EFFECTS OF PRIOR AGING AT ELEVATED TEMPERATURE IN AIR AND IN ARGON ENVIRONMENTS ON CREEP RESPONSE OF PMR-15 NEAT RESIN AT 288°C

THESIS

Joseph L. Broeckert, 1st Lt, USAF

AFIT/GMS/ENY/07-M01

DEPARTMENT OF THE AIR FORCE
AIR UNIVERSITY

AIR FORCE INSTITUTE OF TECHNOLOGY

Wright-Patterson Air Force Base, Ohio

APPROVED FOR PUBLIC RELEASE; DISTRIBUTION UNLIMITED

The views expressed in this thesis are those of the author and do not reflect the official policy or position of the United States Air Force, Department of Defense, or the U.S. Government.

AFIT/GMS/ENY/07-M01

EFFECTS OF PRIOR AGING AT ELEVATED TEMPERATURE IN AIR AND IN ARGON ENVIRONMENTS ON CREEP RESPONSE OF PMR-15 NEAT RESIN AT 288°C

THESIS

Presented to the Faculty

Department of Aeronautics and Astronautics

Graduate School of Engineering and Management

Air Force Institute of Technology

Air University

Air Education and Training Command

In Partial Fulfillment of the Requirements for the

Degree of Master of Science (Material Science)

Joseph L. Broeckert, BS

1st Lt, USAF

March 2007

APPROVED FOR PUBLIC RELEASE; DISTRIBUTION UNLIMITED

AFIT/GMS/ENY/07-M01

EFFECTS OF PRIOR AGING AT ELEVATED TEMPERATURE IN AIR AND IN ARGON ENVIRONMENTS ON CREEP RESPONSE OF PMR-15 NEAT RESIN AT 288°C

Joseph L. Broeckert, BS

1st Lt, USAF

Approved:

_____	_____
Dr. Marina Ruggles-Wrenn, (Chairman)	Date
_____	_____
Dr. R. B. Hall, (Member)	Date
_____	_____
Dr. G. A. Schoeppner, (Member)	Date

AFIT/GMS/ENY/07-M01

Abstract

Creep behavior of PMR-15 neat resin, a polyimide thermoset polymer, aged in air or argon gaseous environments at 288°C for up to 1000 h was evaluated. Creep tests were performed at 288°C at creep stress levels of 20 and 10 MPa. Creep periods of at least 25 h in duration were followed by recovery at zero stress. Duration of the recovery period was at least twice the time of the creep period. Weight loss and growth of the oxidation layer were also monitored and correlated with aging time. The aging time in both air and argon environments had a strong influence on the creep and recovery response of PMR-15 neat resin. Samples aged in argon for 1000 h and tested at a creep stress level of 20 MPa produced creep strain of 4%, while the as-processed samples accumulated creep strain of 16%. In general there was little difference in the creep and recovery response of samples aged in air or argon for the same time and test conditions. Samples aged in air for periods longer than 250 h and tested at 20 MPa failed either during creep or during loading to creep stress. DMA tests were performed to examine any changes in the glass transition temperature (T_g) of the PMR-15 neat resin. DMA results revealed an increase in T_g from 331°C to 336.5°C after 1000 h in argon at 288°C. Results suggest that the rise in T_g is due to an increase in cross link density. Increase in T_g due to aging in both air and argon environments is likely behind the changes in elastic modulus and in creep and recovery behavior.

Acknowledgments

I would like to express my sincere appreciation to my faculty advisor, Dr. Marina Ruggles-Wrenn, for her guidance and support throughout the course of this thesis effort. Without her knowledge and patience this thesis would not have been completed. I would like to thank Dr. Charles Lee of AFOSR, Dr. Greg Schoeppner and Dr. Rick Hall at AFRL/MLBC for their support and effort in making this research possible. I would also like to thank the support staff in the Structures and Materials Testing Laboratory as well as AFRL/MLBC staff for their support, experience, and hard work making everything come together for the completion of this work. Finally I would like to thank my wife for her continued support and listening.

Joe Broeckert

Table of Contents

Page

Page

Page

Table of Figures

Page

Page

Page

Page

Page

Page

Page

Page

Page

Page

List of Tables

Page

EFFECTS OF PRIOR AGING AT ELEVATED TEMPERATURE IN AIR AND IN ARGON ENVIRONMENTS ON CREEP RESPONSE OF PMR-15 NEAT RESIN AT 288°C

I. Introduction

Background

In the 1960's and 1970's National Air and Space Administration and other research organizations began experimenting with new types of polymers that could withstand temperatures above 200°C the temperature limit of most epoxy resins used at that time for extended periods of time. The first application of these polymers would be in radomes on supersonic platforms where the air friction increased the surface temperature over what the epoxy based composites could withstand. Polyimide polymers became prime candidates as matrix materials in developing composites that would perform in these relatively extreme conditions. As a result of this research many polyimide and other thermoset polymer resin systems were developed. Today the aerospace industry is considering using these composites in engine components, which experience service temperatures ~300°C for extended periods of time. At the same time, consumer products such as automobiles are starting to use composites in many structural applications including engine components, auto body panels and truck beds and seats [1]. These automotive applications also benefit from the development of stable high temperature polymers and high temperature polymer matrix composites (HTPMCs).

Polyimide resins such as PMR-15 (Polymerization of Monomeric Reactants -15) are of particular interest today because of their superior high-temperature properties and ease of processing compared to many other high-temperature thermosetting resin systems. These materials are being designed for use at temperatures that approach their glass transition temperatures (T_g) for extended periods of time. These conditions demand a thorough understanding of the mechanical stability of the material over time.

PMR-15, developed by NASA Lewis Research Laboratory in the 1970's has become the benchmark of high performance aerospace thermoset polymer resins. It is named for the type of reaction used to manufacture the resin, while the 15 alludes to the average molecular weight of 1500 g/mole of the oligomers before the final cure. There have been many different PMR resins developed but none have been embraced and utilized as widely as PMR-15. There have been three decades of research to characterize it chemically and mechanically by academia, industry and the government laboratories [1].

All polymers have a temperature at which their covalent bonds start to break down independent of the gaseous environment, called pyrolysis. Pyrolysis occurs rapidly when a polymer is heated well beyond its T_g. This polymer degradation occurs at lower temperatures as well, albeit at a much slower rate and can affect the mechanical properties over time [2]. Chain scission and additional crosslinking occurs in thermoset resins as a result of pyrolysis, not only degrading the polymer itself, but changing its morphology and mechanical properties. This is commonly observed as a resin becomes

brittle and stiff over time. These changes can also be due to physical aging as a result of the polymer network changing over time to lower its conformal energy.

The stability of a polymer at high temperatures in the presence of oxygen, or the thermo oxidative stability (TOS), of a polymer resin has been the focus of most PMR-15 research literature since it has been found to have a significant influence on the mechanical properties and performance of a typical composite subject to loading at high temperatures in air. It has been reported that generally a layer of highly oxidized polymer forms on the outer surface of the PMR-15 sample after a relatively short exposure to high temperatures [3]. The mechanical properties of this oxidized layer are drastically different from those of the remaining bulk polymer. The presence of the oxidized layer in general degrades the structural integrity and performance of the overall composite part.

Additionally, some studies on pyrolysis and thermal-oxidative stability (TOS) of PMR-15 examined exposure to either inert gases or air to distinguish between the pyrolytic and oxidative degradation mechanisms. This exposure is commonly called "aging" of the material. However it is important to note that the term aging implies nothing more than high temperature exposure following the intended cure cycle. The studies of aging in inert gas serve as the base line of the oxidative studies since one has little control over the inherent thermal stability of a given polymer. A polymer that acts similar in an inert environment and in an oxidative environment is considered to be thermally oxidatively stable. In order to design and utilize PMR-15 components with confidence, designers need a database of classical material behavior, limitations and performance under use conditions.

This thesis explores the effects of both pyrolytic and thermal oxidative degradation on the mechanical properties and creep response of PMR-15 neat resin due to high temperature aging (288°C) in an argon (inert) or an air (oxidizing) environment. Results of this research will enhance the existing information data base pertaining to thermal and thermo-oxidative-stability, mechanical properties and creep response of PMR-15. These results are critical to the safe use of PMR-15 components in high performance applications such as jet engines.

Problem Statement

The change of mechanical properties with time, temperature, and environment ultimately defines the stability of a composite or resin system. Depending on the design of the part and use environment, the degradation or oxidation of the polymer matrix will play different roles in the degradation of the mechanical properties of the overall composite. A unidirectional composite which is only loaded along the fiber direction will see very little mechanical performance degradation even after the matrix is severely damaged. However, unidirectional composites and unidirectional loads are rarely the case in high performance applications. Commonly multidirectional composites are exposed to in-plane stresses and bending moments where forces are applied in all directions. Here the integrity of the matrix will play a large role in the overall performance of the composite. Therefore the characterization of the mechanical properties and creep response of the neat resin after exposure to both inert and oxidizing environments at use temperature for the intended application is critical for the designing of structural components with this material.

Research Objectives

The research objective of this effort is to characterize the mechanical properties and creep response of PMR-15 neat resin that was exposed, or aged, for extended periods of time in an inert (argon) atmosphere or air at elevated temperatures (288°C). The results of this research will further illuminate mechanical property degradation of the PMR-15 neat resin subjected to extended periods of prior exposure at high temperature. This data will form a foundation for experimentally-based life prediction methodologies needed for safe use of PMR-15 neat resin and PMR-15 based composite structural components. The study will discuss the evolution of elastic modulus and creep response with prior aging time. Furthermore, weight loss, dynamic modulus and oxidized layer growth of PMR-15 neat resin are analyzed as functions of exposure time in both environments at high temperature.

Methodology

This research was completed in several steps. The first step was to document the elastic modulus of the as-processed neat resin to capture the specimen-to-specimen variability in the elastic modulus. The second step involved aging the samples for various duration in either argon or air environment at elevated temperature. After aging, the samples were tested in tensile creep. Elastic modulus, creep response, oxidation layer growth, weight loss and dynamic modulus were characterized.

Assumptions/Limitations

There are several underlying assumptions utilized in this thesis. The most important is that oxidation of the PMR-15 is negligible at ambient temperatures. This has implications specifically as regards to intermittent opening of the aging chamber for inspections and sample removal and the exposure of the samples to ambient air at room temperature during weight measurements. This assumption is common and is necessary since the resin was exposed to air immediately after initial manufacturing and prior to the actual testing. Any oxidation that is present on the surface of each sample is deemed unavoidable and will have negligible effect on the overall mechanical properties of the sample. It is also assumed that the thermal cycling of the samples during these limited heating and cooling periods does not introduce additional factors contributing to degradation of PMR-15. This assumption is common to many aging studies. The number of thermal cycles was kept to a minimum and didn't exceed 10 for any set of samples, which could be considered negligible in terms of thermal fatigue. A third assumption is that the mechanical properties of the pyrolytically aged samples will approximate the mechanical properties of the inner material of thermal-oxidatively aged samples. The assumption is further discussed and supporting evidence in current literature is presented in Chapter 2.

Finally, the assumption that all testing was done in a dry environment is necessary to classify all data collected as dry data, meaning that the polymer was devoid of moisture that may have introduced additional effects not taken into consideration. This assumption will be supported with some elementary calculations in Chapter 3.

Implications

This thesis research has implications for the continued understanding and development of high temperature polymer matrix composites. Designers of systems employing these materials require classical mechanical property data and lifetime statistics to accurately design and produce parts. Studies such as this expand the pool of reliable mechanical property data for PMR-15 neat resin before and after exposure to certain environmental conditions similar to the operating conditions of PMR-15 polymer and composite in applications. Without this type of data each part designed would need to be tested independently greatly increasing the cost of implementation for such components.

II. Literature Review

The purpose of this chapter is to cite publications that address the issues central to this thesis. Much of the literature also addresses the assumptions that enable this work, and in many cases have proven the assumptions to be true. Additionally, the literature reviewed demonstrates the current level of knowledge on the topic of pyrolitical and oxidative degradation of PMR-15 neat resin and its composites. In some cases the basic science of the chemistry was addressed while in others the ramifications of applications have been addressed.

Thermal Degradation

PMR-15 resin is formulated from 3 monomers: dialkylester of benzophenone tetracarboxylic acid (BTDE), 4,4'-methylenedianiline (MDA) and monoalkyl ester of 5-norbornene-2,3-dicarboxylic acid (NE), all of which are dissolved in a low boiling alkyl alcohol (typically methanol). The first step in polymerization is to take the low viscosity fluid and heat it to 150-200°C for several hours for imidization to form the prepolymer. This step creates oligomers with an average molecular weight of 1500 g/mol. This pre-PMR-15 material is used as the prepreg material. Then the resin or prepreg is heated to 250-320°C to crosslink the oligomers via a reverse Diels-Alders addition reaction creating the final resin system [4]. A schematic of this process is shown in Figure 1. This addition reaction does not generate any byproducts enhancing the processabilty of PMR-15 [2]. The third step involves a post cure at 320°C to drive out any remaining solvent and to raise the glass transition temperature (T_g) to the required level [5].

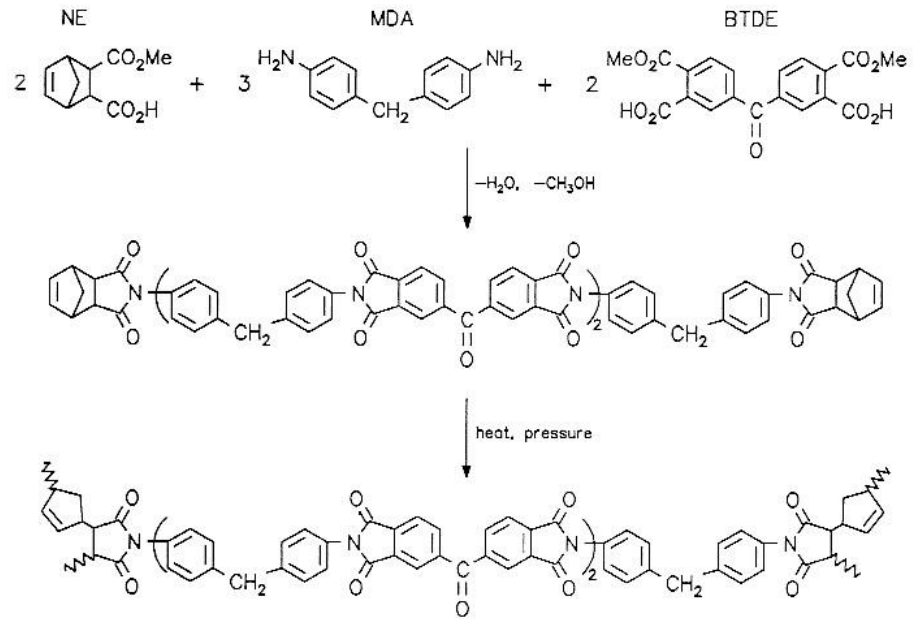

Figure 1 - Classical chemistry of PMR-15. Figure from Ref. [5].

One of the great advantages of PMR-15 over other resin systems is that its polymerization can be broken into two steps. The first step releases byproducts and solvent, but is easily controlled in the prepreg form, not to mention that the prepreg is then relatively easy to handle. The second step does not release byproducts and very little solvent is used limiting the number of gaseous voids found in the final composite product.

There has also been much documentation on the toxicity of one of the monomers, MDA, used in the initial formation of the oligomers. Health and safety studies have found that MDA can cause mutations in animals and is a suspect carcinogen in humans [6]. Consequently many researchers have attempted to develop a chemistry system that

generates PMR-15 without the use of MDA [4,6]. Examples of resins considered for replacement include Avimid N, AMB21 and PMR-II. Avimid N resin was examined for its superior oxidative resistance, but processing it is difficult due to the large amounts of byproducts released during the one step cure. The resulting resin is very porous and has disappointing mechanical properties. AMB21 was found inferior due to its reduced fatigue resistance and lower T_g.

A pyrolytic thermal stability study was carried out by Bowles et al. al. at NASA Glenn Research Center in 2001 [3]. This study attempted to determine the degradation of mechanical properties of PMR-15 neat resin and carbon composite as a function of depth from the exposed surfaces. The samples were exposed at several temperatures (204, 260, 288, 316°C), in air and nitrogen. The processing conditions used in this study are typical for other PMR-15 neat resin and composite studies. The composite used was T650-35/PMR-15 composite (24 by 23, 8 harness satin weave graphite fiber fabric). The neat resin was cured at 316°C for 2 h in matched metal molds and post cured for 16 h at 316°C. All samples were dried for 24 h at 125°C before testing to ensure dry conditions. The quality of the polymer and composites was verified by nondestructive evaluation (NDE) and metallographic photography. The samples were cut with a water cooled micromachining diamond saw to reduce the surface flaws on the cut surfaces. All samples were kept in a desiccator before measurement. Glass transition temperature (T_g) was measured with a dynamic mechanical analysis machine and was determined by the intersection of the two tangents of the linear segments of the stored shear modulus curve.

The average T_g of the samples in that study was found to be 347°C. Compression tests were conducted in accordance with the procedure in ASTM D-695M [3].

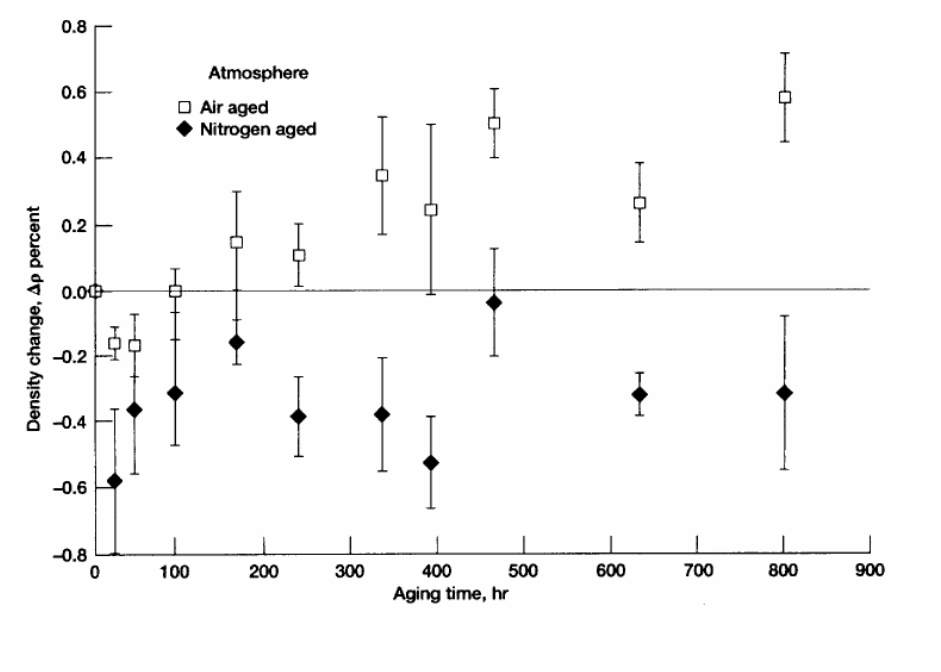

Figure 2 - Density change for PMR-15 neat resin as a function of aging time for 2 aging atmospheres at 316°C. Figure from Ref. [3].

Figure 2 illustrates the dramatic difference between pyrolytic and thermo-oxidative degradation. Samples aged in nitrogen show a decrease in density over time while the specimens aged in air continuously increased in density as matrix continued to oxidize. The reduction in density for the nitrogen aged samples was explained by the release of gaseous products while the increase in density for the air aged samples is due to the adsorption of oxygen throughout the part. Ref. [3] emphasized the importance of using samples with the same surface areas when assessing the oxidation since it occurs mainly on the surface of the sample.

A common method to track thermal degradation is through sample weight loss. The weight loss is attributed to the vaporization of low molecular weight molecules released through chain scission [4]. Shrinkage and density are also measured to show an increase in crosslink density. The weight changes can be normalized by surface area. However when comparing weight loss of samples aged in an inert environment the volumes should be matched as well since the aging takes place throughout the volume of the sample. Figure 3 shows a plot of the weight loss of PMR-15 neat resin as a function of aging time for various aging temperatures. Figure 4 shows plots of weight loss normalized by the surface area as a function of aging time for samples with various surface areas and volumes. The importance of normalization is evident.

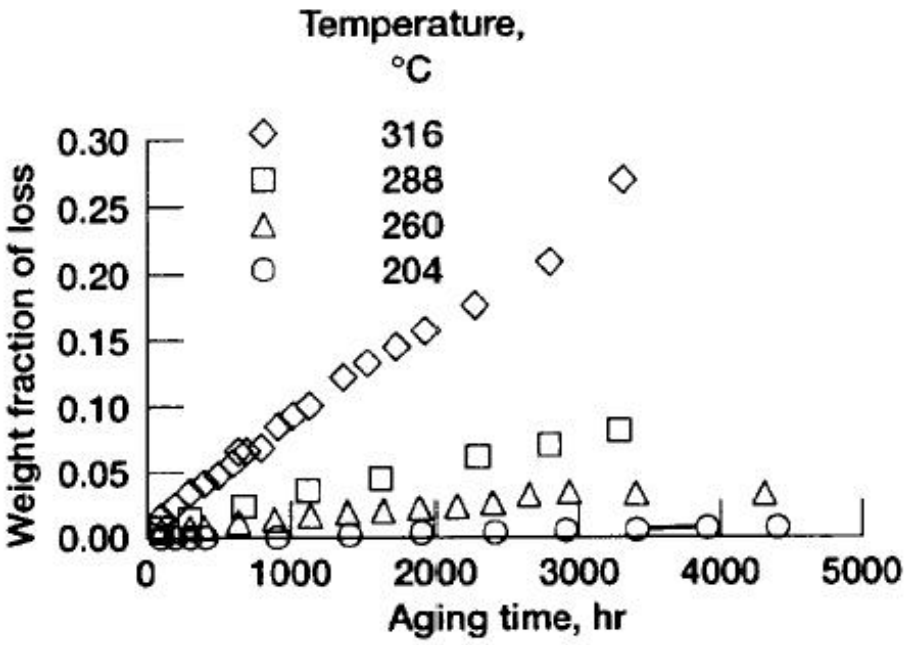

Figure 3 - Weight fraction loss as a function of aging time in air for PMR-15 neat resin. Figure from Ref. [3].

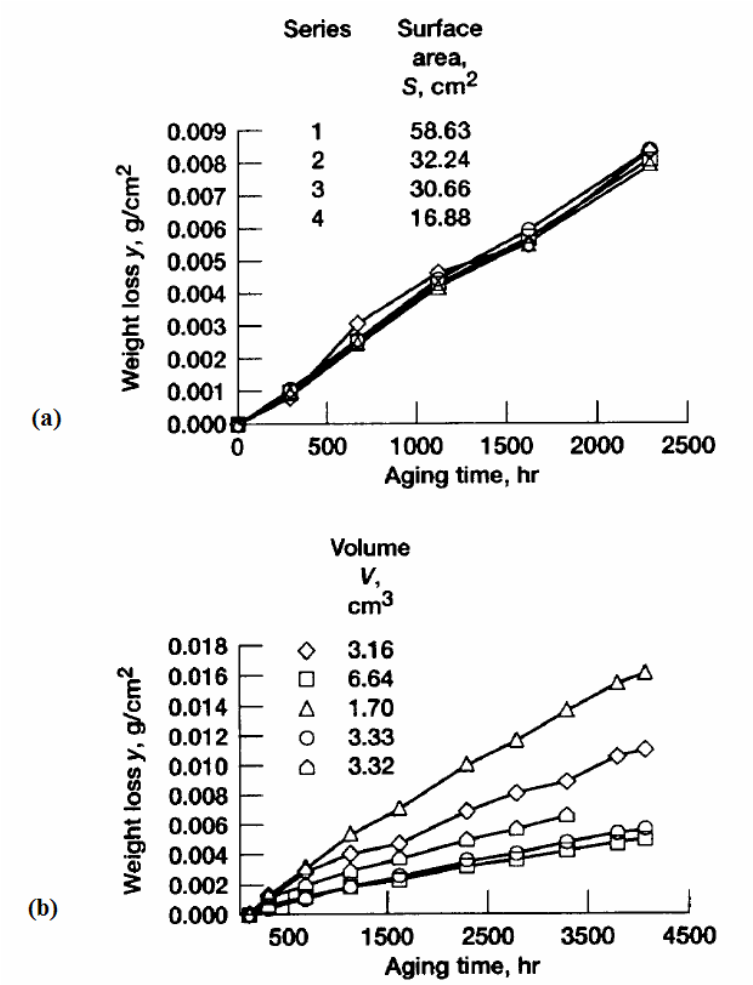

Figure 4 - PMR-15 neat resin aged in air at 288°C. Weight loss normalized by surface area as a function of aging time for (a) various sample surface areas and (b) various sample volumes. Figure from Ref. [3].

Figure 3 shows the expected weight loss at 288°C for up to 1000 h of aging in air. Figure 4 shows the dependence of weight loss in air on surface area. However neither figure shows the difference between weight loss in an inert and that in an oxidizing environment. It is noteworthy that Bowles [3] also found a region of weight gain in samples aged below 250°C. This weight gain was attributed to a slower rate of diffusion

of the gaseous products out of the sample compared to the weight gain mechanism of oxidation at these lower temperatures.

Xie et al. [7] examined gases evolved from PMR-15 neat resin as the exposure temperature was increased to 950°C in nitrogen. The study found that the first molecules to be water, CO, CO2 and CH_4 and NH_3. Using mass spectroscopy and gas chromatography, it was possible to determine that NH_3 was released during the majority of the weight loss at ~ 500°C. Following the degradation, larger molecules vaporized at high temperatures as a result of the degraded backbone. CO and CO_2 were found at lower temperatures, but these molecules are derived from side groups and did not appear related to backbone degradation. It was concluded that the pyrolytic degradation is due to the cleavage first from the C-N and then the C-C bonds while additional weight loss can be attributed to degradation of side groups on the polymer chain [7].

Thermal Oxidative Degradation

Verdu and Colin [8, 9] proposed several mechanisms for the thermo oxidative degradation of organic matrix composites. They presented several general chemical reactions that define oxidation of the polymer (P) and the creation of free radicals (P*) shown in Figure 5.

To explain the appearance of the polymer radical (P*), Verdu postulated that for a generally thermally stable polymer, the weakest bond was the first to break. Commonly the hydroperoxides, POOH, would contain the weakest bond and above 130°C its unimolecular decomposition will dominate. [8]

1. $P^* + O_2^* \rightarrow PO_2^*$
2. $PO_2^* + PH^* \rightarrow POOH + P^*$
3. $POOH \rightarrow 2P^*$

Figure 5 - Oxidizing chemistry proposed for a general thermally stable polymer. Figure from Ref. [8].

In the case of the PMR-15 resin, (Figure 1), there are no hydroperoxides to provide the radicals necessary for oxidation. However, Bowles et al. [4], claim that in the case of PMR-15, it is the nadic end group that introduces the weakest bond into the polymer. The N-CO-C link is the first to be broken down and attacked by O_2 [4].

Another factor that must be considered is the mechanism by which O_2 is introduced into the polymer. Bowles [3] concluded that it was the diffusion rate, and not reaction rate, controlled the oxygen degradation process in PMR-15. A diffusion barrier or a sacrificial additive may help slow down the rate of oxidation of the polymer by slowing down movement of oxygen. Although this was not addressed in [3], it appears that this may be the topic of current research as found in [10]. However solid conclusions have yet to be drawn.

The formation of voids and cracks on the surface of the composite/matrix has also been found to play a role in the extent of oxidative degradation. Bowles [11] also measured the activation energy of formation for the early onset of an oxidized layer, at 5.5 kcal/g-mol, much less than that of late time oxidation, at 22.7 kcal/g-mol. Therefore, the formation of voids in the oxidized layer will consume oxygen before the oxygen will diffuse further in to the composite [11]. This serves to limit the growth of the oxidized layer into the polymer.

Bowles [11] also discovered that the thickness of the severely oxidized layer on the surface of the polymer would stop growing at 0.17 mm regardless of temperature for up to 4000 h of aging.

Bowels [3] reported that the mechanical properties vary with distance from the surface of the T650-35/PMR-15 composite. He measured the strength and modulus of individual layers of the PMR-15 resin in the composite aged at 260°C for 20,000 h. This was accomplished by cutting sections out of an aged composite and testing them independently without further aging. Figure 6 shows the cuts made and the compressive strength and modulus measured for each layer. Modulus was determined by dynamic mechanical analysis [3].

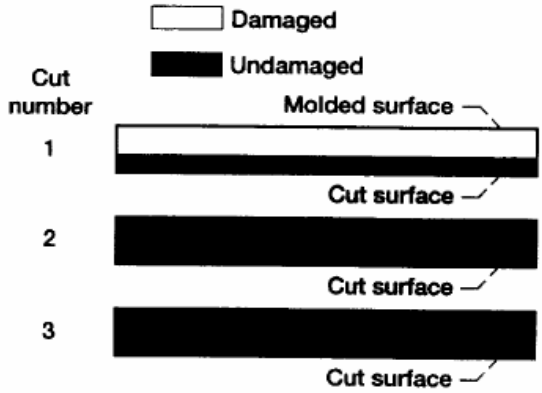

COMPRESSION STRENGTHS AND MODULI OF COMPOSITE SPECIMENS*

Cut number	Strength, MN/m^2	Modulus, GN/m^2
1	137.3	56.9
2	299.6	56.7
3	264.6	62.9

*Taken from different depths through the thickness of thick laminate aged at 260 °C for 20 000 hr.

Figure 6– Geometry of layers cut from a single composite aged at 260°C for 20,000 h. Strength and modulus values shown for each layer are shown. Figure from Ref. [3].

The strength of the surface layer was significantly less than that of the layers shielded from the oxidation while the modulus was generally unaffected. In the case of a composite aged at 360°C for 2090 h, it was found that the T_g decreased with increasing distance from the surface and that the storage modulus was two orders of magnitude lower at the surface than near the center. A plot of stored shear modulus for the layers of the composite aged at 360°C for 2090 h is shown in Figure 7. It is seen that while the surface of the composite is undergoing severe oxidation the center of the composite continues to degrade by thermal mechanisms only.

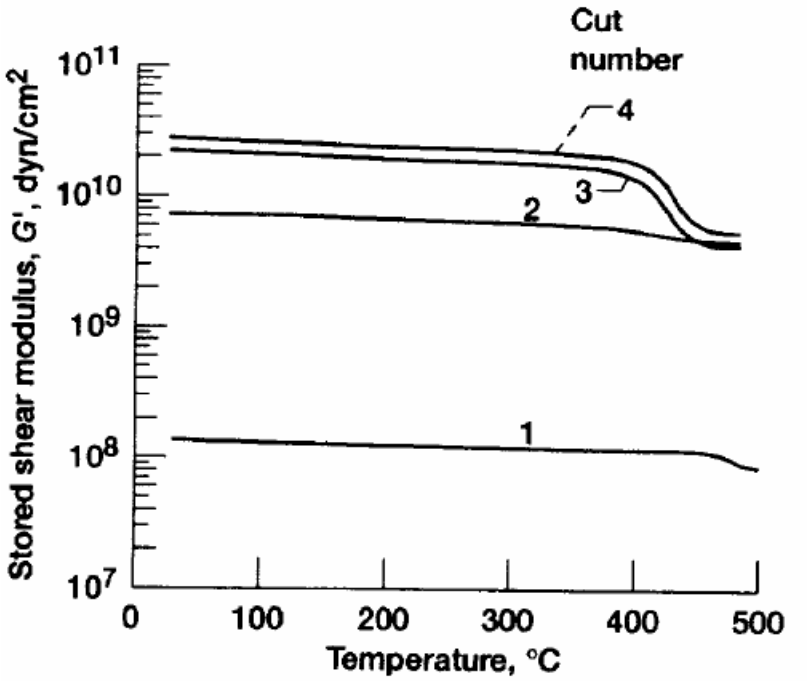

Figure 7 – Stored shear modulus of T650-35/PMR-15 composite as a function of temperature for various depth cuts. Samples aged in air at 360°C for 2090 h. Sample #1 is the surface sample. Figure from Ref. [3].

Additional data from this same study published in 2003 [12] revealed that the compression strength and modulus of the T650-35/PMR-15 composite samples were

affected by aging temperature and time, Figure 8. Results in Figure 8 demonstrate that at very high temperatures relatively little time is needed to severely degrade the compression properties.

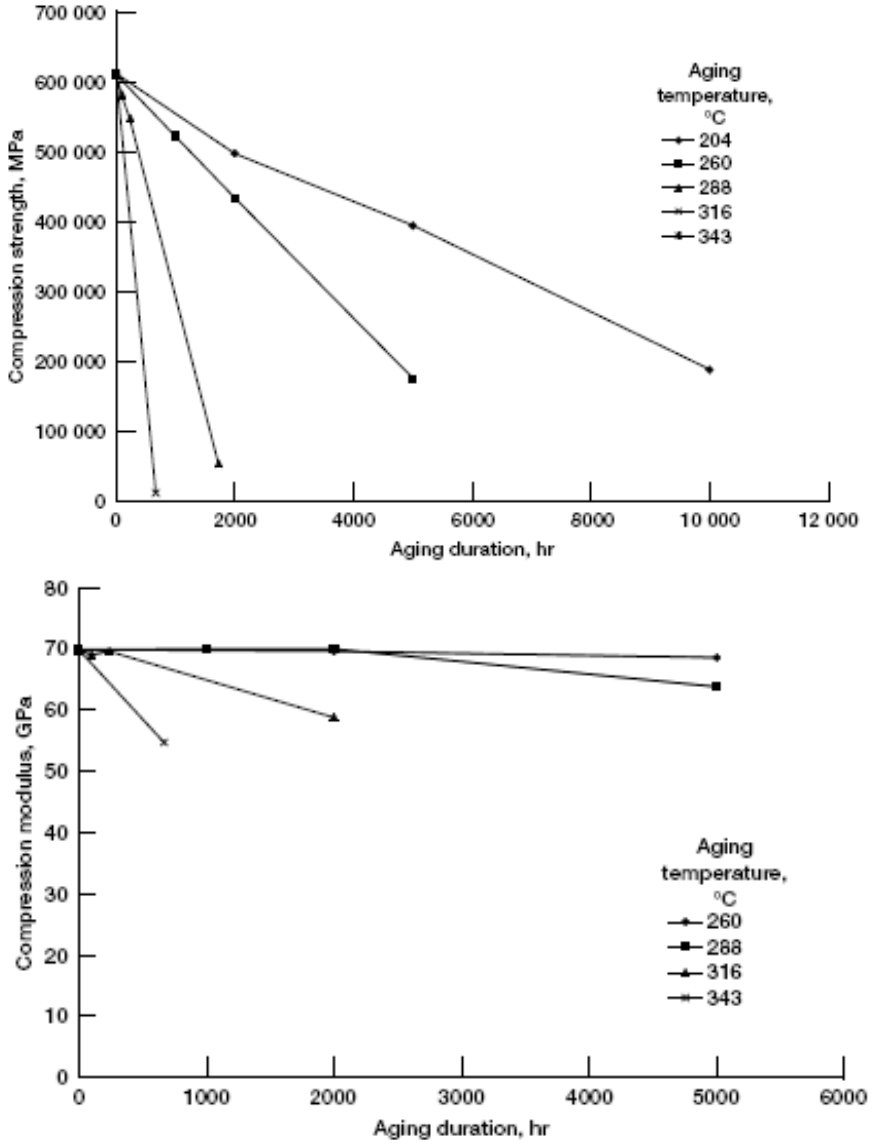

Figure 8– Compression strength and modulus of T650-35/PMR-15 composites as functions of aging time in air at various temperatures. Figure from Ref. [12].

Further studies have explored the difference between the TOS of cut surfaces, molded surfaces and edges where fibers are exposed. It was shown by Bowels et al. [13], that cut surfaces and surfaces containing exposed fiber oxidize faster than a molded resin-rich surface. It was suggested that surface microcracks introduced during cutting were the major contributors to the increased rate of oxidation. On the surfaces containing exposed fiber, the fiber/polymer interface provided a fast track for both water and oxygen diffusion into the center of the composite. Additionally, a difference in TOS of a unidirectional composite and crossply laminate was found. Significant differences in the rate of weight loss between the samples were observed. The crossply samples exhibited dramatically increased weight loss compared to the unidirectional samples. It was concluded that the increase in surfaces containing fiber ends contributed to the increase in weight loss as compared to the unidirectional composites. Large surface cracks formed along the fiber matrix interface and opened a pathway for oxygen to oxidize previously protected resin [13].

Tsuji et al. [14] studied the mechanical properties of PMR-15 neat resin as functions of aging time at 316°C and atmosphere. Tsuji attempted to determine the mechanical properties of the oxidized layer alone and compare those to the properties of the resin that was pyrolytically degraded. He assumed that the properties of the specimens aged in nitrogen would be the same as the properties of the inner unoxidized material in the specimens aged in air. Tsuji found that the bending modulus of the oxidized layer was higher than that of the inner resin. The same trend was found for shrinkage, while the opposite trend was observed for the coefficient of thermal expansion

(CTE). Figure 9 shows the 4-point bend modulus and the CTE for the oxidized and unoxidized samples as functions of aging time at 316°C [14]. The increase in bending modulus was attributed to the increase in crosslink density of the degraded polymer.

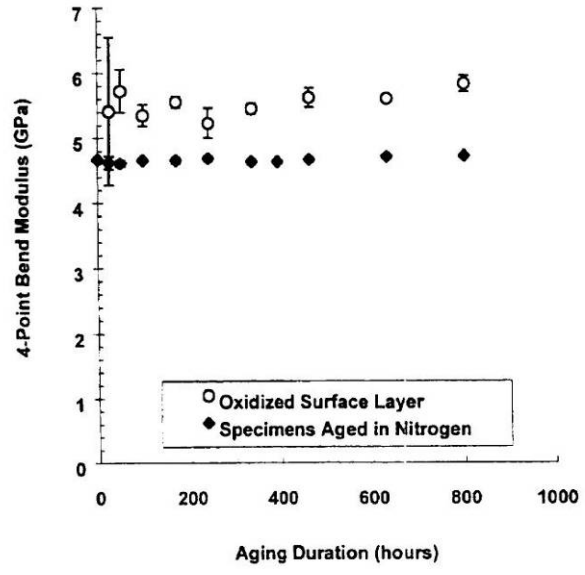

(a)

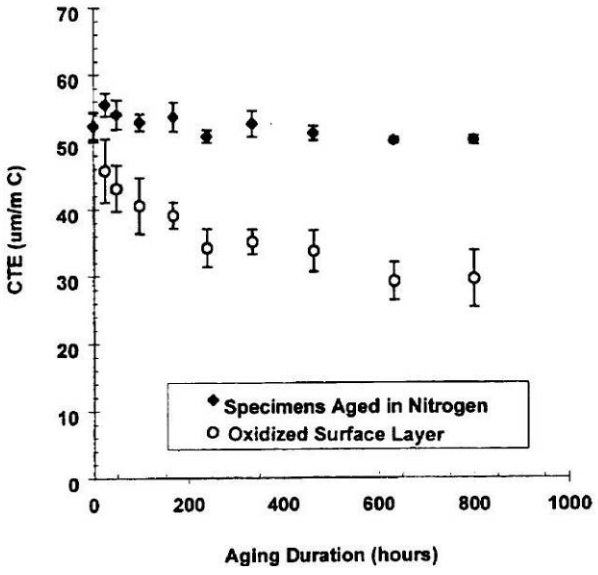

(b)

Figure 9 – (a), 4 point bend modulus and (b) CTE for both oxidized and unoxidized material as a function of aging time at 316°C for PMR-15 neat resin. Figures from Ref. [14].

It was also noted in [14] that this data explains why large surface cracks are found after long aging times in PMR-15. There is a CTE mismatch between the inner and outer layers, the outer layer has a higher bending modulus and expands less producing tensile stresses in the brittle outer oxidized layer [14].

The TOS of composites using high temperature thermoset resins as matrix materials is almost completely dependent on the TOS of the resin. However, fibers do play a role. Not only does the fiber/polymer interface serve as a fast track for diffusion, but some fibers can also react with the O_2. Colin et. al. [9] showed that carbon or graphite fiber reinforced composites carbon in the fibers also reacts with the O_2 thereby minimizing the degradation of the matrix. Colin found that this stabilization was independent of the particular fiber type or temperature [9].

Owens et al. [15] performed a study focusing on aerospace engine applications. As discussed earlier, Bowels [3] found that the oxidative degradation of PMR-15 composites was limited to the outer layers of the composite. However, in those studies the aging was carried out without load or load cycles imposed on the sample. The application of PMR-15 composites in aerospace engines would generally involve thermo-mechanical loads throughout the high temperature use of the composite. Owens found significant microcracking as well as thermal and thermal-oxidative degradation of the PMR-15 composites that were exposed to cyclic thermo-mechanical loading histories.

The study dealt with a Celion 3000 carbon fiber fabric - PMR-15 prepreg and examined both 0/90 and ± 45 laminates, that were subjected to thermal cycles between -55°C and 232°C with 43°C/min heating rates and 10°C/min cooling rates, and

compression fatigue cycling with the ratios of minimum and maximum stress of 0 and 0.3. Prior to thermo-mechanical cycling, the specimens were subjected to 1000 h of thermal aging at 232°C in air. Table 1 summarizes the test conditions used in this study.

Table 1– Grouping of environmental and load histories for PMR-15 carbon fabric samples. Table from Ref. [15].

Grouping of Laminates According to their Conditioning	
Group 1	datum (as moulded)
Group 2	datum + 1 000 hours isothermal ageing at 232°C
Group 3	datum + 1 000 fatigue cycles
Group 4	1 000 thermal cycles
Group 5	1 000 thermal cycles + 1 000 hours isothermal ageing at 232°C
Group 6	1 000 thermal cycles + 1 000 fatigue cycles
Group 7	1 000 thermal cycles + 2% thermal cycles from −55°C → 232°C
Group 8	1 000 thermal cycles + moisture conditioning to 1% + further 10 cycles
Group 9	2 000 thermal cycles
Group 10	2 000 thermal cycles + 1 000 hours isothermal ageing at 232°C
Group 11	2 000 thermal cycles + 1 000 fatigue cycles
Group 12	2 000 thermal cycles + 2% thermal cycles from −55°C → 232°C
Group 13	5 000 thermal cycles
Group 14	5 000 thermal cycles + 2% thermal cycles from −55°C → 232°C

Microcracking was observed and quantified before and after the various treatments and correlated with the mechanical property results. The tensile and compressive strength and modulus are reported in Table 2 and Table 3 respectively.

Table 2– Tensile and compressive strength for 0/90 and ±45 samples subjected to various treatments, tested both at RT and at 232°C. Data from Ref. [15].

Tensile and Compressive Strength at RT and 232°C

Group	*Tensile strength* $(0/90°)_6$ *laminates* (*MPa*)		*Tensile strength* $(\pm 45°)_6$ *laminates* (*MPa*)		*Compressive strength* $(0/90°)_6$ *laminates* (*MPa*)	
	RT	*232°C*	*RT*	*232°C*	*RT*	*232°C*
1	736·6 (2·1%)	689·5 (15·8%)	97·0 (3·0%)	72·9 (6·2%)	623·4 (8·1%)	460·8 (5·5%)
2	820·4 (2·6%)	818·4 (2·9%)	80·3 (3·1%)	71·1 (2·5%)	468·3 (10·9%)	518·5 (8·7%)
3	—	—	—	—	624·3 (19·0%)	433·2 (4·5%)
4	667·3 (6·2%)	661·8 (3·8%)	92·2 (2·6%)	74·2 (3·9%)	555·5 (3·9%)	321·4 (36·5%)
5	753·6 (5·6%)	802·8 (4·6%)	80·7 (1·4%)	74·8 (1·1%)	394·1 (5·6%)	382·9 (8·0%)
6	825·8 (4·9%)	826·5 (8·6%)	88·1 (3·5%)	73·5 (2·0%)	528·7 (2·7%)	344·3 (23·8%)
7	770·3 (4·1%)	638·4 (9·0%)	90·6 (2·5%)	77·6 (4·4%)	634·0 (9·1%)	468·0 (15·7%)
9	751·6 (7·6%)	838·7 (5·4%)	92·7 (4·0%)	69·4 (3·3%)	457·3 (6·7%)	409·2 (4·7%)
10	729·4 (5·4%)	764·4 (4·0%)	73·7 (2·6%)	67·2 (2·2%)	379·2 (5·4%)	335·4 (7·1%)
11	823·2 (6·3%)	800·6 (8·9%)	87·7 (2·7%)	61·1 (16·7%)	599·3 (18·7%)	435·5 (14·9%)
12	700·1 (6·1%)	706·0 (8·4%)	91·8 (1·6%)	74·5 (2·0%)	461·1 (6·0%)	425·9 (14·0%)
13	759·4 (4·0%)	771·8 (3·8%)	63·7 (0·9%)	60·5 (3·0%)	328·7 (16·5%)	228·5 (37·8%)
14	747·4 (5·5%)	790·3 (4·2%)	66·7 (1·3%)	54·8 (3·8%)	252·4 (5·1%)	250·5 (20·1%)

Coefficients of variation are shown in parentheses.

Table 3– Tensile and compressive modulus for 0/90 and ±45 samples subjected to various treatments, tested both at RT and at 232°C. Data from Ref. [15].

Tensile and Compressive Modulus at RT and 232°C

Group	*Tensile modulus $(0/90°)_6$ laminates (GPa)*		*Tensile modulus $(\pm 45°)_6$ laminates (GPa)*		*Compressive modulus $(0/90°)_6$ laminates (GPa)*	
	RT	*232°C*	*RT*	*232°C*	*RT*	*232°C*
1	69·5 (4·5%)	67·5 (3·6%)	4·52 (6·7%)	3·59 (2·9%)	60·7 (9·4%)	57·44 (6·1%)
2	65·6 (3·5%)	67·0 (6·0%)	4·35 (2·3%)	3·42 (8·8%)	57·1 (12·3%)	74·3 (12·2%)
3	—	—	—	—	—	—
4	66·4 (4·5%)	66·7 (4·0%)	4·67 (17·0%)	3·67 (5·4%)	56·7 (13·4%)	63·2 (5·9%)
5	66·3 (6·2%)	70·5 (7·0%)	4·55 (2·2%)	3·55 (8·3%)	65·7 (3·3%)	71·7 (13·7%)
6	69·6 (2·2%)	67·6 (2·4%)	4·71 (2·1%)	3·14 (3·2%)	62·2 (11·1%)	55·8 (12·2%)
7	66·8 (4·5%)	65·4 (3·5%)	4·46 (4·4%)	3·96 (7·5%)	61·3 (6·0%)	77·5 (13·8%)
9	64·2 (6·2%)	70·5 (8·4%)	5·0 (4·0%)	3·23 (3·1%)	57·7 (6·8%)	66·6 (10·1%)
10	63·6 (3·6%)	68·0 (4·6%)	4·56 (4·3%)	3·44 (5·9%)	59·1 (9·1%)	78·5 (8·2%)
11	66·0 (4·5%)	65·8 (4·2%)	4·19 (7·1%)	2·34 (13·0%)	68·9 (14·2%)	75·4 (12·3%)
12	67·4 (6·0%)	65·9 (5·3%)	4·90 (2·0%)	3·10 (6·4%)	61·5 (8·0%)	81·6 (6·5%)
13	64·6 (6·0%)	73·4 (10·5%)	4·0 (5·0%)	3·88 (7·7%)	63·6 (12·5%)	77·5 (7·4%)
14	66·7 (3·2%)	73·0 (7·8%)	4·07 (2·4%)	3·15 (6·4%)	63·3 (9·9%)	85·4 (10·6%)

Coefficients of variation are shown in parentheses.

The most significant findings include: (1) the thermal cycling generates surface microcracks initially, followed by internal microcracks; (2) the number of microcracks was still increasing after 5000 thermal cycles; (3) internal microcracks reduced matrix-dominated properties at both RT and 232°C, although modulus was not affected; (4) fiber

dominated properties were not affected by microcracking. Owens [15] concluded that in order to use PMR-15 carbon composites for long periods of time in an aircraft engine, additional work must be completed to stabilize or protect the material from cyclical degradation affects [15].

Creep Behavior

There is relatively little published data on the creep behavior of PMPR-15 neat resin. Marais [16] aimed to model the initial linear creep behavior of PMR-15 neat resin at several elevated temperatures and stress levels. Marais tested PMR-15 in creep and recovery at 250, 275, 285, 300°C and creep stress levels ranging from 30% to 70% of the ultimate tensile strength (UTS), also measured in this study. The UTS of the PMR-15 was found to be 47 MPa at all temperatures investigated. In the majority of tests, 5 h creep periods were followed by 16 h of recovery at zero stress. The study monitored samples for an additional week of recovery and found no change in recovered strain after 16 h. Figure 10 shows the results of the 5 h creep tests for all temperatures and stress levels used in this study.

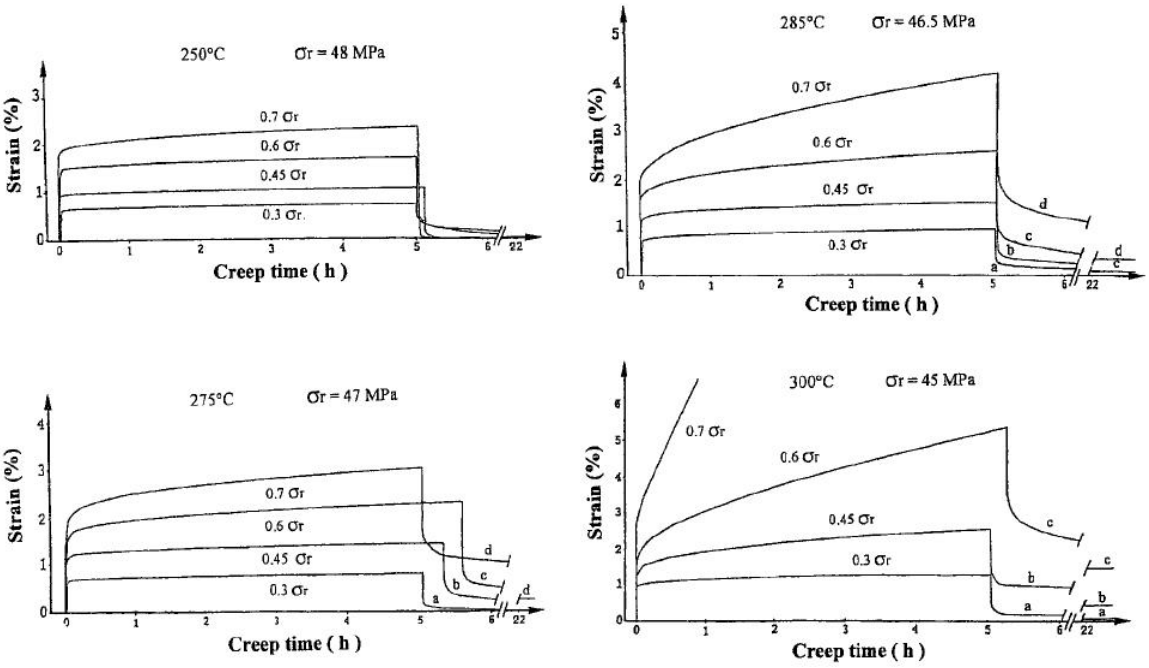

Figure 10 –Creep and recovery curves at multiple temperatures and stress levels for PMR-15 neat resin. Figures from Ref. [16].

It is interesting to note the strong temperature dependence of creep and recovery strains. Marais reported full recovery for any prior creep stress level at 250°C at 275°C noticeable residual strain was found only for high prior creep stress levels. Marais employed the Burgar's model to represent the linear viscoelastic behavior and the Kohlrausch or KWW function to model the creep compliance of PMR-15 neat resin. Although modeling is not the focus of this thesis, it is noteworthy that Marais successfully modeled the viscoelastic response in linear region with a combination of a Burgers model and a generalized Kelvin-Voigt model. However, in the cases where strain accumulation did not approach an asymptotic solution, i.e. at high stress and temperature, this approach was not applicable. The shape of the creep and recovery

curves presented in [16] will serve as a reference for the viscoelastic behavior of the PMR-15 expected in this thesis.

General Theories of Polymer Degradation and Resulting Mechanical Behavior

There are many specific theories on the degradation mechanisms of different polymer systems. Although important for continued fundamental research in polymer science, these degradation theories are not the focus of this research effort. However, these theories do shed light on the chemical, physical and mechanical changes that occur in polymers when exposed to environment and temperature for extended periods of time.

Some references [18:363-365,391-393;21]separate changes that occur in a polymer system due to aging into physical, chemical, and oxidative changes. Physical aging is generally defined as a thermo-reversible process where the polymer rearranges itself into a lower energy state, lowering its free volume. Physical aging has been shown to result in increased yield stress and modulus, and in decreased fracture energy, toughness, and elongation. While physical aging can occur at room temperature it is accelerated by time at elevated temperature.

Chemical aging on the other hand is defined as an irreversible process where chemical bonds of the virgin polymer are broken or rearranged over time. This type of aging is typically defined to specifically exclude effects of oxygen. Chemical aging can occur with or without a reactant. High temperatures have been shown to break chemical bonds leading to the formation of free radicals which can act to either increase or decrease crosslink density. Other chemicals, including water, can also interact with the polymer chains leading to similar results. Chemical aging can result in dramatic changes

in crosslink density and various mechanical properties (modulus, elongation, toughness) depending on the specific environment and polymer chemistry. It may also cause the release of small bits of polymer chains resulting in weight loss and density decrease in the polymer. Typical manifestations of chemical aging include lower molecular weight, etching of the surface, discoloration, voids, and hardening. Chemical aging is relatively under-explored due to the complexity of specific environments and polymer chemistries [18:363-413;20:446-465].

Finally oxidation aging or degradation is defined as the effect of an oxygen reaction with the polymer chains. For a given polymer system in the presence of an oxidizing environment, certain chemical bonds on a polymer chain will be more susceptible to oxidation than others. For example, as discussed earlier it has been reported in literature that for PMR-15 the weak link that is first attacked by oxygen is the nadic end group. The reaction is autocatalytic and results in the breakdown of polymer chains as well as in the formation of free radicals which can in turn trigger further degradation. Oxygen first interacts with the very surface of the polymer and then must either diffuse into the polymer or find a pathway into the polymer for further reaction. For neat resin samples the oxidation degradation is typically limited to a relatively small surface layer. However, in polymer systems with networks of cracks or porosity, or in polymer composites oxidation degradation may take place through the thickness of the polymer. Oxygen degradation can lead to lower molecular weight, lower T_g, embrittlement, additional crosslinking, changes in dielectric properties, change in modulus, change in elongation, just to name a few [18:397-404].

Under most service conditions for high temperature polymers such as PMR-15, all three types of degradation or aging take place simultaneously. The rates of each may differ and may also depend on time and temperature. Therefore, especially when testing for residual mechanical properties after aging over long periods of time it may be possible to see a switch in dominating degradation mechanisms leading to swings in mechanical property trends with aging time. Relatively little has been published on this topic due to the substantial amount of time required to generate the data for a number of polymer systems [18:397-404]. Tracking the specific effects of each type of degradation is difficult and typically studies are only able to track the net resulting effects.

One common statistic tracked is the variation in the T_g of the polymer system with aging time. A thermosetting polymer glass transition temperature is mainly depends on crosslink density, free volume, and average molecular weight between crosslinks. Hence it is obvious that a change in the T_g is related to the changes in the network structure of the polymer. Tests such as Dynamic Thermal Analysis and Differential Scanning Calorimetry are commonly used for this purpose [18:129-138;19:117-121;20:323-370].

Cure during High Temperature Aging

The degree of cure for a thermosetting polymer is defined as the fraction of reacted groups to the total number of reaction groups once available. A degree of cure of one means that every monomer end group has reacted and there are no more possible crosslinks to be made. Because vitrification and gelation reduce chemical mobility and increase the distance between active sites during cure, a degree of cure of one is rarely achieved. After vitrification chemical groups can only move by diffusion and the cure

reaction is effectively stopped. In commercial systems a conversion of one is typically undesirable as the resulting thermoset will be very brittle and hard. A final conversion of 0.8 - 0.9 would be more desirable to give the polymer a reasonable toughness. During the curing process the balance between time, temperature, and degree of cure (X) is often represented by a time-temperature-transition diagram (TTT diagram) and a Conversion-Temperature-Transformation (CTT diagram). Generic TTT and CTT diagrams for typical thermosetting polymers are shown in Figure 11. [20:139-143]

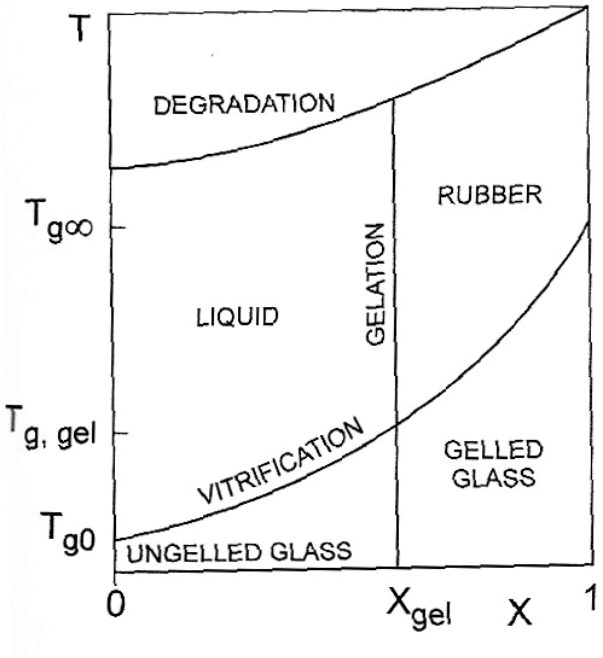

(a)

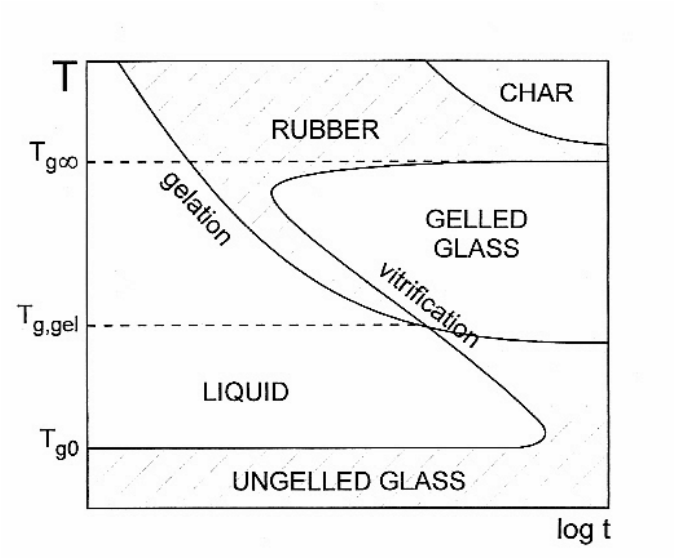

(b)

Figure 11 – (a) CTT diagram for generic thermoset polymer, (b) TTT diagram for generic thermoset polymer. Figures from Ref. [20:139-143].

The CTT diagram can be used to show the various states that a thermoset can exist in as functions of degree of cure and temperature. The diagram also shows that a $T_{g,gel}$ can be defined as the point were the vitrification line crosses the gel line, otherwise stated as the minimum cure temperature for a polymer to gel. If cured at a lower temperature, the polymer solution will vitrify and the cure process is stopped before the irreversible gel point is reached. If an isothermal cure cycle is applied to an uncured polymer solution, a straight line can be drawn across the CTT diagram and the degree of cure at the point of gelation as well as the degree of cure at the point when the gel vitrifies can be found. This method can be helpful when determining the desired cure temperature for a desired final degree of cure. Note that the CTT diagram also shows a $T_{g,\infty}$ where a final degree of cure of one is attainable, however, this is not representative of most practical highly crosslinked polymer systems such as PMR-15. A cure cycle with a cure temperature at or above $T_{g,\infty}$ should be used for maximum degree of cure. Another observation is that at cure temperatures between $T_{g,gel}$ and $T_{g,\infty}$, vitrification occurs soon after geling therefore the T_g of the final polymer will only be as high as the highest cure temperature. This is one of the reasons why a post cure at or above the $T_{g,\infty}$ is done on polymer systems where high T_g is critical. However, curing at temperatures above the degradation line, can lead to chemical degradation of the polymer. This is particularly important over long periods of time as shown with the TTT diagram.

The TTT diagram is a plot of cure temperature versus log time showing the same regions as the CTT diagram, but including a time scale needed to accomplish the phase transformations. This diagram is based on isothermal data and should not be used as a

phase diagram for temperature changes. The TTT diagram is especially helpful when predicting the behavior of a polymer system after long times at a constant temperature. An experimentally derived TTT diagram for an epoxy thermoset polymer in Figure 12 exposure shows the onset of charring at temperatures below $T_{g,\infty}$ after long periods of time [20:139-143;2].

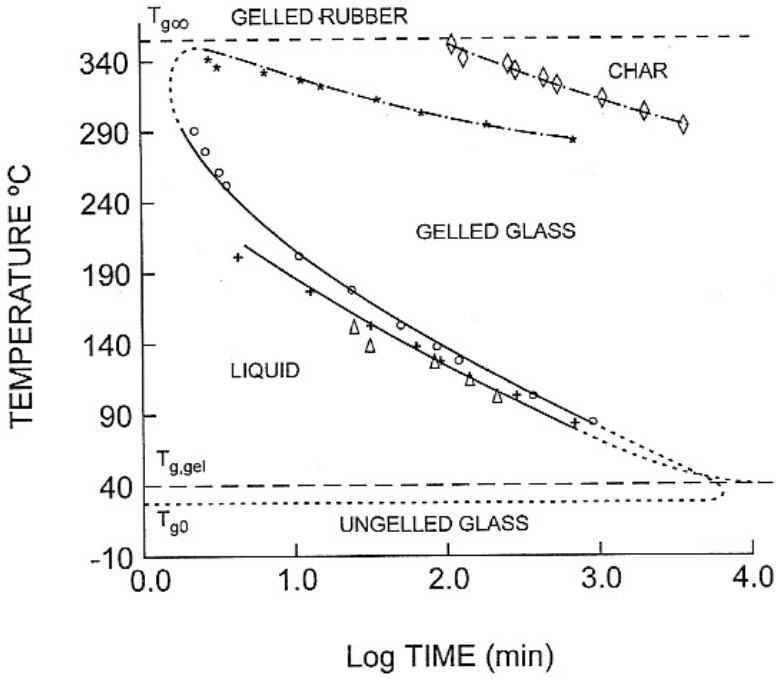

Figure 12 – TTT diagram for an epoxy thermosetting polymer system showing possible degradation after long periods of exposure at temperatures below $T_{g,\infty}$. Figure from Ref. [20:142].

Based on the CTT and TTT diagrams the following conclusions can be made: (1) high temperatures are needed for near full conversion, (2) the highest cure temperature will control the T_g of the final polymer, and (3) degradation of the polymer network can still occur below T_g after long periods of time. In this case, aging a polymer at temperatures near its T_g could also be considered additional curing. [20:193-143]

Summary

This literature review briefly summarizes the current state of the art in the area of mechanical and chemical changes in PMR-15 neat resin and composites due to exposure to high temperatures in both inert and oxidizing environments. It is generally understood that PMR-15 neat resin and its composites will undergo physical and chemical degradation after prolonged exposure to elevated temperatures approaching the polymer's glass transition temperature in both inert and oxidizing environments. The documentation of the resulting changes in mechanical response, the observation and interpretation of the chemical changes on molecular and macro-molecular levels is an ongoing effort.

III. Methodology

Chapter Overview

The purpose of this chapter is to outline and describe the exact procedure used to perform the various portions of this study.

Experimental Arrangements

This study involved exposing (or aging) PMR-15 neat resin samples to either air or argon environments at 288°C for various amounts of time. Aging time was varied from 0 to 1000 h. Four mechanical tests specimens and one rectangular specimen for oxidation layer growth and weight loss measurement were subjected to each aging condition. Previous work [22:65**]** had shown the ultimate tensile strength (UTS) of the PMR-15 material supplied for this study to be ~30 MPa at 288°C. Creep testing was carried out at the applied creep stress levels of 10 MPa (33% UTS) and 20 MPa (67% UTS). Two creep tests were conducted for each creep stress level and aging condition. Table 4 gives the summary of aging conditions. Dog bone shaped tensile specimens were used in all tests. Test specimen is shown in Figure 13. The samples thickness varied slightly, but was nominally 0.15 in.

Table 4 – Summary of aging conditions used in the study. All samples were aged at 288°C.

Sample ID	group	Aged time (hrs)	Aged environment	Sample ID	group	Aged time (hrs)	Aged environment
12-10	1	0		12-05	8	10	air
02-01	1	0		12-17	8	10	air
11-15	1	0		11-05	8	10	air
13-10	1	0		13-01	8	10	air
12-11	2	50	air	12-07	9	50	Ar
02-02	2	50	air	12-09	9	50	Ar
11-12	2	50	air	11-10	9	50	Ar
13-12	2	50	air	13-02	9	50	Ar
12-02	3	50	air	12-14	10	100	Ar
02-03	3	50	air	12-15	10	100	Ar
11-11	3	50	air	11-03	10	100	Ar
11-17	3	50	air	13-03	10	100	Ar
12-16	4	100	air	12-12	11	250	Ar
12-18	4	100	air	12-13	11	250	Ar
02-04	4	100	air	11-18	11	250	Ar
11-16	4	100	air	13-04	11	250	Ar
12-19	5	250	air	12-04	12	500	Ar
02-05	5	250	air	12-20	12	500	Ar
11-04	5	250	air	11-09	12	500	Ar
13-09	5	250	air	13-06	12	500	Ar
12-08	6	500	air	12-03	13	1000	Ar
02-06	6	500	air	11-02	13	1000	Ar
11-07	6	500	air	11-14	13	1000	Ar
11-08	6	500	air	13-07	13	1000	Ar
12-01	7	1000	air	02-10	1	0	
12-06	7	1000	air				
02-07	7	1000	air				
11-13	7	1000	air				

The sample ID uniquely identifies each sample as well as which panel the sample was cut from. The first two digits of the sample ID designate the panel number while the second two digits identify a particular sample within that panel. The samples were separated into groups, with an average of one specimen from each panel per group. The

purpose of this forced randomization was to minimize the effects of the panel to panel variability on experimental results.

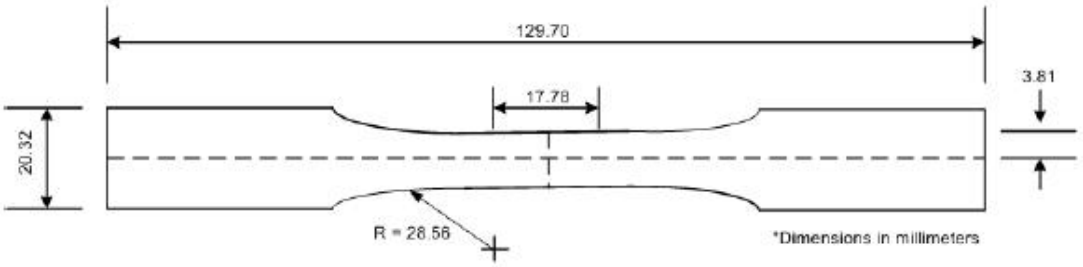

Figure 13 –Dog bone tensile specimens with nominal dimensions shown. Figure from Ref. [22:47].

Material

The PMR-15 neat resin panels were supplied by HyComp and were post cured at the Air Force Research Laboratory/Materials Laboratory Directorate. The condition of the 4 panels delivered was not optimal for use and subsequent high temperature pressing was performed to flatten the panels to attain acceptable test specimens. Unfortunately the exact history of the high temperature treatment for each of the panels used in this study is not available. All that is known is that the panels were post cured. This unconventional treatment of the panels may lead to increased mechanical property variability between panels. This will be accounted for by determining the initial elastic modulus of each of the samples.

The standard free standing post cure cycle used by the Air Force Research Laboratory is shown in Table 5. It is assumed that each of the panels was exposed to this

post cure cycle. The exposure time in this post cure cycle differs slightly from the exposure time in the post-cure cycle recommended by the manufacture.

Table 5 – Steps of the Air Force Research Lab standard post cure cycle for PMR-15 neat resin panels.

Step 1) Heat to 204°C in 2 h and hold for 1 h

Step 2) Heat to 260°C in 1 h and hold of 1 h

Step 3) Heat to 316°C in 2 h and hold of 16 h

Step 4) Cool to room temperature at a rate of 1°C/min

The post-cure cycle recommended by the manufacture specifies heating to 288°C at 5-10°C/min followed by a 5 h hold then heating to 316°C at 0.5°C/min followed by a 10 h hold, and finally cooling to 71°C prior to removing panels from the oven.

Aging

The samples were aged in either argon or in air environment at 288°C for various periods of time. Samples were removed for periodic inspections. The aging in argon was accomplished with a Blue M inert gas oven, model 7780. High purity argon gas (99.999% pure) was supplied to the furnace in a manner designed to maintain a slight positive argon pressure in the heating chamber at all times when the temperature inside the chamber was above ambient temperature. In the case of aging in air, air was supplied to the Blue M oven via a compressed air line with an inline filter and desiccator. The measured relative humidity (RH) of the air fed to the chamber was less than 10% throughout the entire aging period, and most commonly below 5% RH. It is assumed that

any moisture released during aging in both environments was removed by the flowing gas and that any moisture in the chamber was introduced by the air supply creating "dry" aging conditions. The steady state flow rate of the argon and air was approximately 30 standard cubic feet per hour (SCFH) at steady state and 150 SCFH during the purge cycle. When it was necessary to remove or inspect the aging samples, the oven was opened without cooling and closed immediately. The oven then automatically entered the purge cycle to flush out any ambient atmosphere that had entered the chamber. It is assumed that this short exposure did not introduce any additional effects (mainly oxidation and humidity) that were not already present from the production process. It is assumed that the diffusion and reaction kinetics of the oxidation of PMR-15 at room temperature are negligible compared to those at elevated temperatures. This assumption is routinely made in similar published reports. Upon removal of the samples from the aging chamber, the samples were stored in a dry-air-purged desiccator prior to mechanical testing. The desiccator was kept at a constant relative humidity of less than 10%, to ensure the absence of moisture effects. Thus all mechanical properties were considered "dry" mechanical properties. The sample trays in the oven were covered with quartz cloth to prevent contamination of the samples. Prior to use the quartz cloth was kept at 500°C for 1 h to burn off any organic contaminants on the cloth.

Relative Humidity

Even though the aging is carried out in a humidity controlled environment, a question can be raised regarding the exposure of the samples to ambient air during long-term mechanical tests at 288°C. A simple calculation of the expected relative humidity

around the sample during the mechanical test at 288°C shows that even in a very humid ambient environment (RH ≥ 70%) the relative humidity around the sample is very low (RH ≤ 1%) due to high test temperatures.

There are two general definitions for relative humidity: (1) either the actual water vapor pressure divided by the saturation water vapor pressure at the current temperature and (2) the actual water concentration divided by the saturation water concentration at temperature. Using both definitions in calculations yields approximately the same value of RH of the air around the specimens during testing. During testing at e288°C the sample is exposed to heated ambient air. During the summer months the RH of the laboratory did not exceed 70% as measured by a Rotronic, Hygropalm 2 humidity probe, model SC05. The water vapor pressure or water density of the air can be found knowing the saturation point at room temperature. According to the CRC Handbook of Chemistry and Physics, 84th edition, the saturation vapor density is 23 g/cm^3 at 23°C and 8240 g/cm^3 at 288°C. Using the room temperature saturation point and the 70% RH of the laboratory air the actual vapor density is found to be 16.1 g/cm^3. Assuming that this moisture is still present in the air around the test specimen when heated to test temperature with no pressure or volume effects, a new RH at 288°C can be calculated. Using the 288°C saturation point, the RH of the air once heated to 288°C is only 0.002 (0.2%). Even if the laboratory environment was at 100% RH, the heated air would have a RH of 0.3%. Therefore it can be concluded that no moisture effects were introduced during long-term mechanical tests at 288°C. This result also shows that it may not be necessary to supply

the aging oven with dry air to maintain a dry aging environment at 288°C. However, the dry air was supplied for added confidence in the aging environment.

Sample Preparation

Samples used in this study were cut from four different panels. Each panel was C-scanned and any areas within the panel with porosity were not used for the test samples. Some samples were cut using water jet machining and others using a diamond saw and grinding machine. It was found that the diamond grinding introduced fewer defects into the specimens. Any samples with defects in the gauge section were not used for mechanical testing. All samples were washed by hand using common hand soap and rinsed in distilled water to remove oils or other contaminates that might influence the aging process. Gloves were used to handle the samples after this point. Samples were then dried in a vacuum oven at 105°C for at least 24 h to ensure that any moisture was expelled. Before and after testing all samples were held in a desiccator purged continuously with dry air. The samples were marked with silver colored permanent marker for visibility and weighed after the marker was applied and the samples were dried. Fiber glass composite tabs were bonded to the gripping sections of the samples using M-Bond 200, a room temperature cure epoxy adhesive, to protect the samples from the aggressive surface of the grips.

Mechanical testing required the use of a high temperature extensometer designed for use with rough samples or samples pre-marked with small indents or "dimples" for accurate placement and continued contact. Therefore each sample was dimpled before aging and testing so that dimples did not need to be added after aging when a very brittle

oxidation layer may have formed on specimen surface. The dimples were placed using a metal punch provided by MTS and a small hammer. Dimple depth was kept to a consistent minimum as to reduce the possibility of inducing crack propagation from the sites. The effect of the dimples on the UTS has been verified in previous work and was taken into consideration **[**22:65**]**

Mechanical Testing Equipment

All mechanical testing was accomplished using an MTS servo-hydraulic model 810 with a 3 KIP load cell, vertical configured MTS model 318.10 load unit, equipped with the TestStar II's digital controller for input signal generation and data acquisition. The temperature of the specimen gauge section was controlled by a MTS single zone furnace model 653.01A, with a MTS model 409.83 temperature controller. The set point of the furnace required to obtain 288°C on the sample gauge section was determined using a PMR-15 sample fitted with two k-type thermocouples in the gauge section. The furnace set point of 259.5°C was found to yield the required temperature of 288°C. Hydraulic, water-cooled wedge grips, MTS model 647.02B were used and set to a grip pressure of 2.76 MPa in all tests. Strain measurements were taken with a high temperature capable MTS model 6323.53E-14 axial extensometer.

For high-temperature tests the sample was heated to test temperature at a rate of 2°C/min and kept at temperature for 45 min prior to testing. This 45 min period allowed for stabilization of the temperature and thermal strain produced during heating. Typically it was observed that the thermal strain peaked during heating and then stabilized at a

constant but lower value after 30-45 minuets. This effect is attributed to a temperature overshoot upon heating of the sample.

Initial Elastic Modulus Measurements

Prior to aging and further testing the initial room-temperature elastic modulus of each specimen was measured in order to capture the sample to sample and panel to panel variability inherent to this study. The tests were carried out at room temperature in laboratory air environment. The specimen was loaded to 3 MPa at a rate of approximately 1MPa/s and unloaded at the same rate to zero stress. The stress level of 3 MPa and the loading rate of 1 MPa/s were chosen to ensure a linear response, thus no permanent strain was introduced. This linear response region has been documented in similar studies on PMR-15 neat resin tested at 288°C. [23:22,25-27]

Creep Tests

Creep and recovery tests were preformed on all samples. The sample was loaded to creep stress at a rate of 1 MPa/s in all tests. Previous work [23:22,25-27] has shown that loading at a rate of 1 MPa/s or above produced creep during loading at 288°C. Changes of an order of magnitude in the load-up rate are needed to observe the rate dependence in PMR-15 neat resin. The applied load was held constant for a typical period of 25 h followed by unloading to zero stress at stress rate magnitude of 1 MPa/s. Specimen was allowed to recover at zero stress for ~50 h followed by a cool down to room temperature. Data was collected during each phase of the test (i.e. load-up, creep, unloading to zero stress, and recovery data). During the loading and unloading, data was

taken at a fast rate while the data points taken during the relatively long creep and recovery periods were separated by longer time intervals. During creep and recovery, data was taken at 10 second intervals as well as at every change of 0.002 m/m in strain. This allowed for collection of more data during times of fast change but also limited the size of the data files to reasonable levels.

In the cases where the samples failed during testing the fracture surfaces of the samples were observed using an optical microscope to the morphology of the fracture surface. Images were taken using a digital stereo microscope, Zeiss Discovery.V12, at various magnifications. Additionally, all samples were photographed after testing for documentation of the condition of the sample.

Weight Measurements and Oxidation Layer Growth

Each group of sample subjected to a particular aging time and environment included one rectangular blank sample for the purpose of monitoring weight loss and oxidation layer growth as a function of aging time and environment. The initial weight measurements of the blanks were taken after drying and marking. All weight measurements were taken with a Metler Toledo AG245 microbalance with a resolution of 0.0001 grams. After aging, the blank specimens were allowed to cool in the desiccator prior to weight measurements. Next a section of the specimen was cut, mounted and polished for observation with an optical microscope. The samples were mounted in a room temperature cured epoxy, sanded with 600 grit paper and polished with 0.03 micron silica slurry. No staining of the sample was required to view the oxidation layer and its

boundary. A Nikon EPIPHOT digital microscope was employed. Micrographs were captured digitally and dimensioned automatically.

Dynamic Mechanical Analysis (DMA)

Dynamic Mechanical Analysis (DMA) is commonly used to investigate the structure property relationships of cured polymer systems. Although the test can be run in a variety of modes, the most common mode for use with solid polymers is a temperature scan from below T_g to above T_g while stimulating the sample with an insignificant sinusoidal shear stress in torsion to determine both the elastic modulus (G' or storage modulus) and the viscous modulus (G" or loss modulus) as functions of temperature. Depending on the exact tool used this test may also be referred to as to as a Dynamic Mechanical Thermal Analysis (DTMA) or Dynamic Mechanical Rheological Testing (DMRT) [18:129]. In this study the test was conducted at a constant angular frequency of applied torsion, ω. The angular frequency was 1 Hz, with a shear strain amplitude of 0.1%. Temperature was increased at a rate of 1°C/min from room temperature to 450°C. Prior to DMA samples were dried in a vacuum oven at 80°C for 5 days to ensure zero moisture in the samples before testing. The complex modulus, G, can be defined as $G = G'(\omega) \sin \omega t + G''(\omega) \cos \omega t$ [19:117]. The storage modulus is defined as the in-phase portion of the complex modulus and represents the stored and recovered energy in each cycle. The loss modulus is defined as the out of phase portion of the complex modulus and represents the energy lost during each cycle. The ratio of G" to G' call tan δ , can be calculated.

The chemical structure of the polymer directly and indirectly affects modulus of the polymer. The response of a given polymer as a function of temperature has been shown to indicate the extent of crosslinking, provide evidence of polymer degradation, reveal changes in crosslink density, and provide an accurate measurement of T_g. Same results can be obtained by varying the angular frequency and holding the temperature constant. Since the mechanical response of a polymer is related to the free volume and time allowed for its change, tests involving temperature variation (which determines free volume) and tests involving frequency variation (which determines time) have been shown to be related. Either test can be employed to obtain similar results.

In this study an Ares model 3A1 DMA with a nitrogen purged test chamber was used to measure T_g and relate changes in the structure of the PMR-15 neat resin samples to aging time in air and in argon environments [18:129-133,19:117].

Summary

Room-temperature elastic modulus was measured for all samples prior to aging in order to asses the sample-to-sample and panel to panel variability. Samples were aged either in air or in argon at 288°C to simulate both oxidizing and non-oxidizing use conditions. Weight and oxidation layer thickness were measured at periodic intervals to establish dependence of weight change and oxidative layer growth on aging time and environment. Creep tests of 25 h duration were conducted for creep stress levels of 10 and 20 MPa at 288°C in laboratory air. Creep test was followed by unloading to zero stress and 50 h recovery at zero stress at 288°C. Additionally, DMA tests were carried

out to valuate T_g changes in the polymer aged for different durations and in different environments.

IV. Results and Discussion

Chapter Overview

Chapter IV documents the results and presents the analysis of the data collected during this study. Details of the individual experiments will be given and results reported. The discussion section will attempt to correlate the data with theory.

Weight Loss Measurements

The weight of samples aged for various times in either air or argon was measured. It has been shown that in the presence of air the weight loss depends on the surface area of the sample. Therefore the weight loss should be normalized by the surface area of each individual sample for comparison. For samples aged in argon the weight loss depends on the sample volume as the entire sample is releasing various products during the aging process. Weight loss normalized by either surface area or volume of the sample is reported as a weight loss factor, so samples of various geometries and sizes can be compared [3,11,12,13]. Weight loss was measured using a micro balance with an accuracy of 0.0001 grams. All samples were stored in a dry-air-purged desiccator before and after aging to maintain near zero moisture content. The desiccator was kept at relative humidity (RH) of less than 10% at all times while the average value was below 5% RH. Surface area and volume values were measured before aging and no adjustments were made for any dimensional changes. This is a common practice employed in similar studies [3,12]. Figure 14 shows the weight loss factor as a function of aging time in air or argon environments at 288°C.

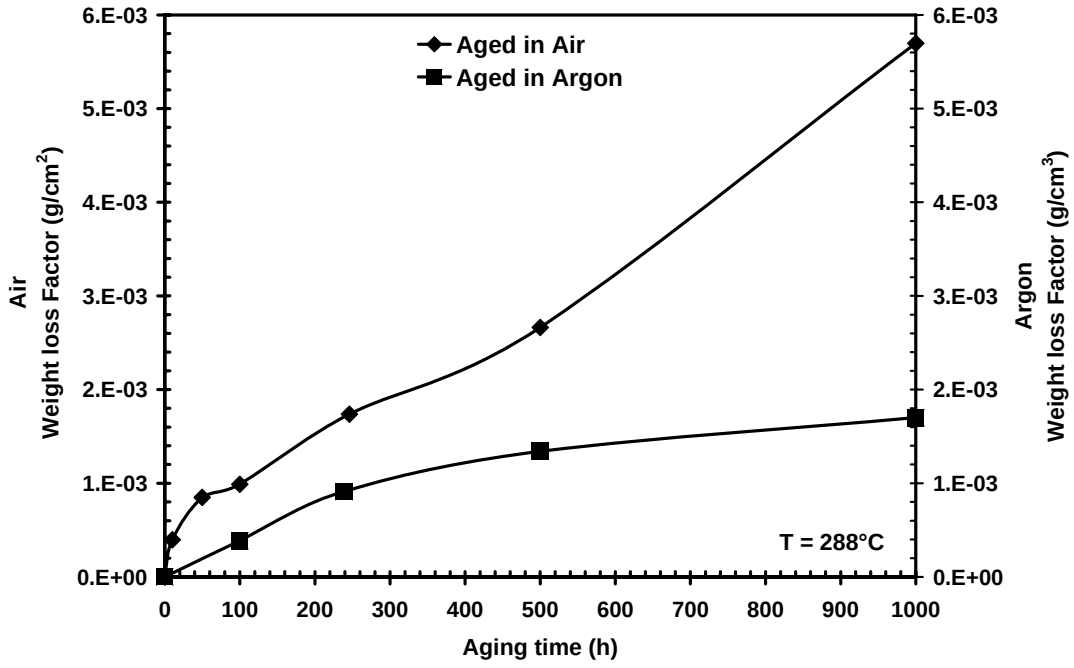

Figure 14 –Weight loss factor as a function of aging time for PMR-15 neat resin at 288°C in air and in argon.

Weight loss in air environment was normalized by the surface area of each sample while the weight loss in the argon environment was normalized by the volume of each sample. The values closely correlate with previously published weight loss measurements indicating that the aging setup in this study performed as expected [3,11,12,13,17]. Note the difference between the initial fast rate of weight loss and the later rate for aging in air. This behavior has been observed in other studies [12] and has been attributed to the combination of both the fast reaction of oxygen with the surface of the sample before the oxygen must diffuse into the sample to react further and the immediate release of low molecular weight particles from the sample. Studies of long-term aging have shown that

in air the steady state weight loss seen at times >1000 hrs continues beyond the period of time examined in this study. The weight loss in the presence of oxygen is attributed to the release of low molecular weight particles by the reaction of oxygen with the polymer chains [12]. In the argon environment a similar trend, but of a smaller magnitude, of weight loss was observed. In previous studies [3] the weight loss has been attributed to the loss of low molecular weight particles as the polymer is degraded by the temperature over time. A direct comparison of the weight loss in the air and in argon environments can also be accomplished since all samples were of very similar size and geometry.

Figure 15 shows percent weight loss for both air and argon environments as a function of aging time.

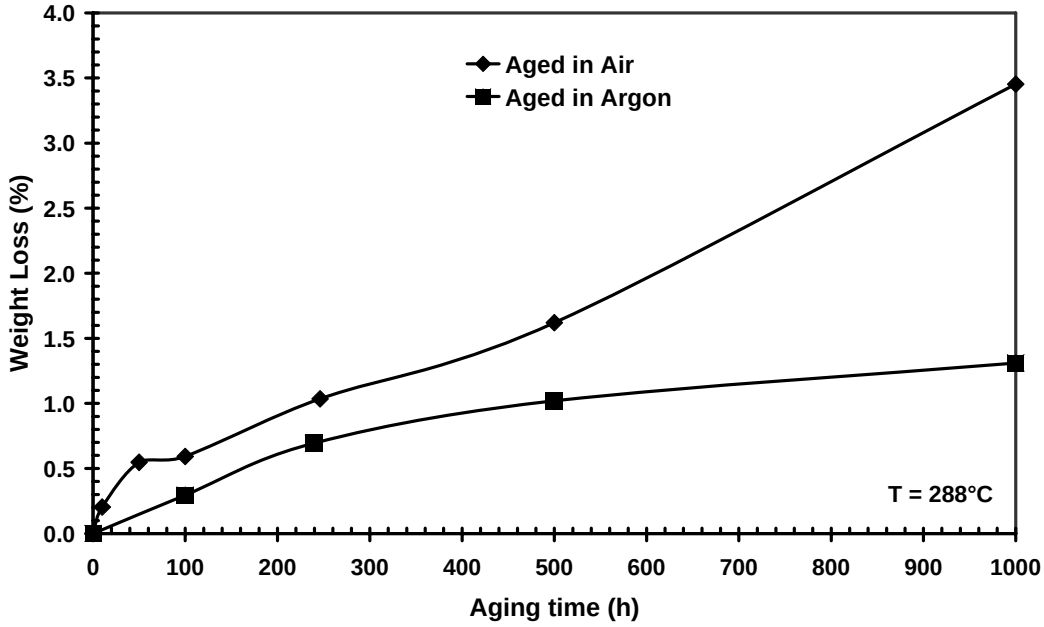

Figure 15 –Percent weight loss as a function of aging time for PMR-15 neat resin aged in air or in argon at 288°C.

It is seen in

Figure 15 that the weight loss in air exceeds that in argon. The visual inspection of the weighed samples revealed no changes in the outer appearance of the samples. A section was cut from each sample to view the formation of oxidation layer or any other micro structural changes. Results are discussed in the next section.

Oxidative Layer Thickness

Samples aged in air develop a layer of oxidized polymer on the surface. A cross sectional cut was taken from each of the rectangular aged samples using a diamond saw. The cut surface was mounted, polished, and observed under optical microscope. The cross sectional cut was taken at least 5 millimeters from the end of the sample to

eliminate any edge effects. The sample was mounted in room temperature curing epoxy puck and ground first with 600 grit paper and then polished with 0.03 micron silica slurry. No etchant was applied. An effort was made to minimize the amount of grinding and polishing in an attempt to maintain the integrity of the relatively soft sample edges. For this reason the micrographs taken show many rough scratches left from the first stage of grinding. Despite the scratched appearance it was decided that further grinding and polishing could impact the vulnerable oxidized edges and could lead to incorrect measurement of the actual oxidation layer. The polished surface was observed under a Nikon EPIPHOT digital microscope because the stereo microscope used for general sample observation was not able capable of illuminating the oxidation layer. A microscope capable of bright field viewing where the light is directed to the sample through the lens was needed.

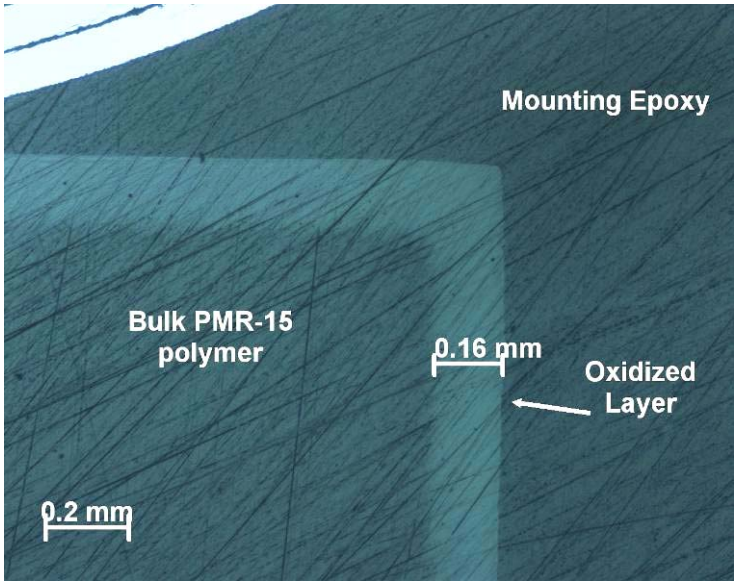

Figure 16 –Optical micrograph showing the oxidation layer on outer surface of PMR-15 neat resin sample aged for 1000 h at 288°C in air.

Figure 16 presents a micrograph of cross sectional cut of a sample aged for 1000 h at 288°C in air. A significant layer of oxidized PMR-15 resin on the outer surfaces is clearly visible. All micrographs were taken at the magnification of 50X, and a calibration using a traceable calibrated microslide was carried out for measurements. In contrast, a micrograph of a sample aged for 1000 h in argon at 288°C, Figure 17, shows no presence of an oxidation layer.

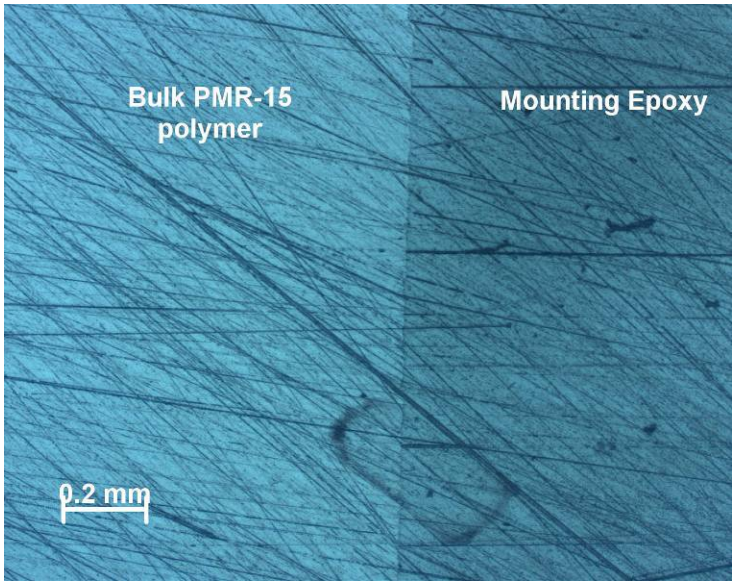

Figure 17 –Optical micrograph showing the absence of an oxidation layer on the outer surface of PMR-15 neat resin sample aged for 1000 h at 288°C in argon.

Micrograph in Figure 17 also confirms that the argon aging setup performed as planned; the oxidation effect at high temperatures appears to be completely eliminated. Note that in the case of samples that fractured during creep testing, the oxidation layer could be observed without mounting and polishing. Micrographs of the samples subjected to all aging conditions, are presented in Appendix D. The observed thickness of oxidation layer for these samples was also measured using the stereo microscope.

Figure 18 shows the fracture surface of a specimen aged in for 1000 h at 288°C in air that subsequently failed during creep testing.

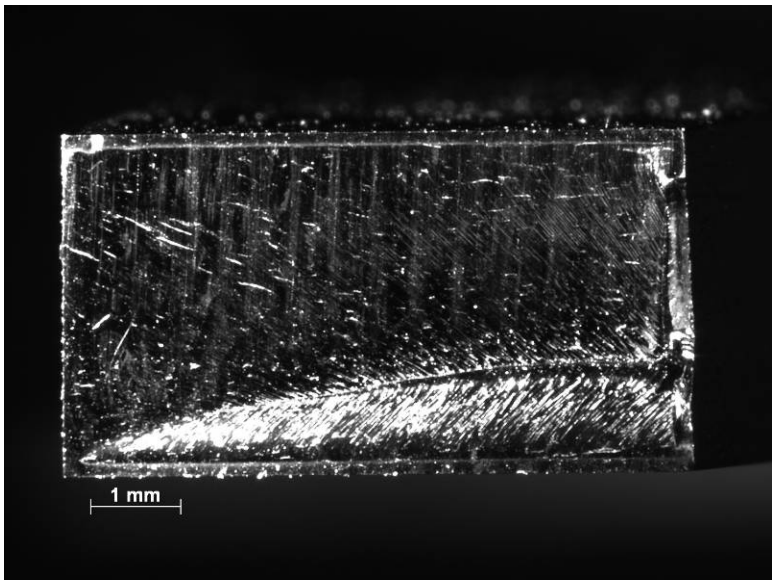

Figure 18 –Photograph showing the visible oxidation layer on the fracture surface of a PMR-15 neat resin sample aged for 1000 h at 288°C in air and tested in creep.

Figure 19 shows the measurement of the apparent thickness of the oxidation layer visible on the fracture surface of the sample in Figure 18. The apparent thickness of 0.16mm measured using the stereo optical microscope is the same as that measured using the digital optical microscope in micrograph of the sectioned sample in Figure 16.

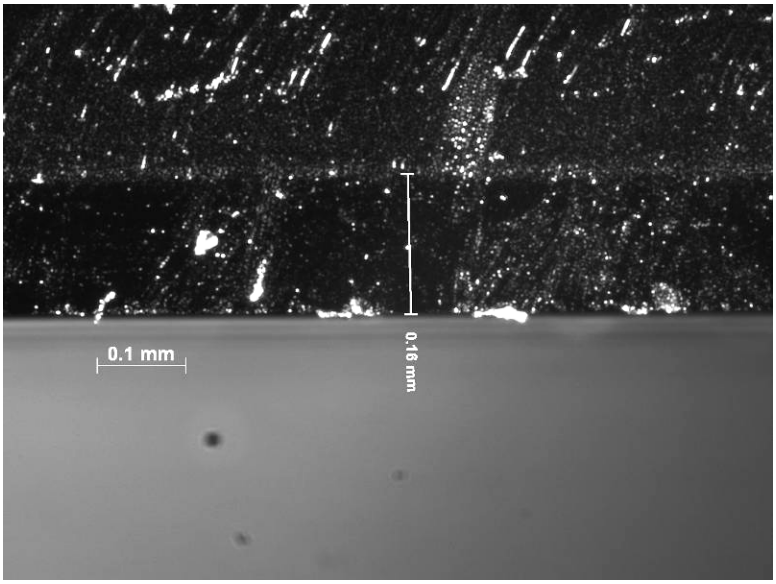

Figure 19 –Photograph showing the visible oxidation layer on the fracture surface of a PMR-15 neat resin sample aged for 1000 h at 288°C in air and tested in creep.

Micrographs of all fracture surfaces obtained in this study are presented in Appendix C. Figure 20 shows a plot of the measured oxidation layer thickness as a function of aging time in air at 288°C, measured on fracture surfaces and on sectioned samples using optical microscopy.

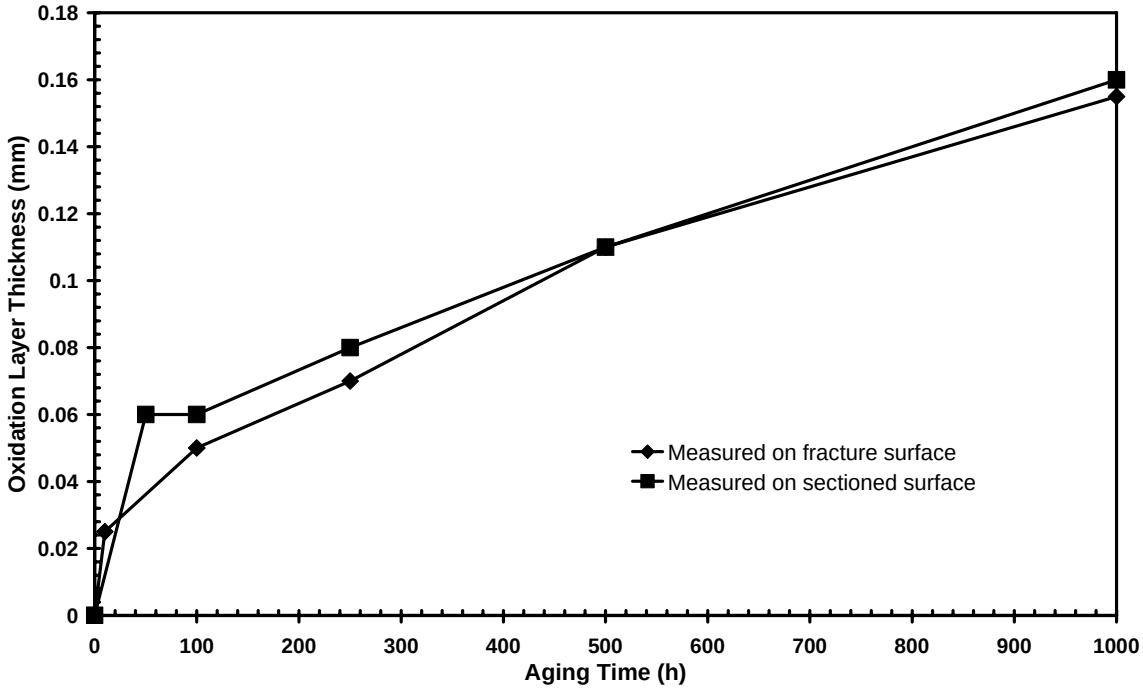

Figure 20 –Oxidation layer thickness measured on both cross sectional cut and fracture surfaces as a function of aging time in air at 288°C for PMR-15 neat resin.

Previous studies by Bowles et. al. [3] also examined the growth of the oxidation layer and found that the oxidation layer stops growing at a thickness of ~0.17 mm even for aging times that significantly exceed those used in the current study. The data in Figure 20 is consistent with results obtained by Bowles [3]. It is also evident that examination of the available fracture surfaces revealed the same layer thickness as the examination of mounted and polished samples that were not subjected to any mechanical loading.

Elastic Modulus

Initial Room Temperature Modulus

The initial room temperature elastic modulus of each sample measured in order to asses the sample to sample and panel to panel variability. A statistical one way analysis of variance test (ANOVA) of the initial room-temperature elastic modulus values was accomplished to determine if there were significant differences between panels or specimens. The analysis showed that with a confidence of 95% there was no statistical difference between any of the panels. The covariance of the elastic modulus for the entire population was 6 percent. Figure 21 shows the output of the statistical program, MiniTab, used to analyze the initial room temperature elastic modulus with 95% confidence intervals for each panel.

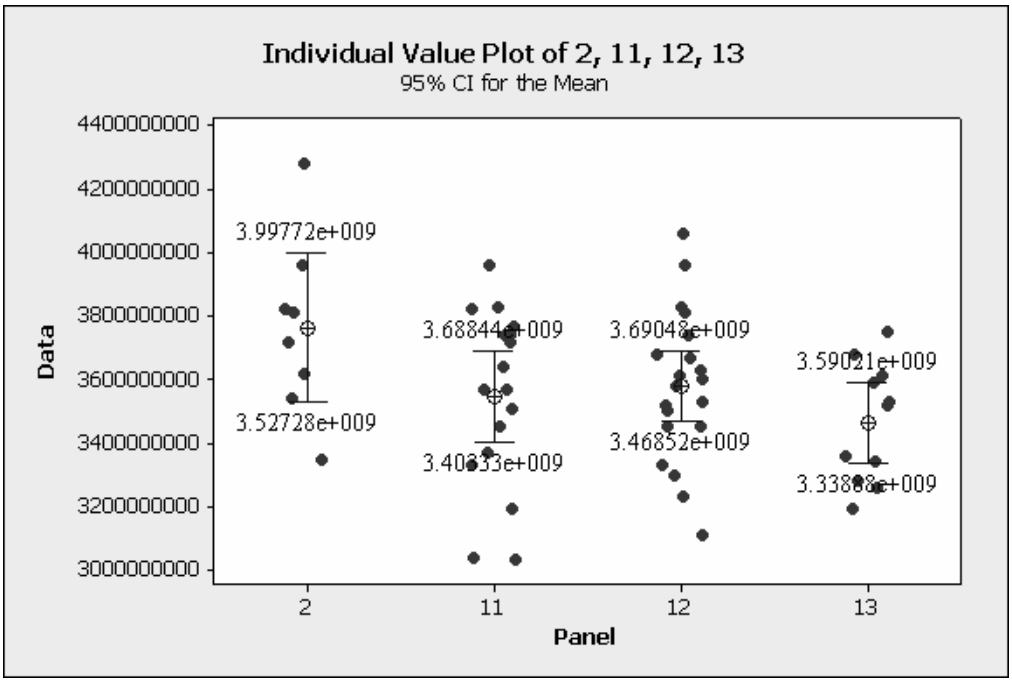

Figure 21 – Initial room temperature elastic modulus data as a function of origin panel number, with 95% confidence intervals for each panel. Figure produced using MiniTab program.

Figure 21 shows that within each panel there was some scatter between samples. However, it was decided that no single sample should be eliminated at this stage based solely on this room temperature elastic modulus measurement. The average room temperature elastic modulus of the entire population of samples was 3.57 GPa.

Identification of Outlier Samples

The elastic modulus at elevated temperature was calculated during loading and unloading after each of the creep tests. It was immediately apparent that although the initial room-temperature elastic modulus values showed limited scatter several samples exhibited anomalies in their mechanical behavior during creep and recovery tests. Their

elastic modulus measured during loading and unloading for several samples did not follow the general trend. Further examination the samples revealed considerable surface defects in these specimens. It was determined that all outlier samples were cut using water jet machining. Figure 22 shows a picture of the machined surface of a sample cut using water jet machining after testing. The dark line in the center of the photograph is the fracture line.

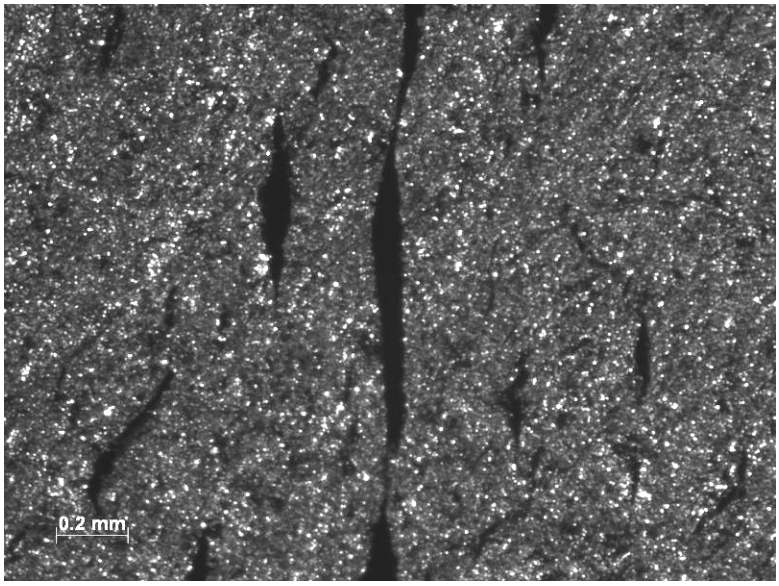

Figure 22 –Sample 12-18 (water jet machined), showing the presence of significant surface micro cracking on the machined surface of the gauge section. PMR-15 neat resin aged for 100 h in air at 288°C.

Sample 12-18 was aged in air for 100 h and subjected to a 20 MPa creep test where it fractured prematurely. Figure 22 reveals extensive micro cracking on the machined surface of the sample, which was seen to correlate with erratic modulus values and creep behavior of the sample and in this case caused creep rupture after only 1.5 h and creep strain accumulation of 8%. Sample 02-04, which was machined using

diamond saw and was tested under the same conditions survived 25 h at 20 MPa and produced creep strain accumulation of 7%. The elastic modulus measured during load-up to creep stress level for specimen 12-18 was 1.73 GPa compared to the modulus of 1.91GPa for specimen 02-04. When samples aged in air were subjected to creep at 20 MPa, water jet machined samples invariably exhibited lower modulus during load-up and accumulated significantly higher creep strains compared to samples machined with diamond saw. In some cases water jet machined samples fractured prematurely during creep. An effect of machining methods was not revealed when comparing the room temperature elastic modulus values from samples of the two types of machining. Detrimental effects of water jet machining were observed only when samples were tested at high temperature after aging. Optical examination of the post test machined surface of the water jet machined samples aged in air and tested at the creep stress of 20 MPa almost always revealed an extensive network of surface micro cracks in the gauge section. In contrast to the specimen machined surface exhibiting extensive microcracking shown in Figure 22, Figure 23 displays a micrograph of sample 02-04 after testing. Note that the machined surface of sample 02-04 machined by diamond grinding exhibits no defects or cracks.

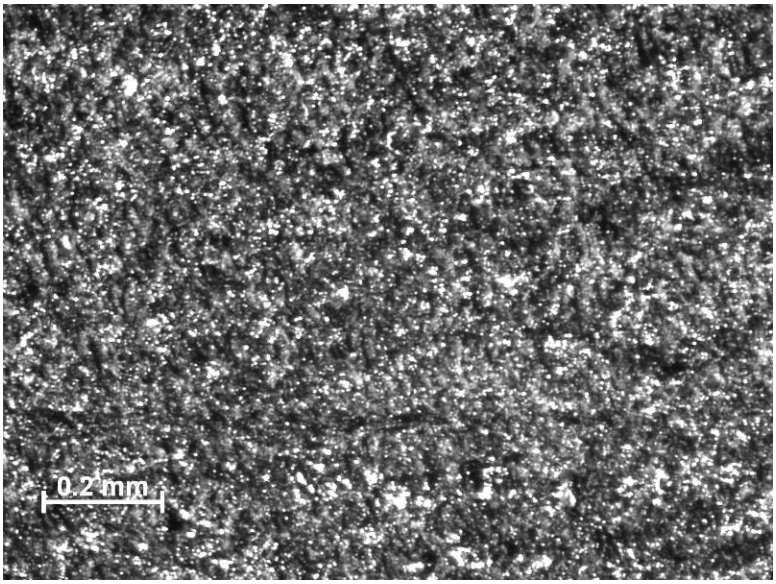

Figure 23 – Micrograph of sample 02-04 (diamond saw machined), demonstrating the substantial difference between the machined surfaces of diamond saw and water jet machined samples of PMR-15 neat resin aged for 100 h in air at 288°C.

The micrographs of the samples machined with a water jet reveal extensive micro cracking on the machined surface of the gauge section. It is therefore believed that the existing micro cracks grew and caused early failure at higher creep stress levels. Water jet machined samples aged in argon also exhibited surface cracking and failed prematurely when tested at 20 MPa indicating that early failure or anomalous creep and recovery behavior was indeed caused by surface microcracking and not by aging environment.

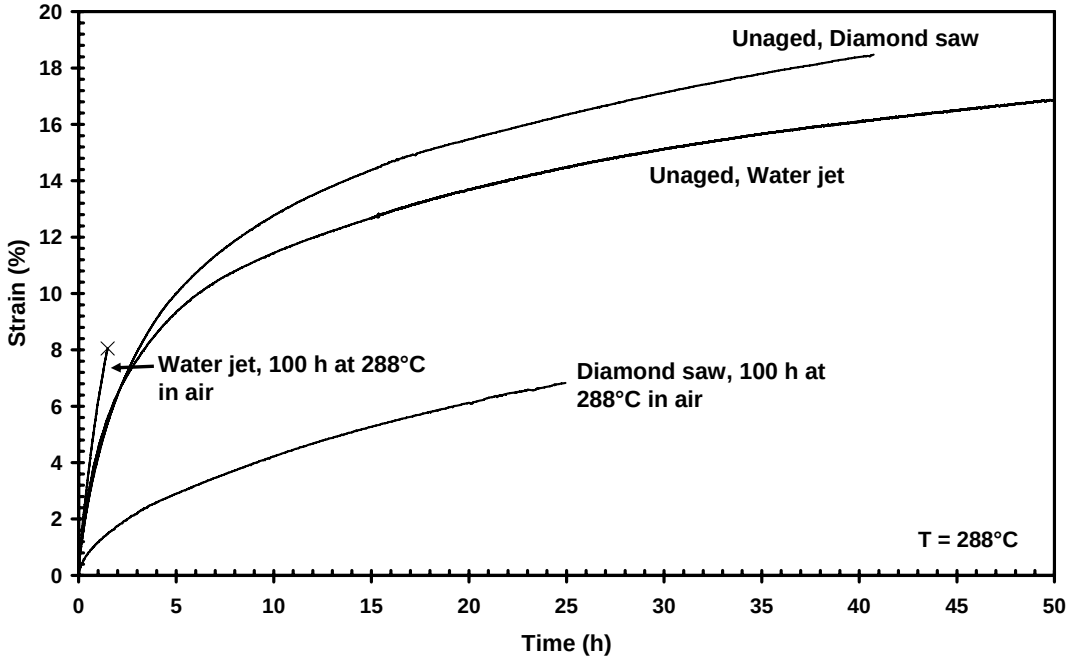

Figure 24 – Creep curves obtained for diamond saw and water jet machined samples. Results for the as-processed (unaged) material and material aged for 100 h in air at 288°C are shown.

Figure 24 reveals a dramatic difference in creep response of samples machined with different methods. It is also seen that the unaged samples are not sensitive to cutting methods. The creep curves produced by unaged samples are with in expected data scatter. Samples aged in argon and in air and tested at 10 MPa did not exhibit this severe sensitivity to the defects introduced by water jet machining. This can be attributed to much lower crack growth rates at lower creep stress levels.

Due to this unexpected sensitivity to the machining method only diamond ground samplers were tested at 20 MPa creep stress levels, thereby limited the number of samples available for testing at 20 MPa so that in many cases only one sample was available for a given aging condition. Note that all samples were photographed before

and after testing to help identify samples which were affected by micro cracking induced during machining. From this point forward all samples were screened for micro cracking and data from any identified "bad" samples were omitted from the report. Furthermore, samples that showed obvious evidence of point defects and fractures outside of the gauge section were also omitted from the reported data. A complete set of before and after photographs of samples is presented in Appendices A and B.

Aged Modulus versus Initial Modulus

The elastic modulus obtained at elevated temperature during loading and unloading portions of each creep and recovery test was recorded to evaluate the effects of aging. The loading rate magnitude of 1 MPa/s was used in all tests. The modulus was calculated from the stress portion of the curve between 0 and 3 MPa, i.e. the most linear region of the curve. No correlation was observed between the room temperature initial elastic modulus values and loading or unloading elastic modulus values produced at elevated temperature regardless of the aging environment. Figure 25 shows a plot of aged loading and unloading moduli of aged samples measured at 288°C versus the initial room-temperature moduli.

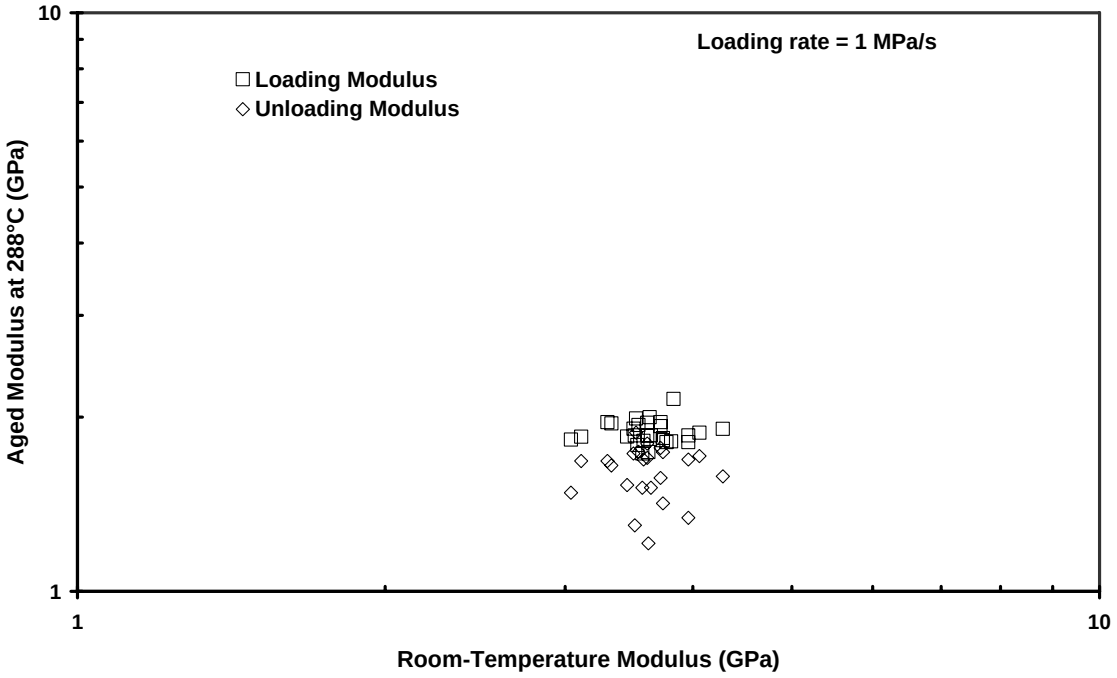

Figure 25 –Elastic modulus of aged samples measured at 288°C versus initial room temperature elastic modulus for PMR-15 neat resin.

It is apparent that the elastic modulus observed during unloading is typically lower than the elastic modulus observed during loading regardless of the sample's initial room temperature modulus. This could be attributed to the accumulation of damage during the mechanical testing.

Elastic Modulus upon Loading and Unloading

Qualitatively all samples produced similar stress strain curves upon both loading and unloading. A very limited linear region is seen for stresses below 3 MPa. Figure 26 presents the tensile stress-strain curves obtained during loading at 288° C for samples aged in air and in argon.

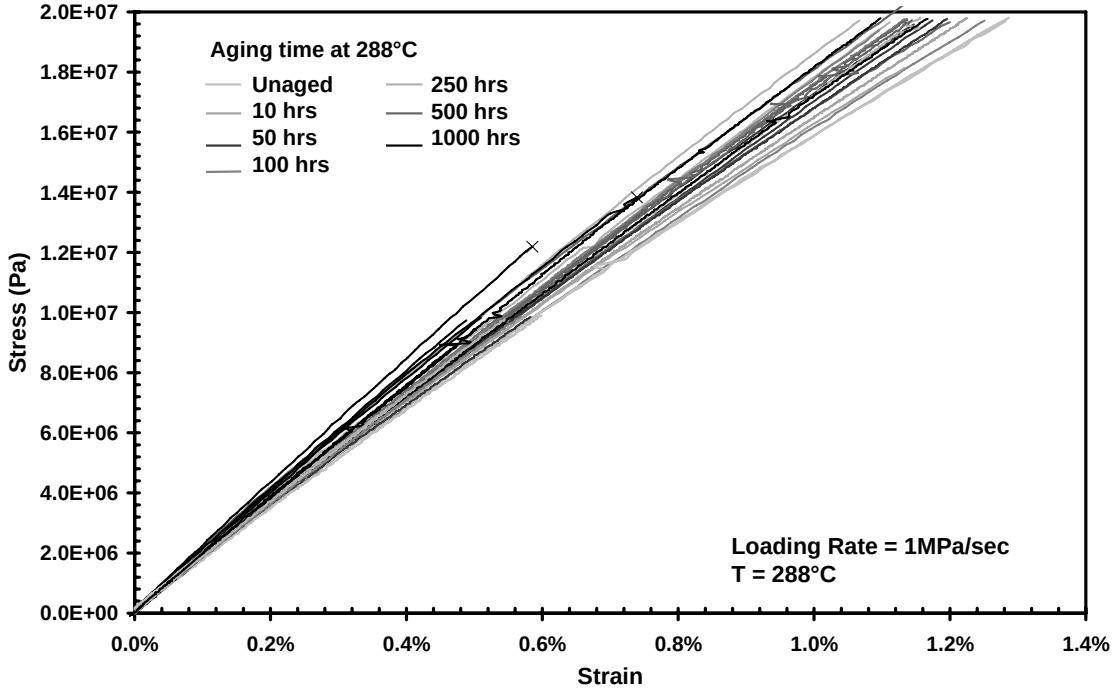

Figure 26 – Tensile stress-strain curves during loading obtained in all tests at 288°C showing qualitatively similar stress-strain behavior. An X indicates a sample fracture.

It was observed that increased aging time in either air or in argon environment caused increases in both the loading and the unloading elastic moduli. Figure 27 shows the loading elastic modulus as a function of aging time in air and in argon. The general trend of modulus increasing with aging time is apparent. The individual data points are shown together with the trending line drawn through the average values.

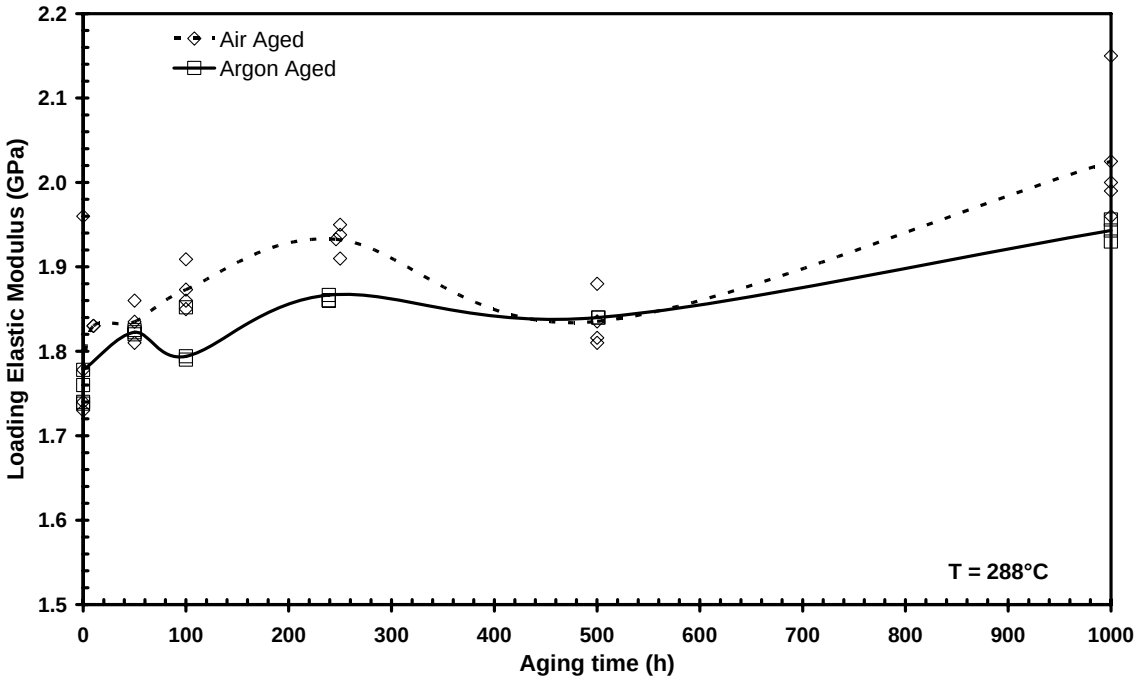

Figure 27 – Elastic modulus upon loading versus aging time in air and in argon at 288°C for PMR-15 neat resin.

The general increase in modulus seen in samples aged in both the air and argon environments suggested that the bulk of the material is stiffening and that the overall sample modulus is independent of the presence of an oxidation layer, for prior aging times ≤1000 h. Both the air and argon aged samples show a steady increase in loading elastic modulus for prior aging times ≤1000 h.

Figure 28 shows the elastic modulus measurements upon unloading as a function of aging time in air and in argon environments. Because unloading modulus may be influenced by prior creep as well, results have been broken down by aging environment and creep stress. While a limited number of samples were tested in creep for 50 h most samples were subjected to 25 h of creep. The data in Figure 28 reveals that specimens

subjected too 50 h of creep produced lower modulus values upon unloading (open symbols in Figure 28) compared to the specimens subjected to 25 h of creep (solid symbols in Figure 28). This indicates that progressive damage is occurring during the creep period.

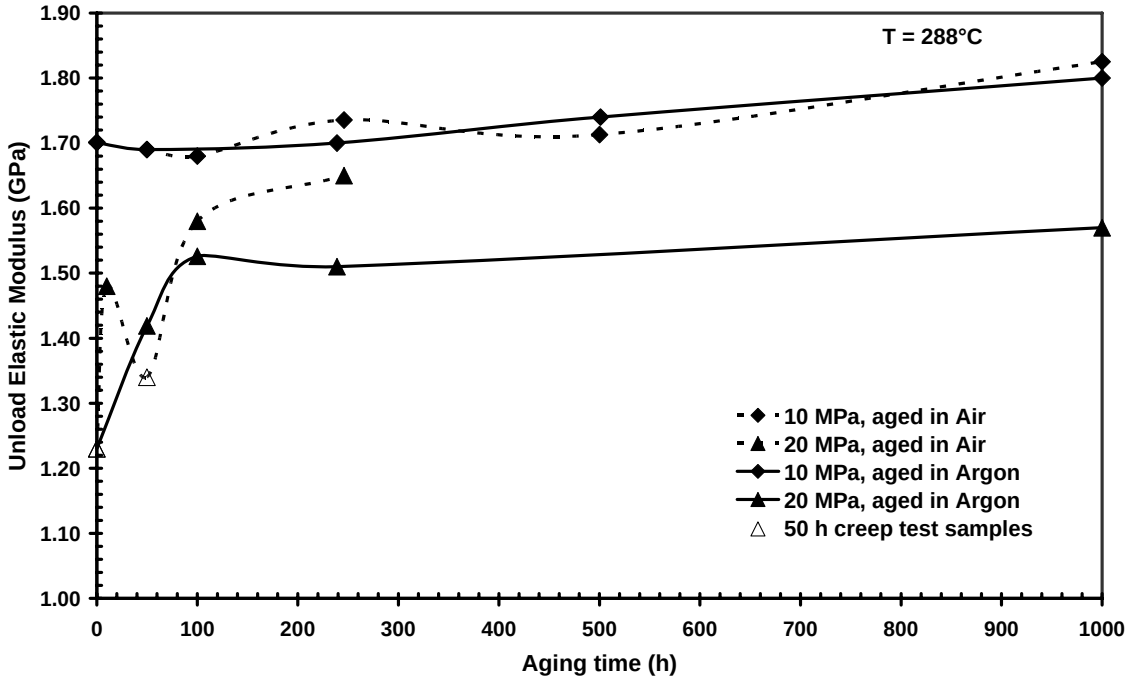

Figure 28 –Elastic modulus obtained upon unloading versus aging time in argon and in air at various creep stress levels. PMR-15 neat resin specimens tested at 288°C.

Elastic Modulus Ratios

The ratios of elastic moduli measured before, during, and after testing are of interest and can help identify any dynamic material changes due to aging and mechanical loading. The ratio of the room temperature elastic modulus (initial modulus, E_O) to the elastic modulus measured upon loading (loading modulus, E_L) at 288°C after aging shows effects of both increased temperature and aging time on the elastic response. A

ratio of the elastic modulus upon unloading (unloading modulus, E_U) to E_L would indicate damage developing in the material during the creep period. A ratio of E_U to E_O may reveal material changes resulting from the entire aging and testing process. Figure 29 shows these three modulus ratios versus aging time for samples tested at the creep stress of 20 MPa and aged in argon at 288°C.

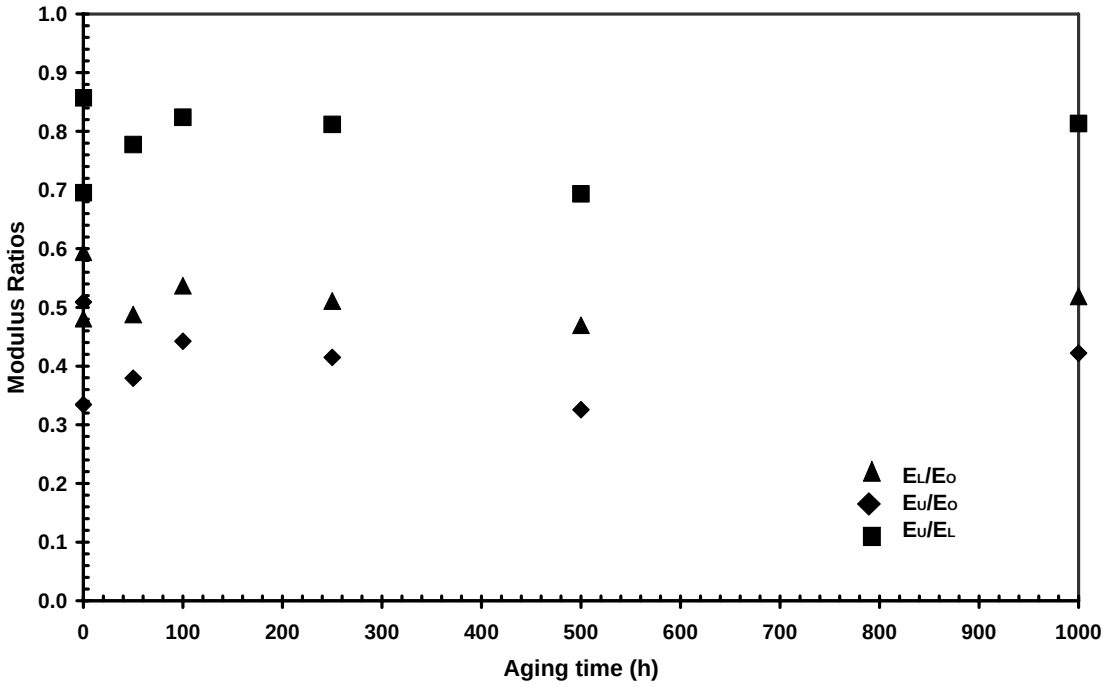

Figure 29 – Elastic modulus ratios versus aging time in argon for PMR-15 neat resin specimens aged at 288°C and tested n creep at 20 MPa at 288°C.

Figure 29 shows that the elastic modulus ratios varied little with aging time. This was also the case for the samples aged in air.

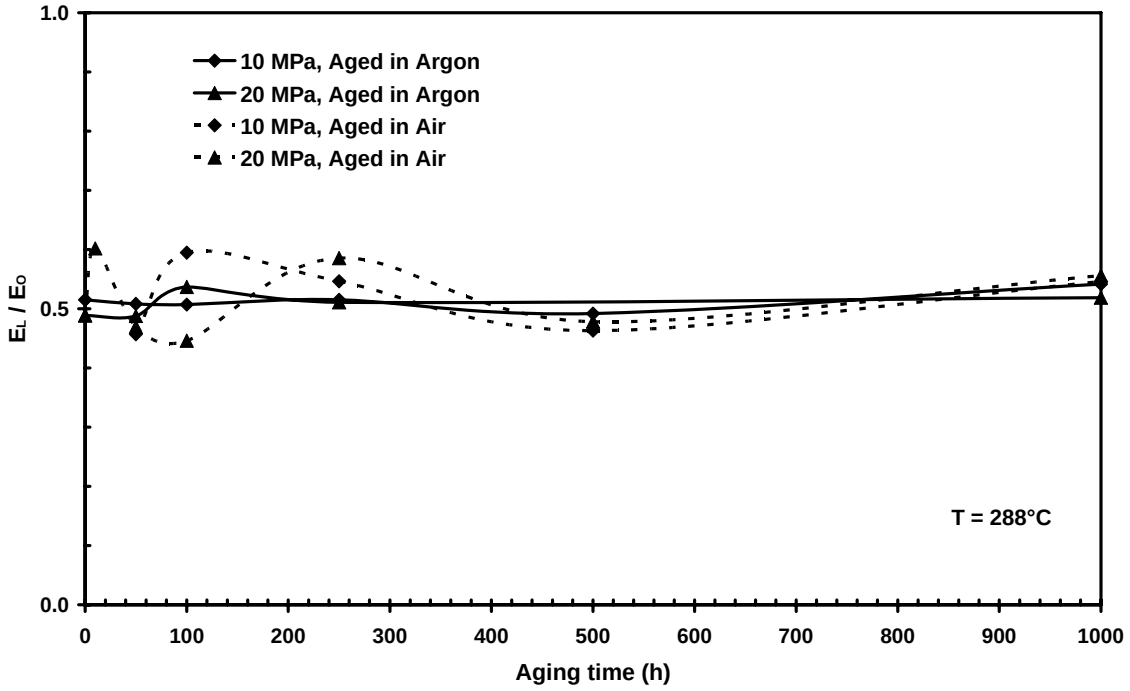

Figure 30 – Ratio of elastic modulus measured upon loading to the initial room-temperature elastic modulus as a function of aging time for various aging environments for PMR-15 neat resin specimens tested in creep at 10 and 20 MPa.

Figure 30 shows ratio of the elastic modulus upon loading to the initial room-temperature elastic modulus, E_L/E_O, as a function of aging time, representing the effect of temperature increase and aging time. The E_L/E_O remains nearly constant at 0.5 (a 50% drop in modulus) for all aging times and environments. This suggests that the aging environment and time have considerably less influence on modulus than the increase in temperature from 23 to 288°C. Figure 31 shows the E_U/E_L ratio as a function of aging time for both aging environments.

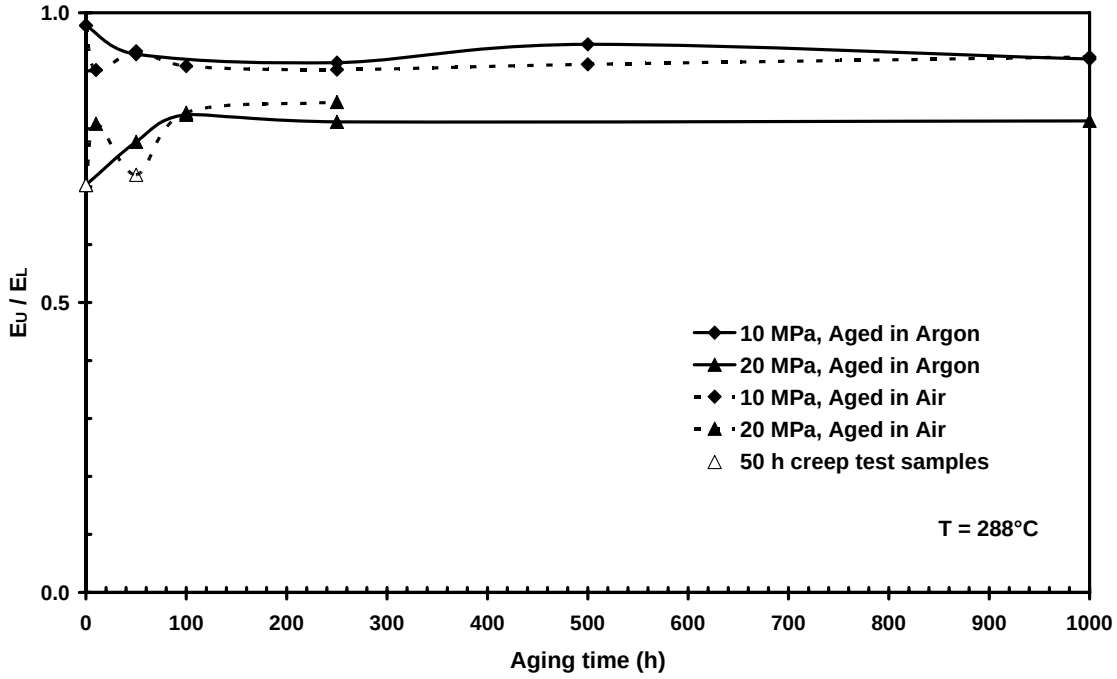

Figure 31 – Ratio of elastic modulus measured upon unloading to the elastic modulus measured upon loading as a function of aging time for various aging environments for PMR-15 neat resin specimens tested in creep at 10 and 20 MPa.

It is seen in Figure 31 that the E_U/E_L ratio is strongly dependent on the creep stress level. The modulus reduction due to damage developed in creep test is not a function of aging time or environment. The samples tested at creep stress of 20 MPa exhibit a 20% reduction in modulus while the samples tested at 10MPa show only a 10% reduction. It is important to note that all samples aged for 250 h or longer failed during the creep period. For those samples unloading to zero stress did not take place and E_U could not be measured.

Results in Figure 31 also indicate that the duration of creep tests have a profound effect on the unloading modulus E_U. Note that the E_U/E_L ratio obtained for an as-

processed specimen and a specimen aged in air for 50 h and subjected to 50 h creep period at 20 MPa (open triangle symbols in Figure 31) is noticeably lower than the E_U/E_L ratios obtained for samples with nearly the same aging history. This result suggests that damage continues to accumulate as the creep test progresses beyond 25 h.

Finally, the E_U/E_O ratio is plotted as a function of aging time for both environments in Figure 32. The E_U/E_O ratio shows the greatest amount of modulus degradation and accounts for modulus changes due to elevated test temperatures, prior aging and creep loading.

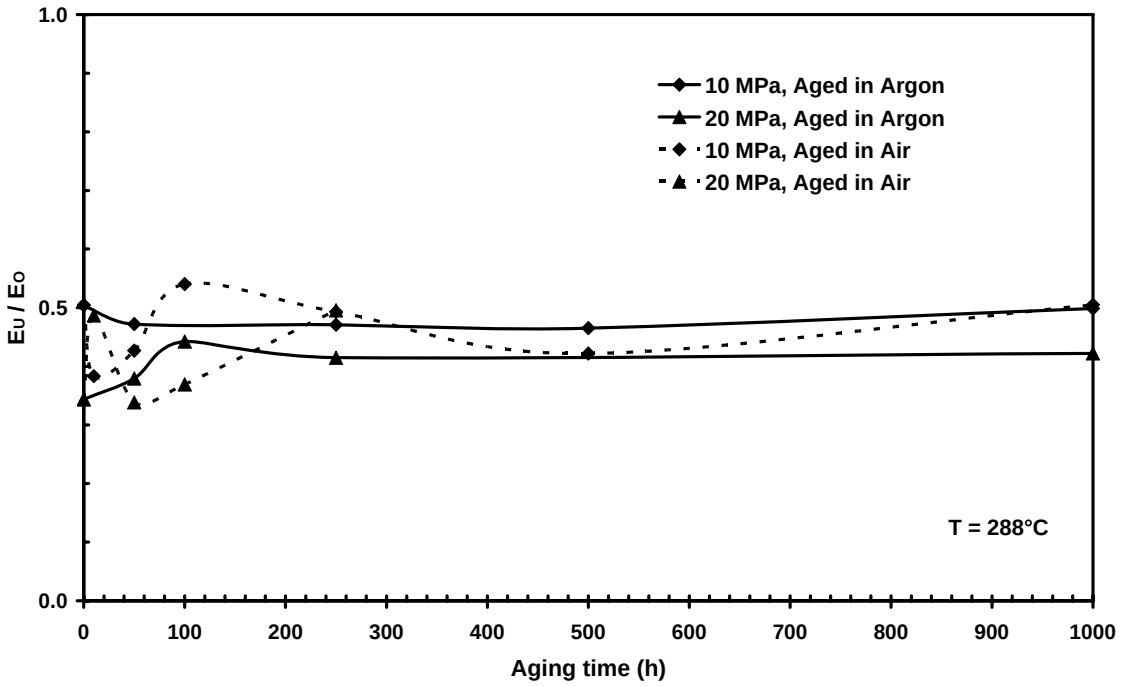

Figure 32 – Ratio of elastic modulus measured upon unloading to the initial room-temperature elastic modulus as a function of aging time for various aging environments for PMR-15 neat resin specimens tested in creep at 10 and 20 MPa.

Modulus loss due to testing at elevated temperature, prior aging and creep damage was limited to 60% in all tests. It may be convenient to view the E_U/E_O ratio as the sum of the E_L/E_O and E_U/E_L ratios for each sample. Examination of the modulus ratios may be more suitable for evaluating the degree of thermal or oxidative degradation of the polymer than the actual modulus values as plotted in Figure 27 and Figure 28. The modulus ratios, in a way, normalize the data for each sample and may be used to separate changes in mechanical behavior due to aging, from those due to elevated temperature, or loading history. Furthermore, changes in mechanical response can be interpreted using traditional structure property relationships for highly networked polymers as chemical or physical aging of the polymer system. The structure of the polymer is actively changing due to prior aging and mechanical loading. DMA testing will attempt to quantify these changes. So far the results reveal that elastic modulus is strongly influenced by test temperature and, in the case of specimens subjected to prior creep, by creep stress level and duration of creep period.

Creep Tests

Thermal Strains, and Strains During Loading and Unloading

In this study specimens were subjected to creep and recovery tests at 288°C. The thermal strains during heating of the sample to test temperature, the strains incurred during loading to creep stress level, and the strains incurred during unloading to zero stress after creep period were measured and recorded in each tests. Thermal strains (ε_T), strain produced during loading (ε_L) and strain produced during unloading (ε_U) are

presented as functions of aging time in Figure 33 for all creep stress levels and aging environments.

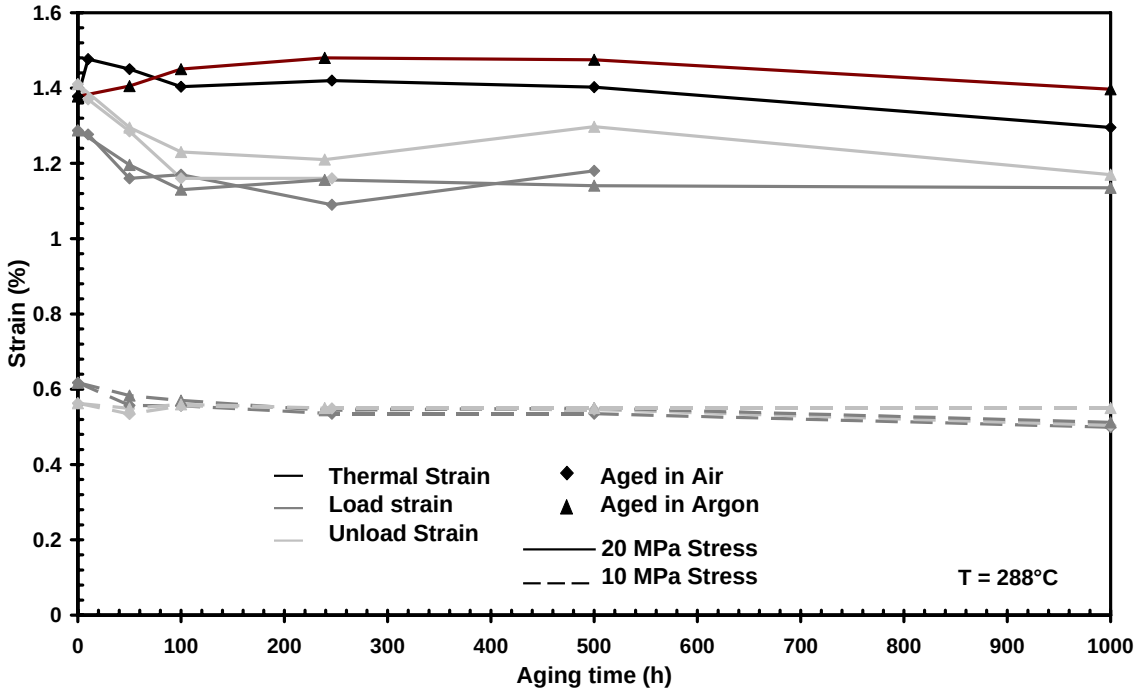

Figure 33 – Average thermal, loading and unloading strains versus aging time for PMR-15 neat resin specimens subjected to prior aging in air or in argon and creep at 10 or 20 MPa at 288°C.

Results in Figure 33 show that for a given applied stress level similar loading and unloading strain values were obtained for specimens with different prior aging histories. It is also seen in Figure 33 that for a given aging time, specimens aged in argon produced slightly higher thermal stains than the specimens aged in air. Bowels [14] published data showing that the oxidized layer on PMR-15 had a lower thermal coefficient of expansion than the unoxidized resin. This may account for the difference between the thermal strains produced by specimens aged in air and those aged in argon [14]. The growing

oxidation layer may not allow for the same amount of thermal expansion as was seen in the argon-aged (unoxidized) samples.

Creep Tests of Unaged Specimens

Creep tests at 10 and 20 MPa stress levels of at least 25 h duration were followed by unloading to a zero stress recovery period of at least 50 h duration, or two times the duration of the creep test. A small number of unaged samples were also tested at in creep tests at 15 MPa. Results are presented in a form of creep strain versus creep time curves. An X symbol at the end of a creep curve denotes specimen failure during the creep test.

The creep curves of unaged samples tested at 10, 15, and 20 MPa at 288°C are shown in Figure 34.

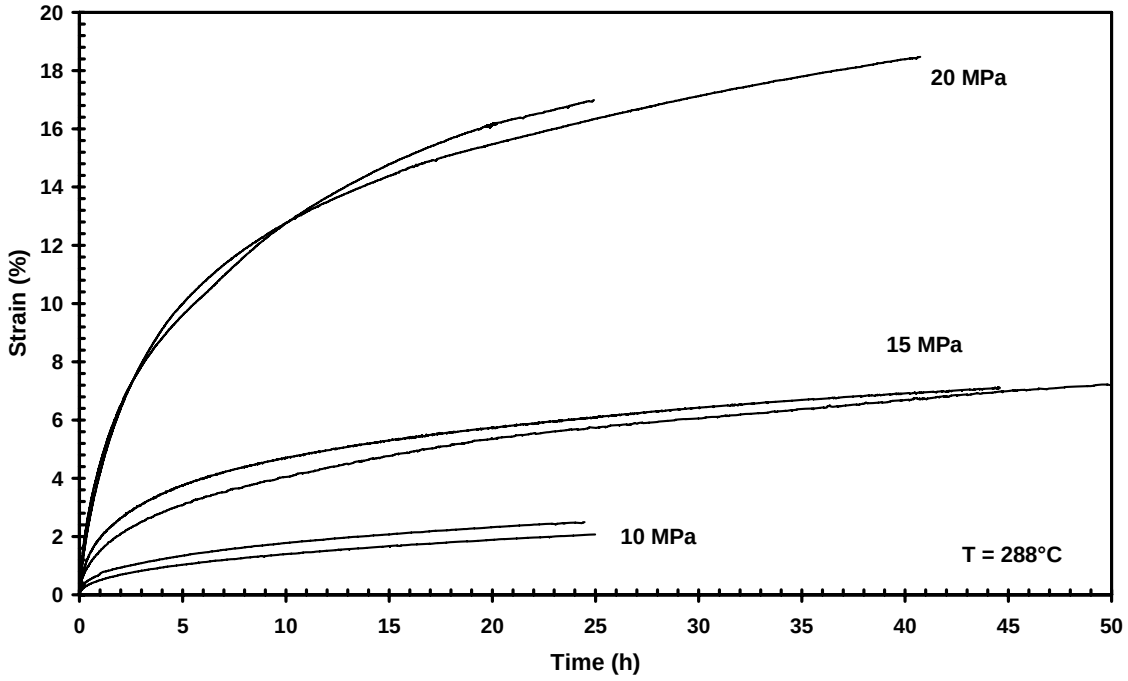

Figure 34 – Creep stress versus strain curves for the as-processed PMR-15 neat resin at 288°C. Primary and secondary creep regimes are present.

All creep curves in Figure 34 exhibit primary and secondary creep regimes. Primary creep transitions to secondary creep after ~5 h. Secondary creep persists for the remainder of the test. Note that in all tests shown in Figure 34 steady-state or secondary creep rates increase with creep stress level.

Creep Tests at 20 MPa

Test specimens aged in argon or air for up to 1000 h at 288°C subjected to creep and recovery tests. Creep stress level was 20 MPa, and duration of creep was at least 25 h, and duration of recovery at zero stress was at least 50 h or twice the creep period. As discussed earlier, the machining of the samples was a major factor in the creep response at this higher stress level. The majority of water jet machined samples tested in creep at 20 MPa either exhibited uncharacteristic strains or fractured prematurely during creep. In most of these cases, surface micro cracks were seen on the sample after testing. Because the majority of samples for this study were water jet cut, the number of diamond saw machined samples was severely limited, frequently only one sample could be tested per test condition. Therefore most conclusions of this research will be qualitative due to a lack of statistical information.

As discussed earlier, the unaged samples tested at 20 MPa creep stress level accumulated relatively large creep strains of ~16% after 25 h under load. It was found that specimens subjected to prior aging at 288°C in either argon or air atmospheres accumulated significantly lower creep strain. For example, specimens aged for 1000 h in argon as well as the specimen aged for 250 h in air produced creep strains $\leq 4\%$. Creep curves obtained for specimens with various aging histories are presented in Figure 35.

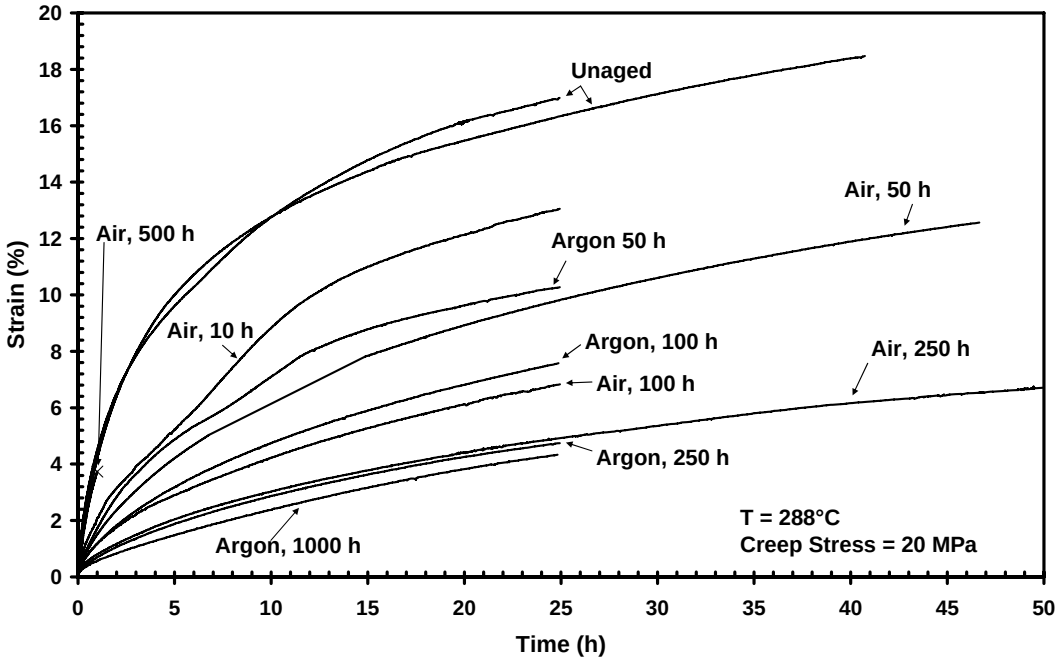

Figure 35 – Creep stress versus strain curves for PMR-15 neat resin aged in air or argon for various durations. Creep stress = 20 MPa, test temperature = 288°C. Decrease in creep strain accumulation with prior aging time is evident.

In the case of samples aged in argon, creep strain accumulation during 25 h decreased with increasing prior aging time. This trend becomes particularly pronounced as the prior aging time exceeds 50 h. Specimens aged for 1000 h in argon accumulated creep strain of only 4% after 25 h of creep, in contrast to the unaged sample which accumulated creep strain of 16% after 25 h of creep. Recall that prior aging in argon also caused an increase in elastic modulus. Consequently a "stiffer" aged sample produces lower creep strain. This "stiffening" of the polymer with aging time may be due to either physical or chemical aging affecting the network structure. In the case of specimens aged in air, a low 4% creep strain accumulation resulted after only 250 h of prior aging.

Samples aged in air for 500 h typically failed during the first 5 h of the creep test. A creep curve obtained for a sample aged for 500 h in air is shown in Figure 35 and marked with an X symbol where the sample failed during creep. While the samples aged for 500 h exhibited rapid strain accumulation compared to the samples aged for 250 h, the elastic modulus of the samples aged for 500 h was higher than that of the samples aged for 250 h. Samples aged for 1000 h consistently failed during loading of the sample, typically at the stress ~12 MPa. Samples aged for 1000 h produced the highest elastic modulus values. In previous sections it was shown that samples aged for either 500 or 1000 h exhibited significant oxidation layers. It is possible that these samples may have failed at a lower load due to a considerable reduction in load bearing area and/or early crack nucleation in a porous and brittle oxidation layer. It is also interesting to note that for the aging times of 250 h and less, aging environment had negligible effect on creep response.

Creep Tests at 10 MPa

Specimens that were aged at 288°C for up to 1000 h in air or argon were subjected to creep and recovery tests with a creep stress of 10 MPa. Duration of creep and recovery periods were at least 25 h and 50 h respectively. Unaged samples tested at 10 MPa produced creep strains of ~2% after 25 h of creep. Samples aged for 1000 h in air or argon produced creep stains of less than 1% in the same amount of creep time. Creep curves obtained at 10 MPa for samples aged at 288°C in air and argon environments for various amounts of time are presented in Figure 36.

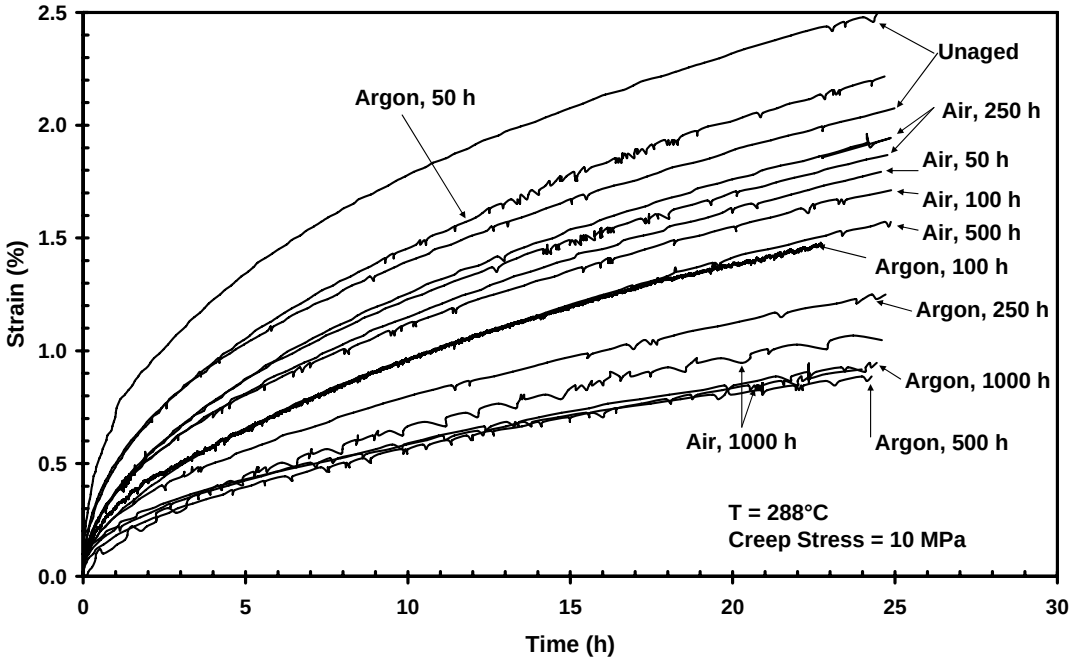

Figure 36 – Creep stress versus strain curves for PMR-15 neat resin aged in air or argon for various durations. Creep stress = 10 MPa, test temperature = 288°C. Decrease in creep strain accumulation with prior aging time is evident.

Results in Figure 36 reveal the same general trend in creep strain variation with prior aging time that was observed in the 20 MPa creep tests. Increasing aging time generally resulted in lower creep strain accumulation for a given amount of time. However, in this case the influence of aging time is less pronounced. All creep strains are lower and there is more overlapping of strain curves obtained for specimens with different aging conditions. Samples aged in air for 500 h or less could be considered relatively unchanged from the unaged condition. Samples aged for 1000 h in air; however, showed a 50% reduction in creep strain accumulated in 25 h. In the case of samples aged in argon, the trend is more distributed. There is a steady decrease in creep

strain with increasing prior aging time. It should be noted that none of the samples failed during creep tests at 10 MPa, regardless of machining method or prior aging conditions. It is seen that there is little to no difference in the behavior of samples aged in air and those aged in argon for a given time.

While examining the creep curves it may be beneficial to examine creep strain accumulation after 25 h of creep as a function of prior aging time. Figure 37 shows creep strain accumulation after 25 h versus aging time for all samples.

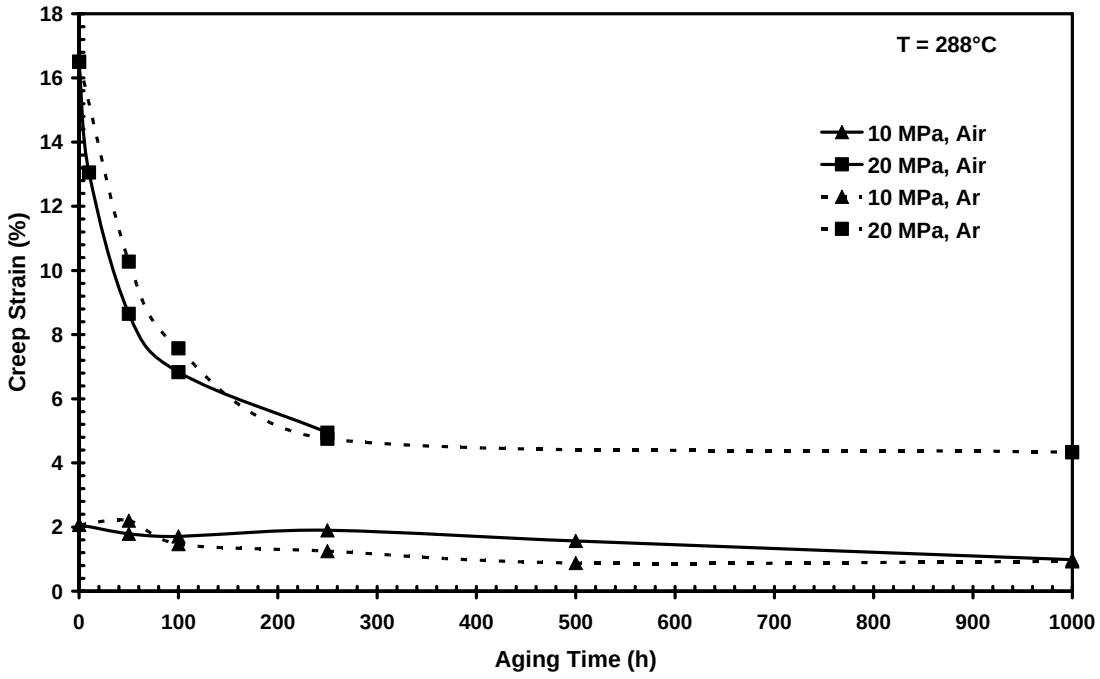

Figure 37 – Creep strain accumulated in 25 h as a function of aging time for PMR-15 neat resin. Creep strain accumulation decreases with increasing prior aging time.

Figure 37 clearly illustrates the inverse relationship between prior aging time and creep strain accumulation as well as similarity in creep response of the samples aged in different environments.

Recovery at Zero Stress after 20 MPa Creep Test

The recovery behavior of a polymer can reveal information as to the condition of the structure of the polymer in relation to the recovery mechanism for the particular material. In this case, for highly crosslinked polymer networks, the recovery mechanism would be a relaxing of strained polymer crosslinks. The amount of creep strain recovered may give clues as to the amount of permanent damage that was accumulated during the creep process and the extent of any chemical damage also caused by creep and/or in this case exposure to temperature or environment.

Samples tested in creep at 20 MPa stress level were held at the creep stress for at least 25 h and then recovered at zero stress for at least 50 h. It is seen in Figure 38 that during the initial stages of the recovery period strain decreases rapidly, then stabilizes and remains nearly constant until the end of the recovery period. This indicates that the recovery process achieved saturation during the allotted 50 h. Extending the recovery period to 160 h did not result in further appreciable decrease in strain. Previous work [16] has shown that full recovery for PMR-15 neat resin was observed only after extremely short duration creep tests, 5 h, followed by long recovery periods of 16 h in duration [16].

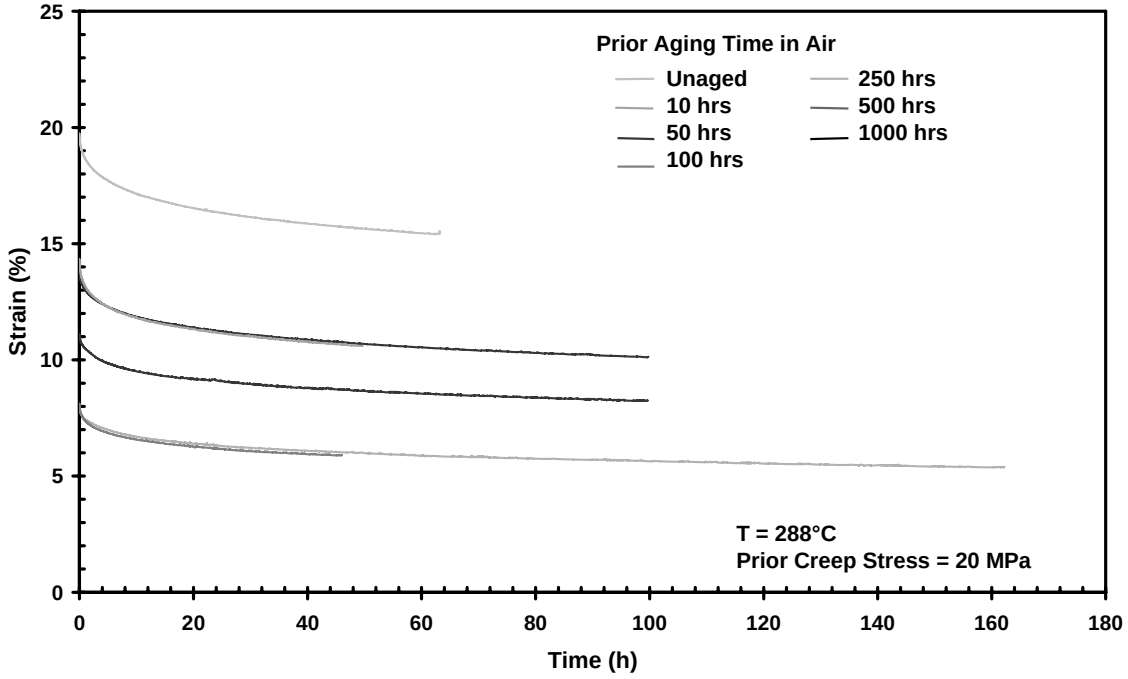

Figure 38 – Recovery curves for PMR-15 neat resin aged in air at 288°C. Prior creep stress = 20 MPa, test temperature = 288°C.

Results in Figure 38 demonstrate that comparing the recovery curves to each other is difficult since their placement depends on the creep strain accumulated prior to recovery.

For the purposes of examining the amount of creep strain recovered it is instructive to examine the recovered strain defined $\varepsilon^r = \varepsilon' - \varepsilon^*$, where ε' and ε^* are the strain after the beginning of the recovery period and at some time t during the recovery period, respectively. Strains ε^r, ε' and ε^* are schematically depicted in Figure 39.

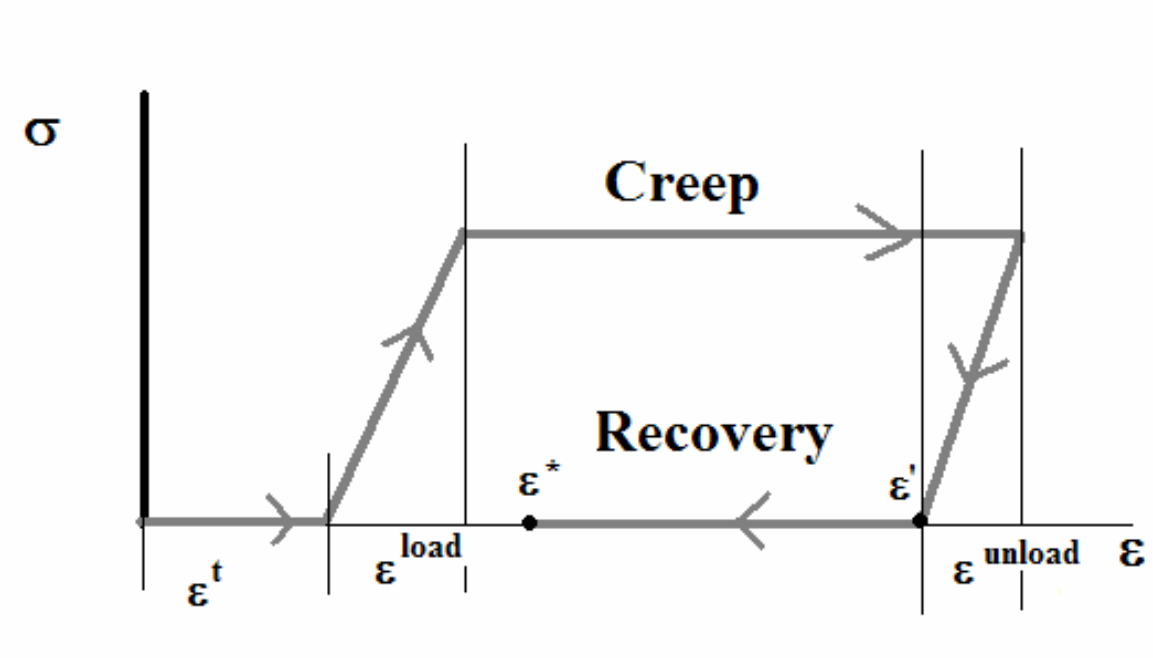

Figure 39 – Schematic stress-strain curve for a constant stress creep period followed by recovery period at zero stress.

The recovered strain as a function of time is shown in Figure 40 for samples tested at the 20 MPa creep stress level and in Figure 41 for samples tested at the creep stress of 10 MPa.

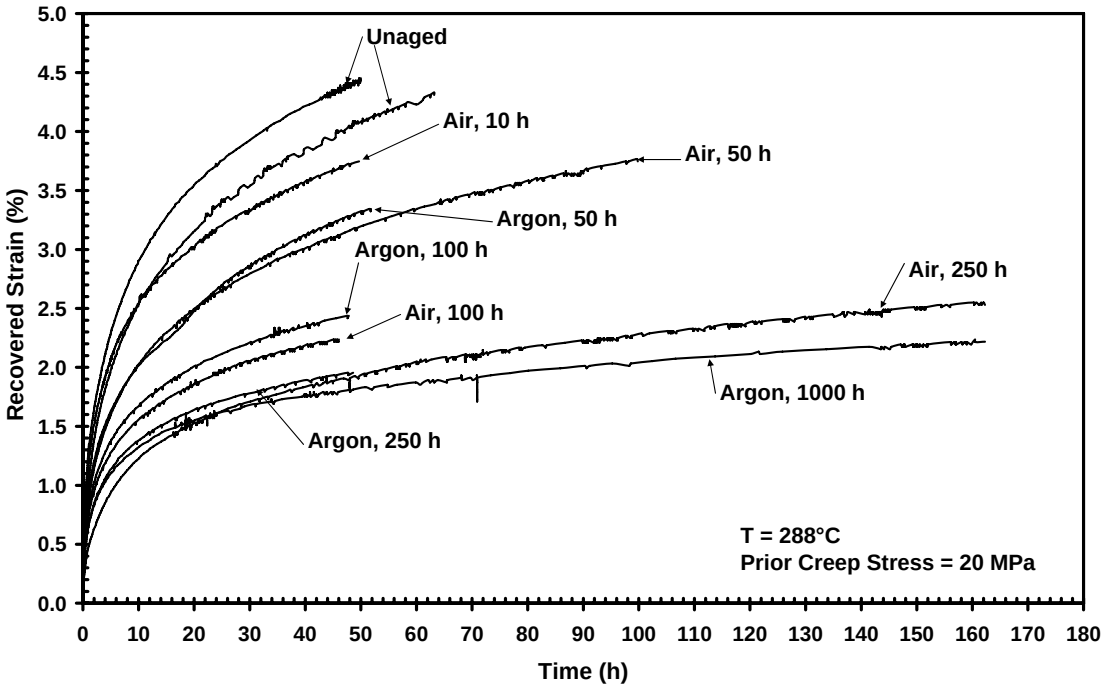

Figure 40 – Recovered strain versus time curves for PMR-15 neat resin aged at 288°C. Creep stress = 20 MPa, test temperature = 288°C. Recovered strain decreases with increasing prior aging time in air or argon.

It is seen in Figure 40 and Figure 41 that recovered strain decreases with increasing prior aging time in air or argon environments at 288°C.

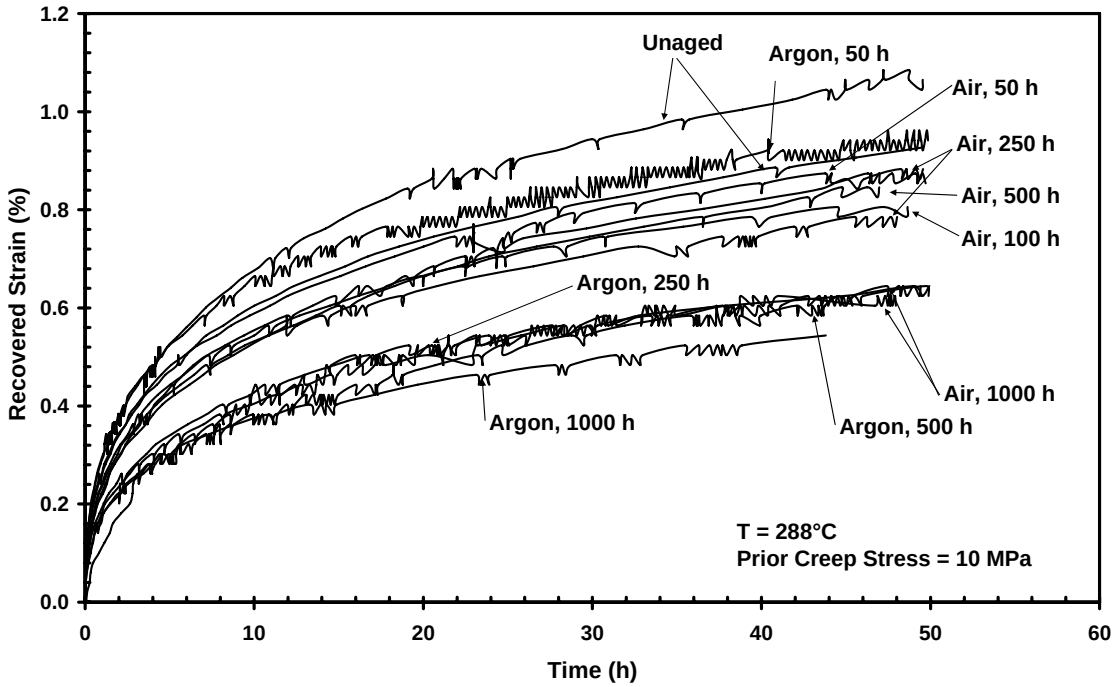

Figure 41 – Recovered strain versus time curves for PMR-15 neat resin aged at 288°C. Creep stress = 10 MPa, test temperature = 288°C. Recovered strain decreases with increasing prior aging time in air or argon.

Strain recovered after 50 h at zero stress is plotted versus prior aging time in Figure 42. It is seen that the amount of strain recovered during a given time at zero stress decreases with increases prior aging time.

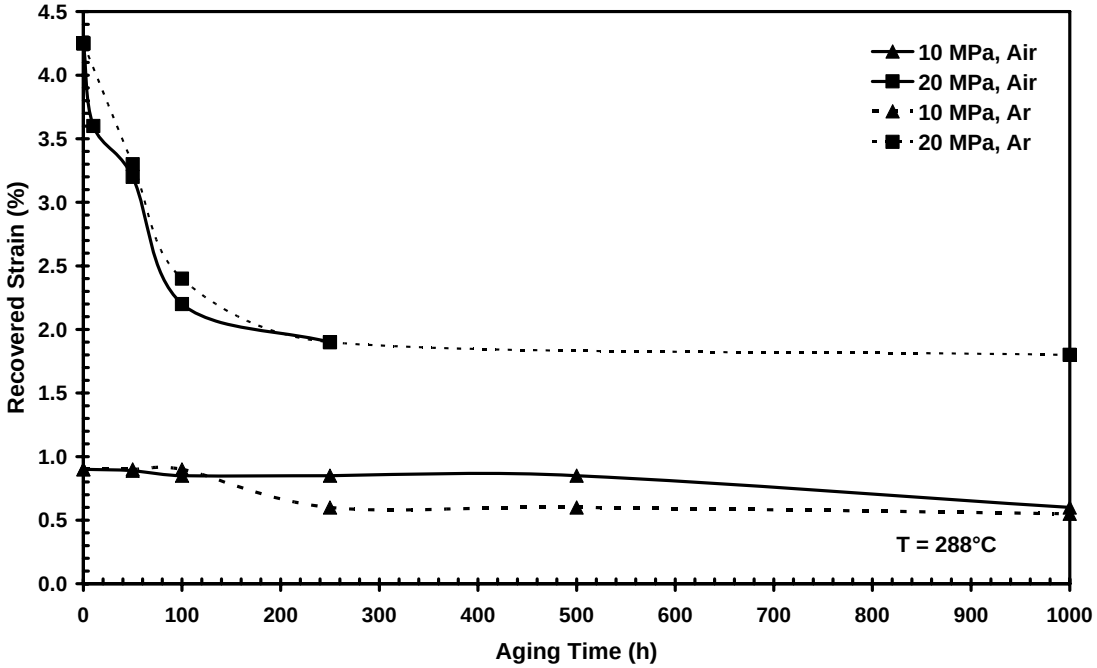

Figure 42 – Strain recovered after 50 h at zero stress as a function of aging time for PMR-15 neat resin. Recovered strain decreases with increasing prior aging time.

Despite the apparent trend seen in Figure 42 it is also necessary to recognize that creep strain accumulation also decreased with increasing prior aging time. It is possible that samples with little prior aging recovered more strain simply because there was more creep strain to be recovered. Therefore it may useful to examine the recovered strain in relation to the amount of previously accumulated creep strain.

It has been chosen to calculate the percent of creep strain recovered for each sample and plot it as a function of time. This percentage was calculated using Figure 39 to define certain strain amounts. Here ε^t is the thermal strain accumulated during heating of the sample, ε^{load} is the strain accumulated during loading, ε^{unload} is the strain recovered during unloading, ε' is the strain value immediately upon reaching zero stress, and ε^* is

the instantaneous strain at any point in time during recovery. Creep strain, ε^{creep} defined as the amount of strain accumulated during creep period, is given by $\varepsilon^{creep} = \varepsilon' - \varepsilon^{t} + \varepsilon^{unload} - \varepsilon^{load}$. It was found that for most tests ε^{unload} was approximately equal to ε^{load} and therefore the expression for ε^{creep} can be simplified to $\varepsilon^{creep} = \varepsilon' - \varepsilon^{t}$. Recovered strain, ε^{r}, was previously defined as $\varepsilon^{r} = \varepsilon' - \varepsilon^{*}$. Finally the ratio of ε^{r} to ε^{creep} can represent the percent of the creep strain recovered as a function of recovery time. This calculation should in effect normalize the recovered strain data to the amount of creep strain accumulated for each sample and allow for easier comparison between results obtained for different samples. Results in Figure 43 show the percent creep strain recovered for samples tested at 20 MPa creep stress level aged in both air and argon environments.

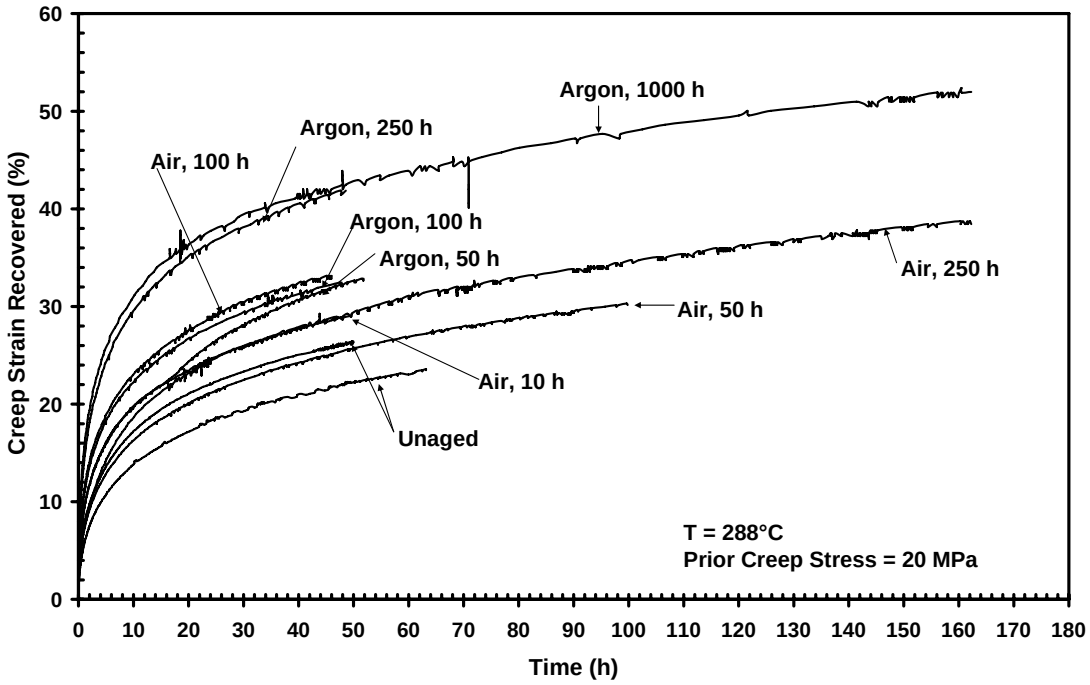

Figure 43 – Creep recovery curves for PMR-15 neat resin aged at 288°C. Prior creep stress = 20 MPa. Recovered creep strain increases with increasing prior aging time.

It is seen in Figure 43 that the unaged samples recovered 20% of the accumulated creep strain after 50 h at zero stress. Samples aged for 1000 h in argon prior to testing recovered 40% of creep strain in the same amount of time. Samples aged for 500 and 1000 h in air are not shown since they failed during the test. It is also interesting to note that even after much longer recovery periods the almost constant rate of recovery is continued without reaching an asymptotic solution.

For specimens tested at a creep stress level of 10 MPa the same general trend was found. Figure 44 shows the percent creep strain recovered for samples tested at a creep stress of 10 MPa.

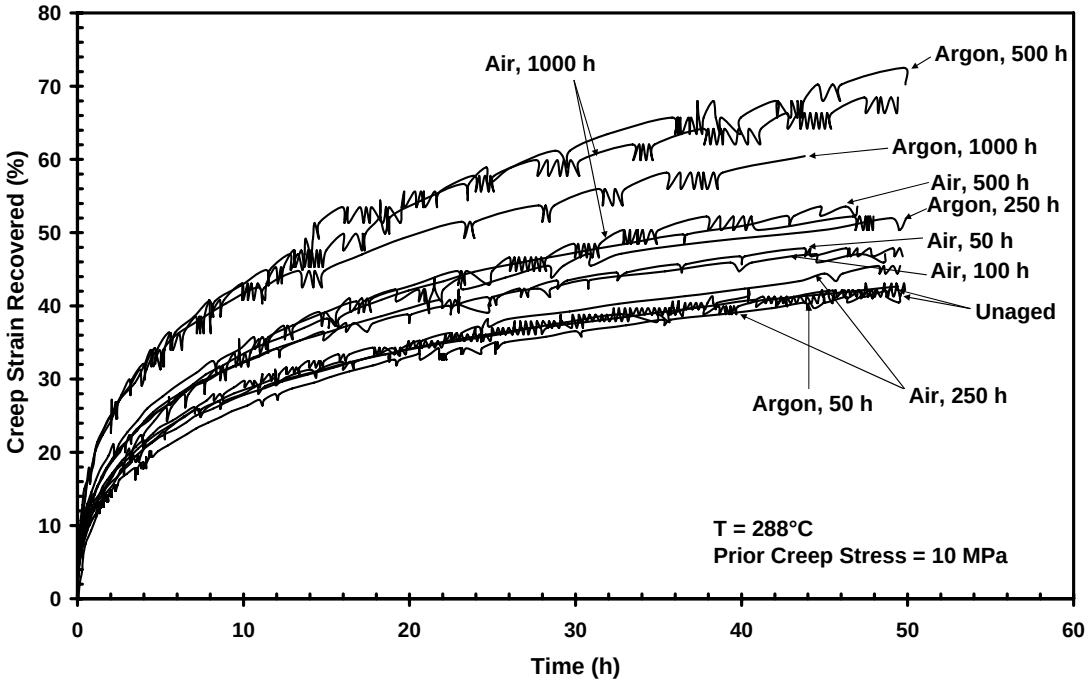

Figure 44 – Creep recovery curves for PMR-15 neat resin aged at 288°C. Prior creep stress = 10 MPa. Recovered creep strain increases with increasing prior aging time.

The unaged samples tested a creep stress of 10 MPa recovered 40% of creep strain after 50 h of recovery. Samples aged for 1000 h in air or argon recovered up to 70% of creep strain during in the same amount of time. Unfortunately no samples were allowed to recover for a longer period to see if full recovery was possible with samples aged for 500 or 1000 h.

Figure 45 shows percent creep strain recovered after 50 h at zero stress versus prior aging time for air or argon environments.

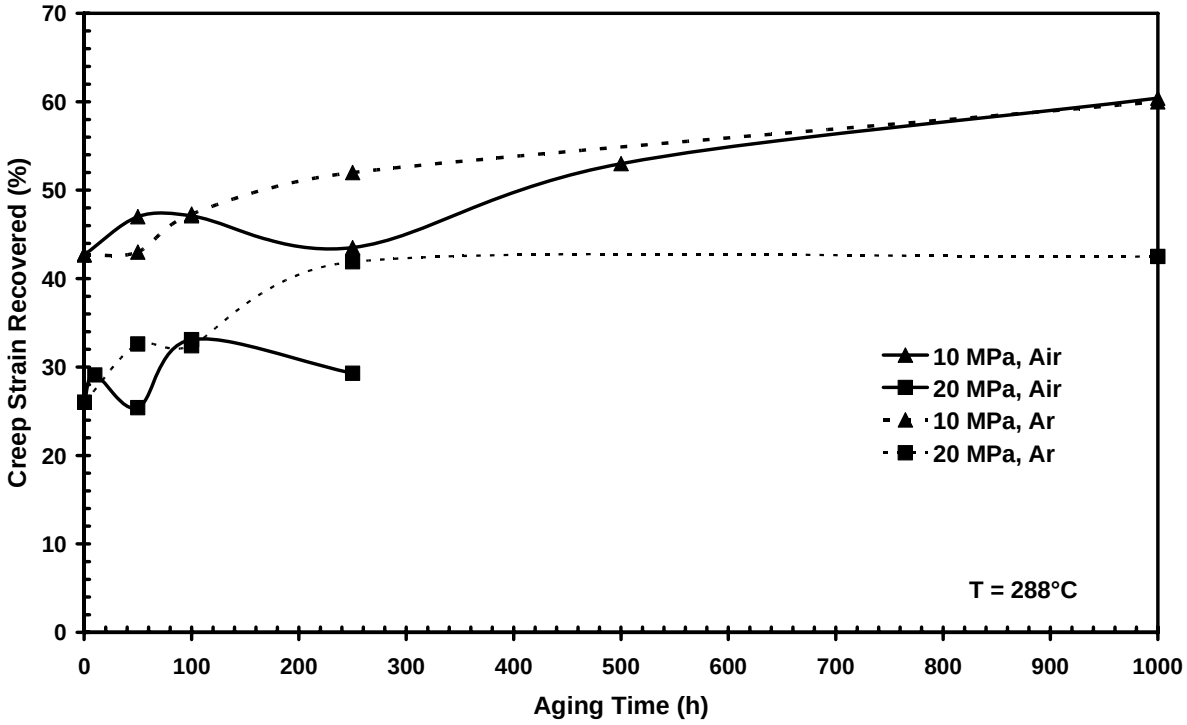

Figure 45 – Creep strain recovered in 50 h as a function of prior aging time at 288°C for PMR-15 neat resin. Recovered creep strain increases with increasing prior aging time in either environment.

Figure 45 shows a trend of increased percent creep strain recovered with increasing prior aging time in both argon and air environments. It was revealed in Figure

42 that creep strain recovered decreased with increased aging time. It is therefore unclear if the recovery behavior is a function of the prior aging condition or the magnitude of creep strain accumulated, or both. The recovery behavior, as the creep behavior, was found to be independent of the aging atmosphere, eliminating the oxidation layer as a large factor in the recovery behavior of PMR-15 neat resin.

Dynamic Modulus Analysis

Portions of the samples used for weight and oxidation layer measurement were also subjected to a Dynamic Modulus Analysis (DMA) test. The torsion test was performed in temperature scan mode and is designed to determine the T_g of a solid polymer as well as the complex modulus for the range of temperatures. Samples were subjected to a 0.1% shear strain, temperature excursion from room temperature to 450°C at a heating rate of 1°C/min and an angular frequency of 1 Hz. Results included storage modulus, loss modulus, and the ratio of the two, tan δ. Samples showed limited blistering during testing, which may be due to trace amounts of moisture. Therefore samples were dried in a vacuum oven at 80°C for 5 days prior to testing to ensure zero moisture effect. Several samples also cracked during the DMA test, particularly the samples aged for 1000 h in air or argon. Fortunately the fractures appeared to occur after the temperature was beyond the T_g, still allowing T_g to be measured. The T_g of a sample can be determined by several commonly used methods. Here the T_g was calculated using the intersection of slopes of the storage modulus at the transition point of the storage modulus versus temperature curve. Bowels [3] determined the T_g using this method to be 347°C for unaged PMR-15 neat resin. The unaged PMR-15 neat resin in this study was

found to have a T_g of 331°C. This discrepancy may be due to differences in material used or may be in part due an unconventional sample geometry used in the tests or different heating rates which has been shown to affect T_g measurements [19:119,18:133]. Typical samples designed for use in a torsion DMA test are ~8mm wide, ~3mm thin, and 50.8 mm long. The only samples available for DMA testing in this study were 6 mm X 4 mm X 50.8 mm. This near square cross section worked well in the grips but it is unknown if there were ramifications on the data due to the sample geometry.

Regardless results of these tests can be used to compare the T_g measurements obtained for different samples. Figure 46 shows the results of the DMA test for an unaged specimen.

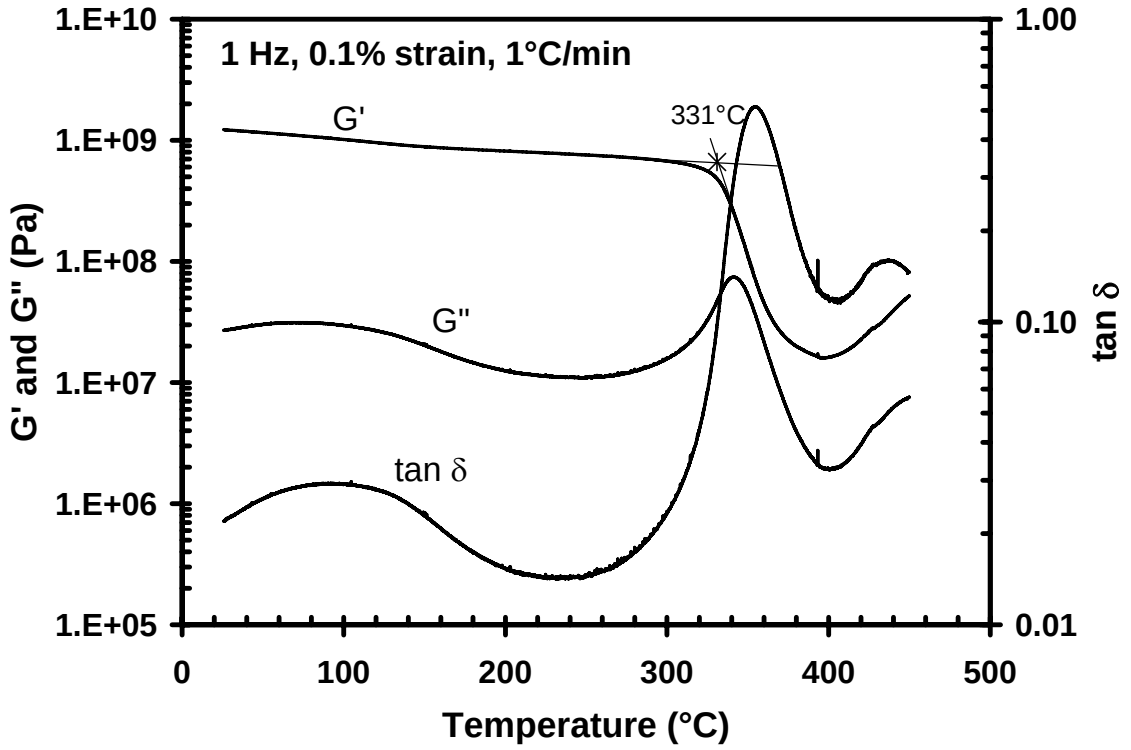

Figure 46 – Results of the DMA tests showing storage modulus, loss modulus and tan δ as a function of temperature for an as-processed PMR-15 neat resin. T_g is determined by the intersection of the two slopes of the storage modulus at the transition.

Samples that were aged for various periods of time in air or in argon at 288°C were also subjected DMA tests. Figure 47 shows the storage modulus as a function of temperature for samples aged in air or argon.

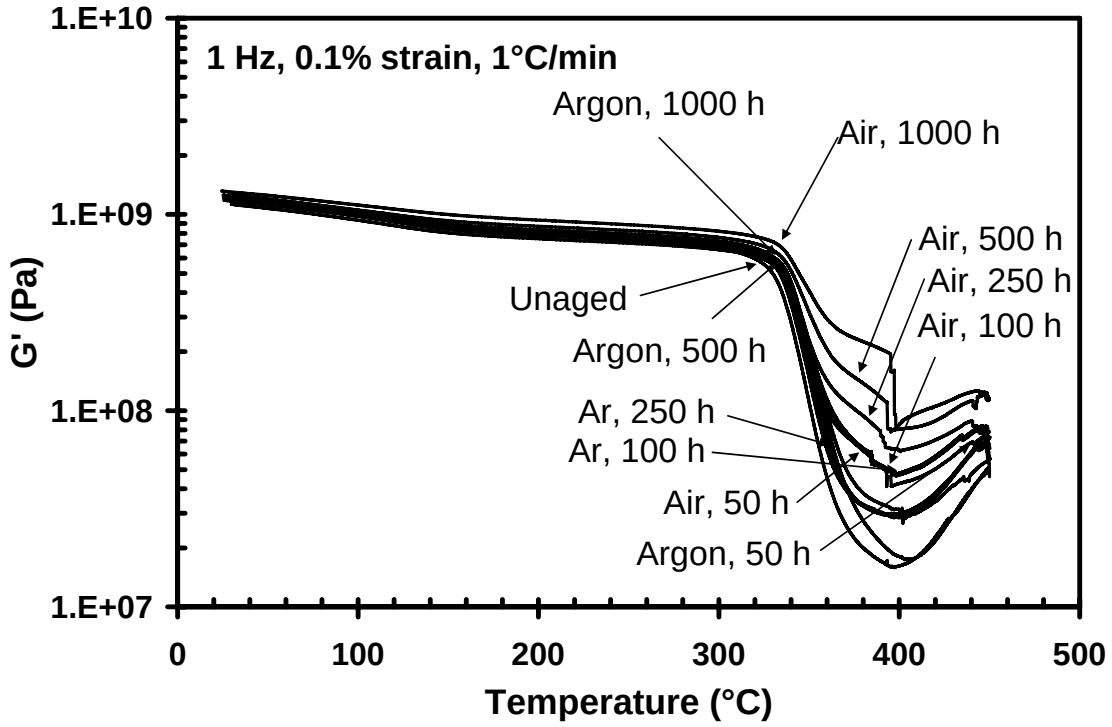

Figure 47 – Storage Modulus versus temperature as determined by DMA for samples aged in air or argon at 288°C. The transition temperature increased with increased prior aging time.

Figure 47 reveals that the transition temperature of the storage modulus increased moderately with increasing prior aging time in either air or argon environments.

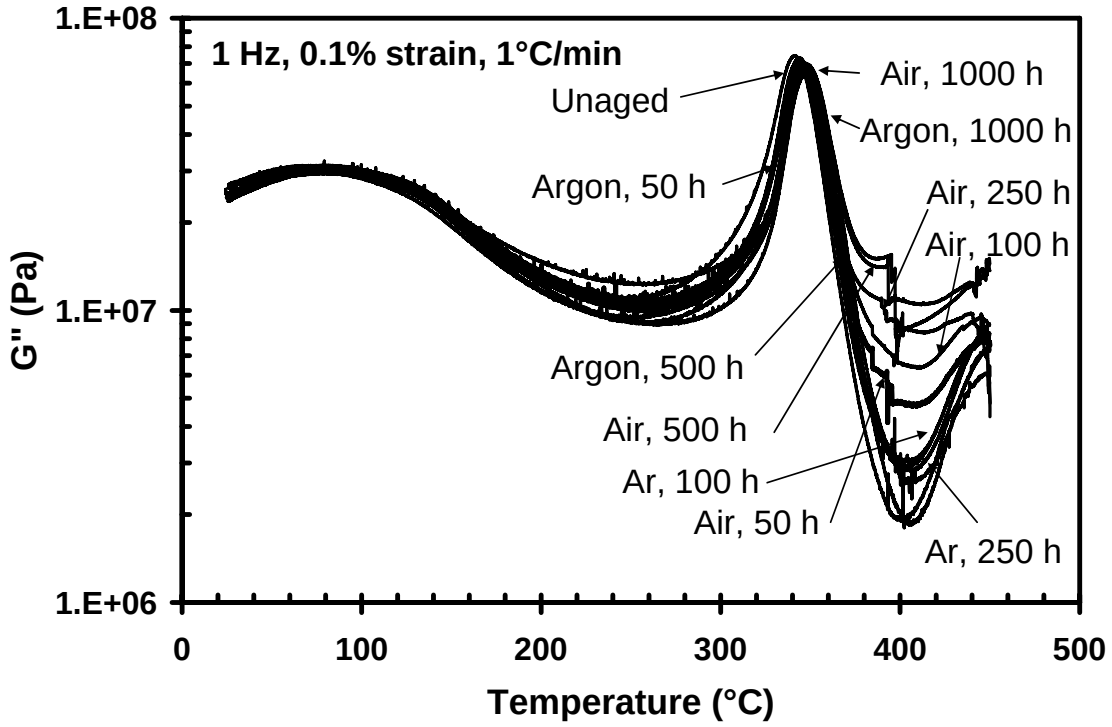

Figure 48 – Loss Modulus versus temperature as determined by DMA for samples aged in air and in argon at 288°C. The temperature at the peak of the curve increased moderately with increasing prior aging time.

Figure 48 shows the loss modulus as a function of temperature as determined by DMA tests for samples aged in air and in argon. It is seen that the temperature at the peak of the curves increases with increasing prior aging time.

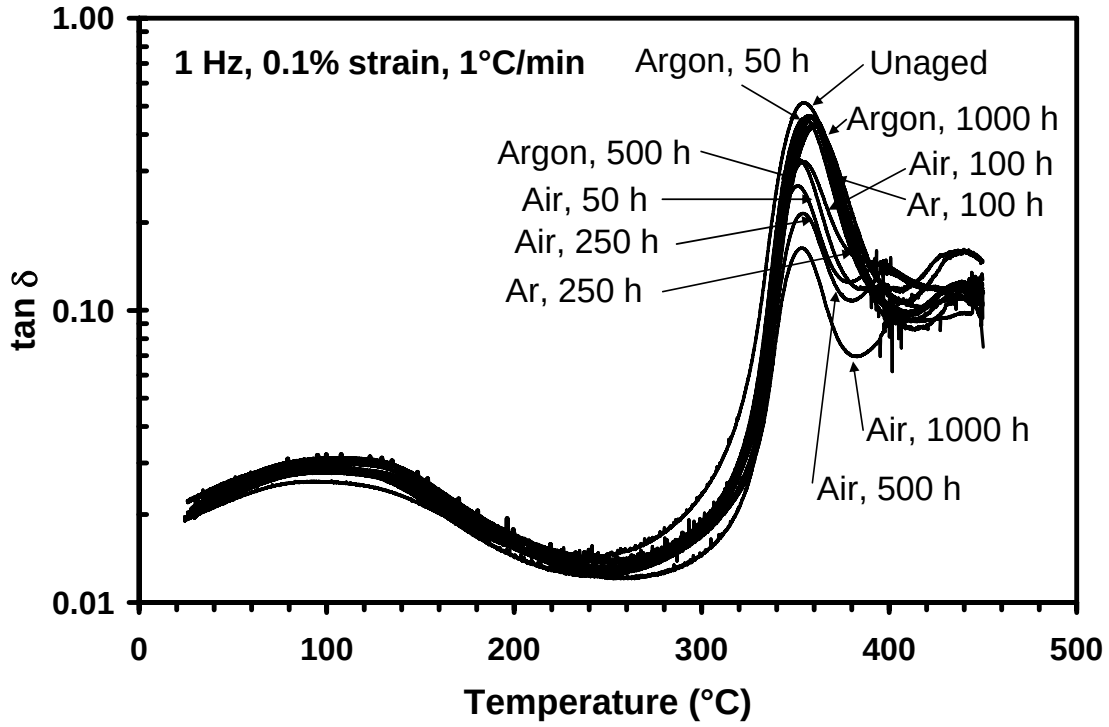

Figure 49 – Tan δ versus temperature as determined by DMA for samples aged in air or in argon at 288°C. The peak value of the ratio decreases with increasing prior aging time.

Figure 49 presents tan δ as a function of temperature as determined by DMA for samples aged in air and argon. It is interesting to note that the sample aged for 1000 h in air had a dramatically lower peak value. This same sample also had a higher storage modulus than the other samples. Since the sample aged for 1000 h in argon did not show this change in storage modulus, it may be attributable to the oxidation layer. For the purpose of tracking the change in T_g with increasing aging time in air or argon, T_g values were measured from the transition in the storage modulus. The measured T_g values are plotted versus the prior aging time in Figure 50.

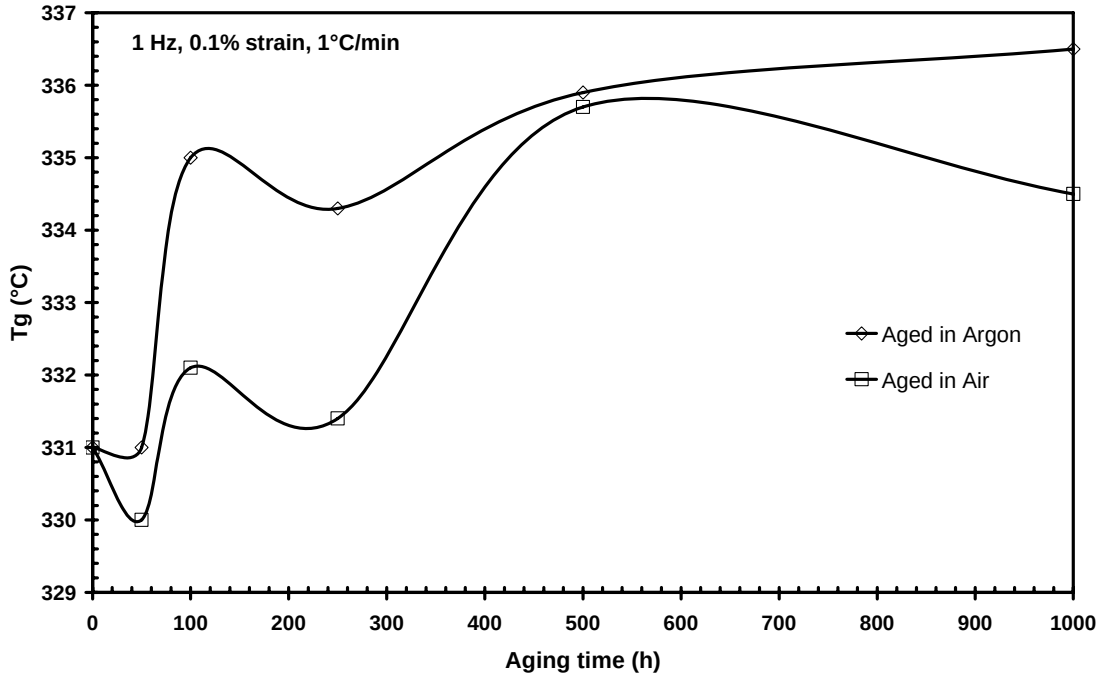

Figure 50 – Glass transition temperature versus prior aging time for specimens aged at 288°C in air or argon as determined by the transition of the storage modulus. T_g increased moderately with increasing prior aging time in air or argon at 288°C

Figure 50 reveals that the measured T_g values increased with increasing prior aging time in air or argon environments at 288°C. The T_g increased from 331.0°C to 336.5° with aging for 1000 h in argon, and increased to 334.5°C with aging for 1000 h in air.

Discussion

Samples that were machined using a water jet exhibited extensive surface cracking when tested in creep at high creep stresses. Therefore the data resulting from those tests were not included in this study. As a result, only a very limited number of samples were available per test condition, making statistically relevant quantitative

statements difficult. Most discussion and conclusions will be limited to the qualitative trends.

Effects of Prior Aging in Argon on Creep Response

Recall that samples aged in an argon environment are thought to represent the non-oxidized material in the interior of the samples aged in an oxidizing environment. This study has shown that the oxidation layer extends up to 0.16 mm after 1000 h of aging in air at 288°C, a relatively small depth compared to the ~3mm thickness of the samples (see Figure 20). These observations also agree with those published in literature [3]. Therefore, on any sample or working component with dimensions significantly greater than the depth of the developed oxidized layer, the interior bulk material would be expected to dominate the mechanical performance of the sample. Note that additional oxidation effects that might result from the presence of fibers or reinforcement lending additional pathways for oxygen penetration.

The samples aged in an argon environment exhibited weight loss, increasing elastic modulus, reduction in creep strains and increase in percent creep strain recovered with increasing prior aging time in the argon environment at 288°C. The T_g temperatures, determined by DMA measurements, increased from 331°C to 336.5°C after prior aging for 1000 h in argon at 288°C, and increased to 334.5°C after prior aging for 1000 h in air (see Figure 50). The weight loss, although not rigorously examined in this study has been shown in [4] to be due to the release of lightweight volatiles or the result of some type of chemical degradation, possibly pyrolytic degradation. However the creep data suggest that the largest change in creep response is seen after the first few

hundred hours of aging. Differences in creep and recovery response as well as the T_g obtained for specimens aged for 500 and 1000 h in argon were relatively small. This observation suggests that the amount of additional crosslinking may be limited. After this crosslinking process is saturated, the polymer would either remain unchanged or begin to degrade with increasing aging time at high temperature as shown in the TTT diagram in Figure 11. Unfortunately, the author was not able to age samples long enough to see evidence of degradation in the data.

Oxidation of PMR-15 Neat Resin and Resulting Creep Response

Having gained an understanding of the effects of prior aging in argon on the creep response of PMR-15 neat resin, the effect of aging in air on creep response can be readily evaluated. Assuming that the samples aged in argon also represent the interior material in the oxidized samples, any differences between the two sample groups can be attributed to the presence of the oxidation layer on the surface. For a given creep stress level, samples aged in air and samples aged in argon showed almost identical creep and recovery behavior. However for the prior aging times of 500 h or 1000 h, specimens aged in air failed early in the 20 MPa creep tests, while the specimens aged for 1000 h in argon survived 25 h at 20 MPa. Examination of the samples aged in air determined that after 250 h a 0.11 mm-thick layer of oxidized/degraded material had formed on the surfaces of these samples (see Figure 20). The brittle and porous oxidative layer contains numerous microcracks [3,14]. Therefore this layer does not contribute to the load-bearing capacity of a sample, which results in a higher stress being applied to the remaining inner material. It is possible that the decrease in the interior bulk material

resulted in stresses approaching the UTS, when the load calculated to produce 20 MPa in the as-processed material was applied. Changes in ultimate tensile strength were not explicitly examined in this study so it is difficult to estimate what stress level was seen that could have lead to fracture. Examination of the fracture surfaces of these samples showed evidence of very little ductility. Specimen fracture was caused by fast crack propagation across the sample. All fracture surfaces were perpendicular to the tensile stress, not on the shear stress plane. This indicates failure due to crack propagation rather than pure tensile failure. The presence of microcracks in the oxidized layer may also have promoted crack growth therefore accelerating the failure.

Besides the premature failure during 20 MPa creep tests, the oxidized layer also caused a slightly increase in elastic modulus values. For a given aging time, specimens aged in air produced slightly higher elastic modulus values than the specimens aged in argon (see Figure 25). Specimens aged in air also exhibited significantly greater weight loss than those aged in argon. This observation is consistent with results reported in literature [3]. The oxidation reaction breaks down the polymer chains, as a result volatiles are released at a much faster rate from the surface of the sample aged in air. Conversely, in the case of specimens aged in argon, release of volatiles is a much slower diffusion-controlled process.

Overall, the presence of the oxidative layer did little to affect the creep and recovery response of PMR-15 neat resin, although it may have played a role in causing premature failure in the 20 MPa creep tests after 500 and 1000 h of prior aging. Because the thickness of the oxidized layer is small relative to the dimensions of the sample, the

unoxidized material dominates the mechanical behavior, including the creep and recovery response.

Creep and Recovery - Structure Property Relationships

DMA results show that T_g increases with increasing prior aging time in either air or argon environments (see Figure 50). An increasing T_g suggests an increase in the crosslink density in the resin, that could affect elastic modulus, creep and recovery behavior, and ultimate strength of the samples [18:133]. In general, a higher crosslink density causes an increase in strength while reducing the strain at failure for a highly networked thermoset polymer. When relating this to creep and recovery behavior it is important to recognize that the creep mechanism for a highly networked structure would be the alignment and extension of the crosslink networks. A higher crosslink density would increase the stress needed for extension and alignment and limit the strain available until fracture.

Samples with a T_g increase due to prior aging produced a lower creep strain at a given stress level (see Figure 37). The recovery response may likewise be dependent on the remaining network structure of the polymer. The recovery mechanism for a highly networked polymer is the relaxation of the previously strained crosslinks. In the absence of crosslinks there is no driving force for recovery. The more crosslinks, the higher the driving force for recovery.

Overall, it is likely that aging at 288°C in air or argon increased the crosslink density of the PMR-15 neat resin, as evidenced by a higher T_g. It is speculated that the increase in crosslink density caused the observed increase in elastic modulus and

decrease in creep strain. Unfortunately, speculations regarding the recovery response can not be created from this study since it is unknown if the change in recovery behavior is a function of the prior aging or the prior creep response. Degradation of the elastic modulus during creep testing, as evidenced by the reduction in E_U, with increasing creep duration, may reveal evidence of polymer degradation of some type; however, it is not possible to speculate on the mechanisms of degradation.

V. Conclusions and Recommendations

Chapter Overview

The purpose of this chapter is to draw conclusions from the experimental data and related discussion. Recommendations are also made for the continued experimental investigation of PMR-15 neat resin and its composites. Finally any practical implications are discussed.

Conclusions of Research

PMR-15 neat resin was aged in either air or argon environments at 288°C for various times up to 1000 h. Samples were then subjected to creep tests at either 10 or 20 MPa followed by unloading and recovery at zero stress. Duration of the creep period was at least 25 h and duration of the recovery period at least 50 h. All creep and recovery tests were conducted 288°C. Additionally a separate group of samples were monitored for variations in weight with aging time. These samples were examined with an optical microscope to observe the oxidation layer that was formed during aging in air. Finally, sections of these samples were used in DMA tests to identify any effects of aging on the T_g of the polymer.

Results showed that prior aging in either air or argon environments significantly influenced the creep behavior of the PMR-15 neat resin. Unaged samples produced creep strains of ~15% and 2% at 20 and 10 MPa creep stress levels, respectively. Samples aged in argon for 1000 h produced creep strains of 4% and 1% at 20 and 10 MPa, respectively. This represents a near 75% reduction in creep strain accumulation due to aging tin argon for 20 MPa tests, and a ~50% reduction in creep strain for 10 MPa tests. Furthermore,

creep strain accumulation for a given creep stress level decreased with increasing prior aging time.

Percent creep strain recovered was calculated as $\varepsilon^r/\varepsilon^{cr}$ X 100%. The unaged samples recovered 22% and 43% creep strain accumulated in the 20 and 10 MPa tests, respectively. The samples aged for 1000 h in argon recovered 43% and 60% of the creep strain accumulated in the 20 and 10 MPa tests, respectively. In general samples aged for the same length of time and tested under the same conditions performed nearly identically regardless of the aging environment provided the aging time was ≤ 250 h. Specimens aged in air for 500 and 1000 h failed during the first 5 h of creep test or during loading to creep stress level. Examination of the fracture surfaces and the oxidation layer indicates that the oxidation layer acted as a stress riser as well as a crack initiation site leading to premature failure of these samples. Therefore, it is concluded that the inner, unoxidized, material dominates the mechanical properties and creep and recovery response of PMR-15 neat resin.

Examination of the oxidation layer in samples aged in air revealed a uniform oxidized region of material on the surface of the samples that reached 0.16 mm in thickness after 1000 h of aging in air at 288°C. This result correlates well with previously published data [3]. Weight measurements documented a significant difference in the weight loss of samples aged in argon and those aged in air. Samples aged in air experienced 3.4% weight loss after 1000 h while samples aged in argon for 1000 h experienced 1.3% weight loss. The data from this study agrees well with weight loss results published in literature [3].

DMA tests were performed in order to check for changes in T_g due to prior aging. It was found that aging in argon or air for 1000 h raised the T_g of the PMR-15 neat resin by 5°C from 331°C to 336.5°C. This increase in T_g is thought to be attributable to an increase in crosslink density in the polymer. An increased crosslink density can have far reaching effects on the mechanical properties and creep response of a highly networked thermoset such as PMR-15. It is likely that the aging in either air or argon caused an increase in crosslink density in the polymer, which in turn caused an increase in elastic modulus and a decrease in creep strain. Results suggest that additional polymer damage occurs during creep tests, as evidence by a decrease in elastic modulus upon unloading, E_U, with increasing creep test duration. All data point to a strong relationship between the creep response and the polymer network integrity and crosslink density. Data also suggests that a limit to the increase in crosslink density exists, as there was little change to the creep and recovery response when aging time exceeded 500 h in either environment.

Significance of Research

Due to the limited amount of time and material available for this study the conclusions resulting from the work are largely qualitative. Never the less several important observations have been made. It was found that samples aged in either air or argon performed almost identically in creep and recovery tests for aging times $\leq$ 250 h. This indicates that the inner, unoxidized, material dominates the majority of the creep and recovery response of a PMR-15 neat resin sample. Additionally, the combination of creep and recovery data and DMA results suggest that the crosslink density increases

with aging time at 288°C, causing a change in mechanical properties and in creep response.

These observations improve the current understanding of the mechanical response one could expect from PMR-15 components when used at elevated temperatures under sustained loading. This study has shown that consideration should be given to the dynamic nature of the material, when exposed to high temperatures and/or moderate stress levels for extended periods of time. This work may also help development of new materials or processing conditions to better control the properties of PMR-15 components in the future.

Recommendations for Future Research

For solid and statistically sound conclusions to be drawn regarding the creep response of PMR-15 neat resin when exposed to prolonged time at elevated temperatures, more data must be taken with multiple samples for each test condition. Efforts should be made to eliminate or reduce additional effects, especially sample to sample material variations. Any additional examination should attempt to further the understanding of the polymer network and its dynamic changes due to both high temperature exposure and testing conditions.

Due to the relatively short aging times used in this study there was no evidence of any polymer network breakdown, either by oxidation or pyrolytic degradation, although it is known that the two processes are concurrent. Longer aging times would be needed to show evidence of this eventual degradation.

Finally, similar studies should be accomplished using PMR-15 based composite to investigate the additional influence of increased oxidation pathways and material interactions between the neat resin and reinforcement material.

Summary

This study has shown that the creep and recovery response of PMR-15 is a function of aging time at 288°C and creep stress level. Significant changes in the mechanical response and properties where observed after relatively short exposure times. Creep strain was reduced with increasing prior aging in both air and argon environments. It was shown that for prior aging time ≤ 250 h, the creep and recovery response of samples aged in air was similar to that of samples aged in argon suggesting that the inner, unoxidized, material is responsible for the bulk mechanical response of the material. As the aging time exceeded 250 h, specimens aged in air developed an oxidative layer which may have acted as both a stress riser and crack initiation site.

DMA results suggest a strong relationship between crosslink density and creep response, and explain changes in elastic modulus with increasing prior aging time.

Bibliography

[1] "DMBZ Polyimides Provide an Alternative to PMR-15 for High-Temperature Applications", *NASA/Lewis Research Center*, published 2005-08-25.

[2] Klosterman, Don, Class handout, MAT 510, Thermosetting Polymers, Department of Material Science, University of Dayton, Spring 2006.

[3] Bowles, K.J., Papadopoulos, D.S., Ingrahm, L.L., McCorkle, L.S., Klan, O.V., "Longtime Durability of PMR-15 Matrix Polymer at 204, 260, 288, and 316°C", *NASA/Glenn Research Center*, TM—2001-210602 (July 2001).

[4] Bowles, Kenneth J., McCorkle, Linda, Ingrahm, Linda, "Comparison of Graphite Fabric Reinforced PMR-15 and Avimid N Composites After Long-Term Isothermal Aging at Various Temperatures", *Journal of Advanced Materials*, 2:27-35 (1998).

[5] Stenzenbereger, H.D., "Addition Polyimides", *Advances in Polymer Science*, 117:166-220 (1994).

[6] Brian Shonkwiler, Ramesh Talreja, Ashraf. Badir "Fatigue Property Characterization of T60-35/AMB21 Laminates Under Room and Elevated Temperature", *American Institute of Aeronautics and Astronautics*, AIAA 2002-1679 (2002).

[7] Xie, W., Pan, W.P., Chuang, K.C., "Thermal Degradation Study of Polymerization of Monomeric Reactants (PMR) Polyimides", Journal of Thermal Analysis and Calorimetry, 74:477-485 (2001).

[8] Colin, X., Verdu, J., "Strategy for studying thermal oxidation of organic matrix composites", *Composites Science and Technology*, 65:411-419 (2005).

[9] Colin, X., Marais, C., Verdu, J., "Kinetic modeling of the stabilizing effect of carbon fibres on thermal ageing of thermoset matrix composites", *Composite Science and Technology*, 65:117-127, (2005).

[10] Ndalama, Tchinga, Hischfeld, Deidre, "Analysis of the Effect of Surface Modification on Polyimide Composites Coated with Erosion Resistant Materials", *New Mexico Institute of Mining and Technology*, NASA/CR 2003-212190.

[11] Bowles, Kenneth J., Jayne, Douglas, Leonhardt, Todd A., "Isothermal Aging Effects on PMR-15 Resin", *SAMPE Quarterly*,24:no. 2,2-9 (1993).

[12] Bowles, Kenneth J., Tsuji, Lusi, Damvouris, John, Roberts, Gary D., "Long-Term Isothermal Aging Effects on Weight Loss, Compression Properties, and Dimensions of T650-35 Fabric-Reinforced PMR-15 Composites – Data", *NASA/Glenn Research Center*, report TM-2003-211870.

[13] Bowles, K.J., Jayne, D., Leonhard, T.A., Bors, D., "Thermal Stability Relationships Between PMR-15 Resin and Its Composites", *NASA/Lewis Research Center,* 1993 TM-106285.

[14] Tjuji, Lewis C., McManus, Hugh L., Bowels, Kenneth J., "Mechanical Properties of Degraded PMR-15 Resin", *NASA/Lewis Research Center,* TM—1998-208487.

[15] Owens, G.A., Scholfield, S.E., "Thermal Cycling and Mechanical Property Assessment of Carbon Fibre Fabric Reinforced PMR-15 Polyimide Laminates", *Composites Science and Technology*, 33:177-190 (1988).

[16] C. Marais, G. Villoutreix, "Analysis and Modeling of the Creep Behavior of the Thermostable PMR-15 Polyimide", *Journal of Applied Polymer Science*, 69:1983-1991 (1998).

[17] Gregory Schoeppner, G. P. Tandon, "Anisotropic Oxidation and weight loss in PMR-15 Composites", *Composites: Part A*, 38:890-904 (2007).

[18] John Scheirs C*ompositional and Failure Analysis of Polymers*. John Wiley & Sons Ltd., 2000.

[19] Rakesh K. Gupta *Polymer and Composite Rheology*. (2nd Edition), Marcel Dekker Inc, 2000.

[20] Pascault, Sautereau, Verdu, Williams *Thermosetting Polymers*. Marcel Dekker Inc., 2002.

[21] Gregory Scheoppner, G.P. Tandon "Modeling of Oxidative Development in PMR-15 resin", *Polymer Degradation and Stability*, 91:1861-1869 (2006).

[22] Falcone, Christina M. *Rate Dependence and Short-Term Creep Behavior of PMR-15 Neat Resin at 23 and 288°C*. MS Thesis, AFIT/GAE/ENY/05-S07. Graduate School of Engineering and Management, Air Force Institute of Technology (AU), Wright-Patterson Air Force Base, OH, September 2005 (ADA441549)

[23] Westberry, Candice M. *Some Aspects of the Mechanical Response of PMR-15 Neat Resin at 288°C: Experiment and Modeling*. MS Thesis, AFIT/GAE/ENY/06-S03. Graduate School of Engineering and Management, Air Force Institute of Technology (AU), Wright-Patterson Air Force Base, OH, September 2006 (ADA456776)

Appendix A – Creep Sample Micrographs, Aged in Air at 288°C

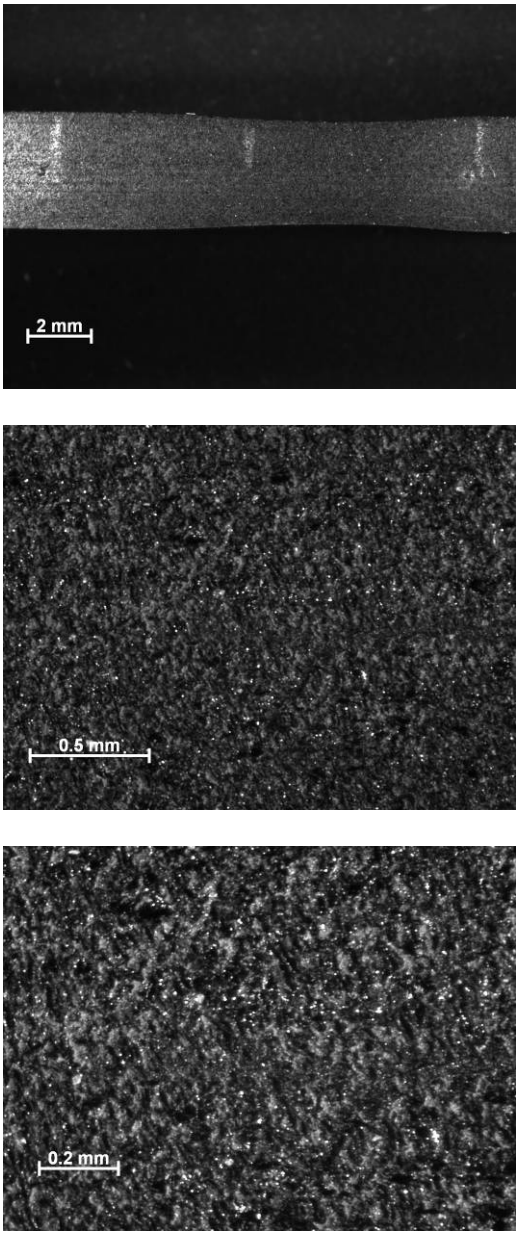

Figure 51 – Sample 02-01, as-processed PMR-15 neat resin, Creep stress = 20 MPa. Machined with diamond saw.

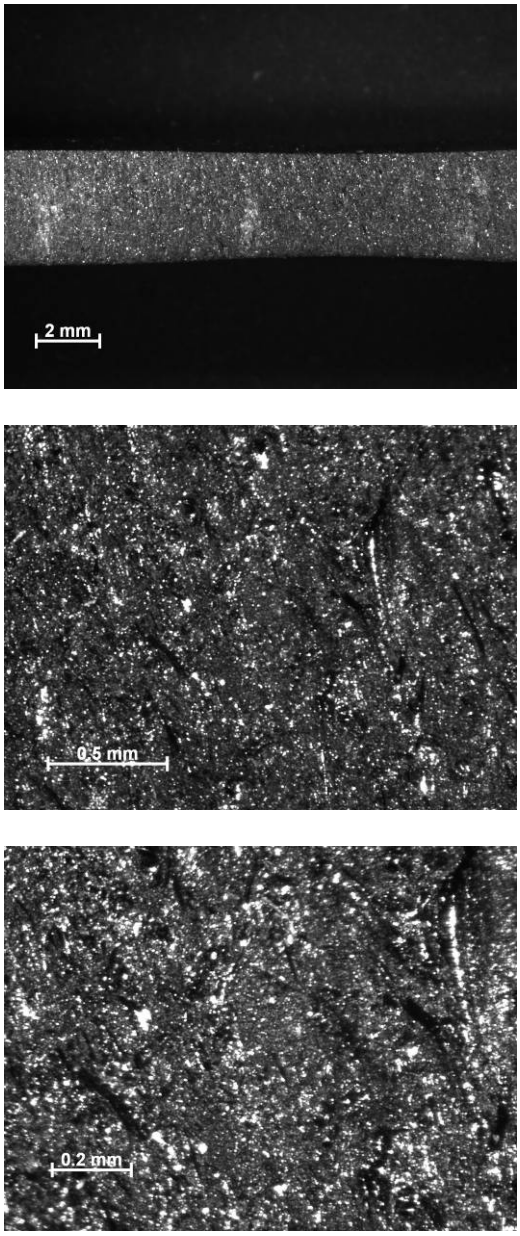

Figure 52 –Sample 13-10, as-processed PMR-15 neat resin, Creep stress = 20 MPa. Machined with water jet, showing microcracks.

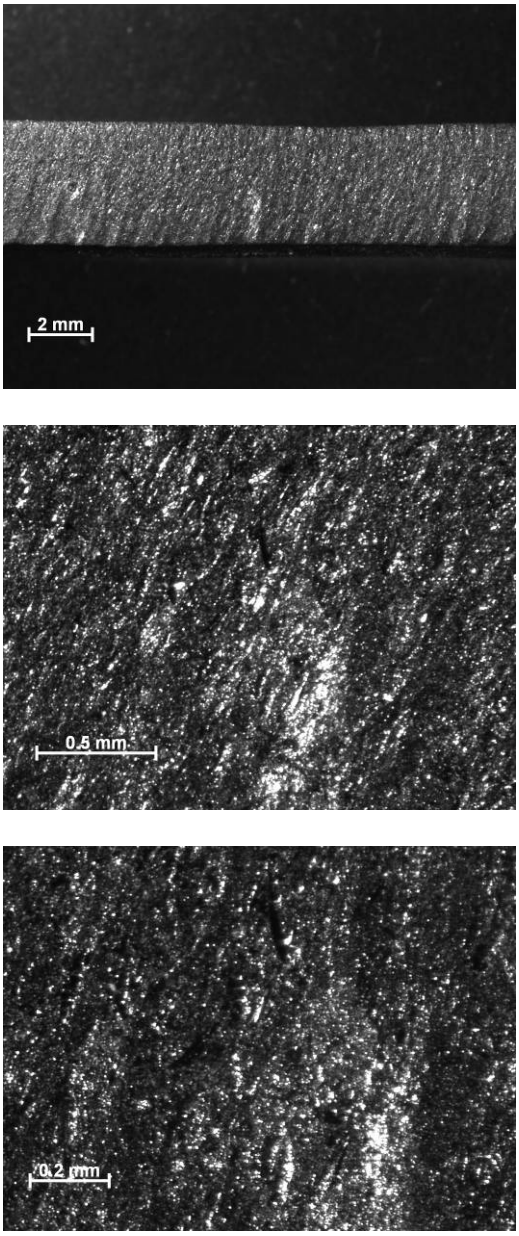

Figure 53 – Sample 12-10, as-processed PMR-15 neat resin, Creep stress = 15 MPa. Machined with diamond saw, showing slight microcracking

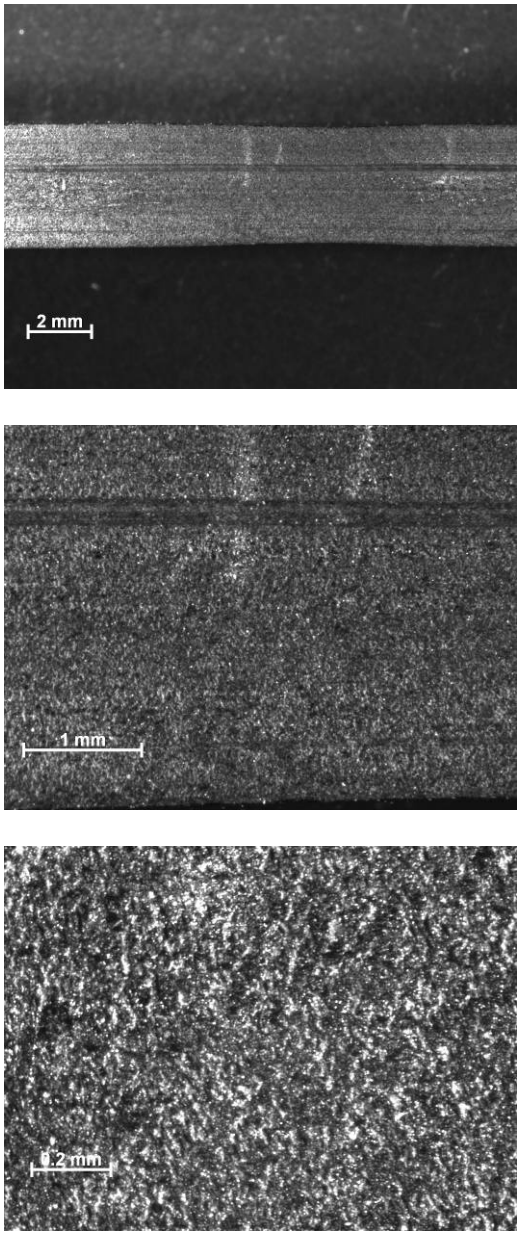

Figure 54 – Micrographs at several magnifications of sample 11-15, as-processed PMR-15 neat resin, Creep stress = 15 MPa. Machined with diamond saw.

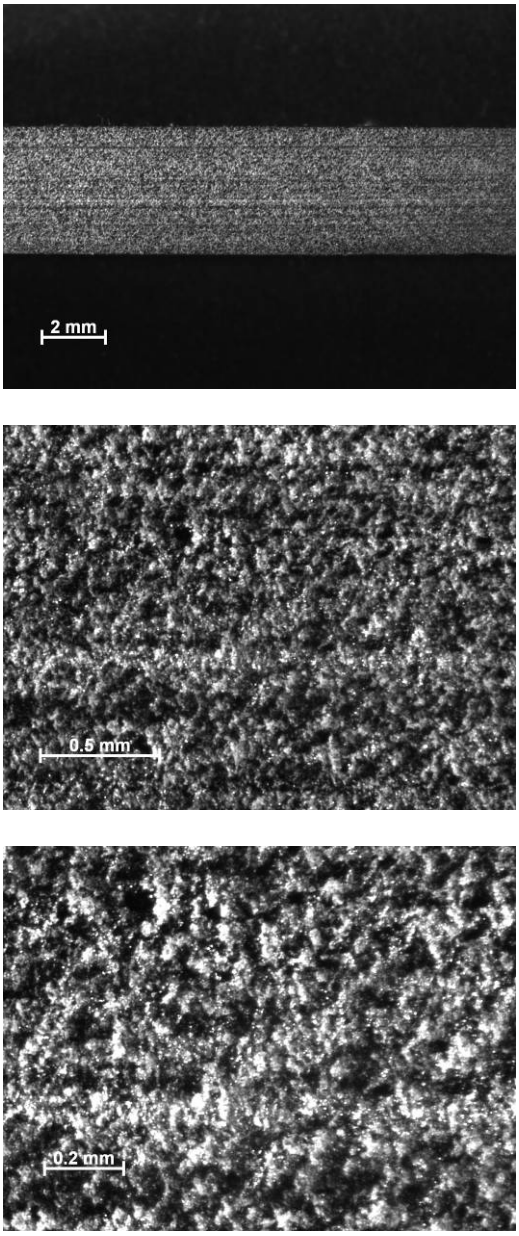

Figure 55 – Sample 02-08, as-processed PMR-15 neat resin. Before testing, Machined with diamond saw.

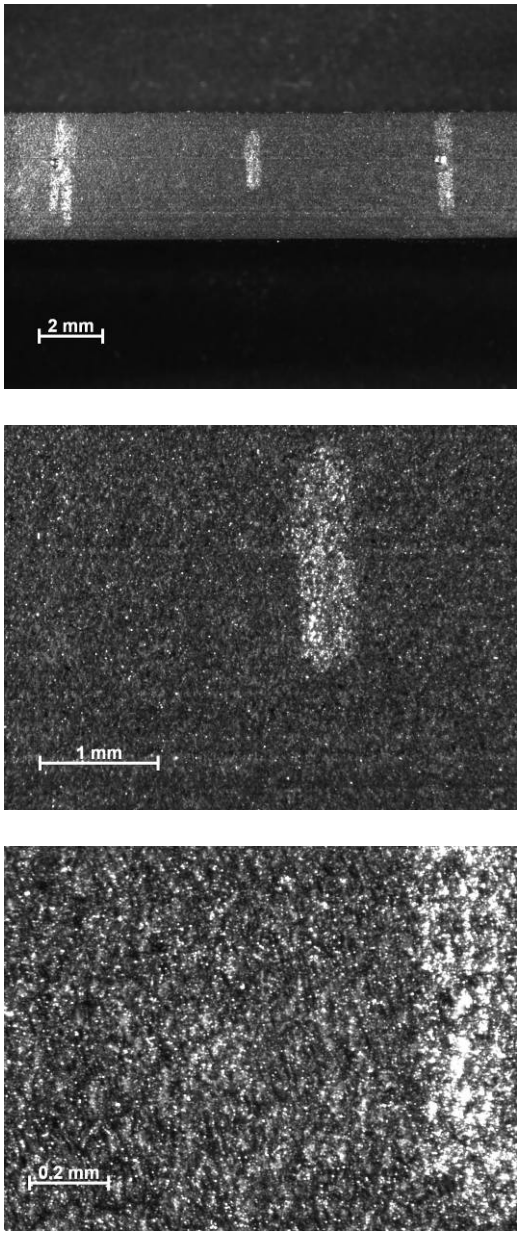

Figure 56 –Sample 02-08, as-processed PMR-15 neat resin, Creep stress = 15 MPa. Machined with diamond saw.

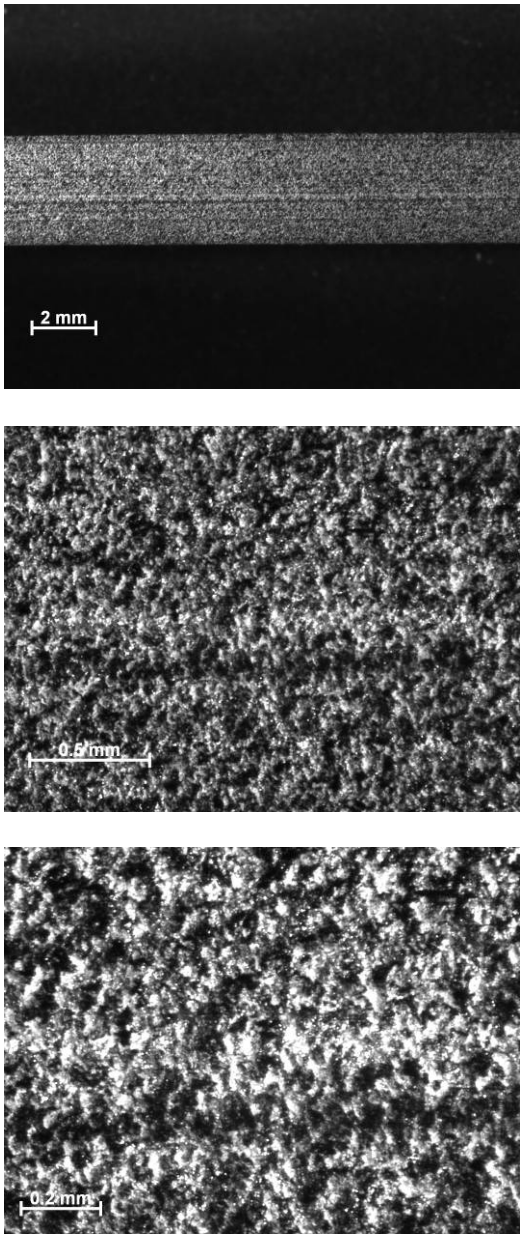

Figure 57 –Sample 02-10, as-processed PMR-15 neat resin. Before testing, Machined with diamond saw.

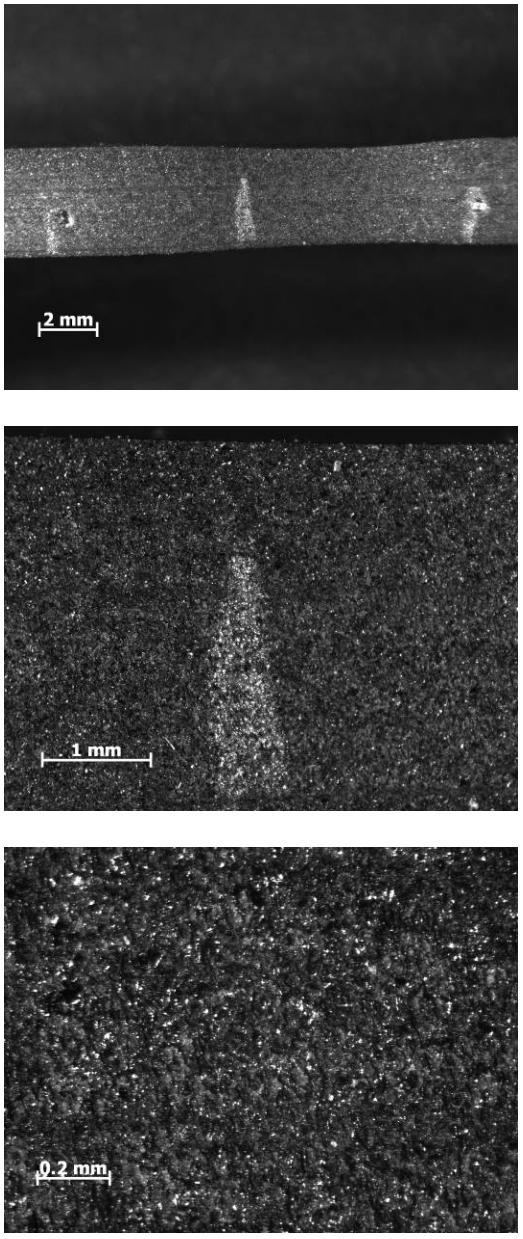

Figure 58 –Sample 02-10, as-processed PMR-15 neat resin, Creep stress = 20 MPa. Machined with diamond saw.

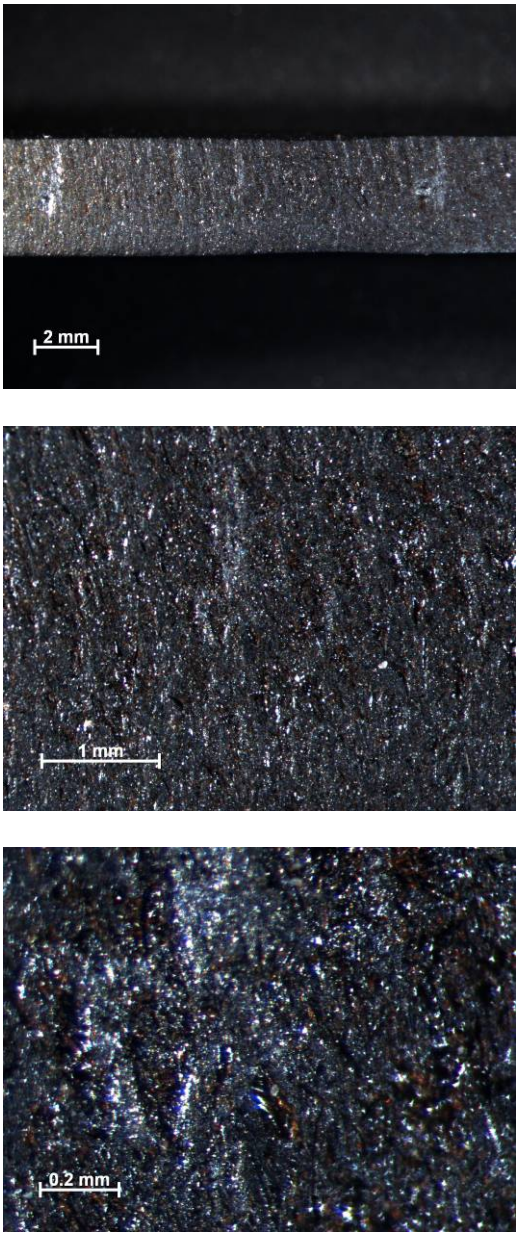

Figure 59 –Sample 13-11, as-processed PMR-15 neat resin, Creep stress = 10 MPa. Machined with diamond saw.

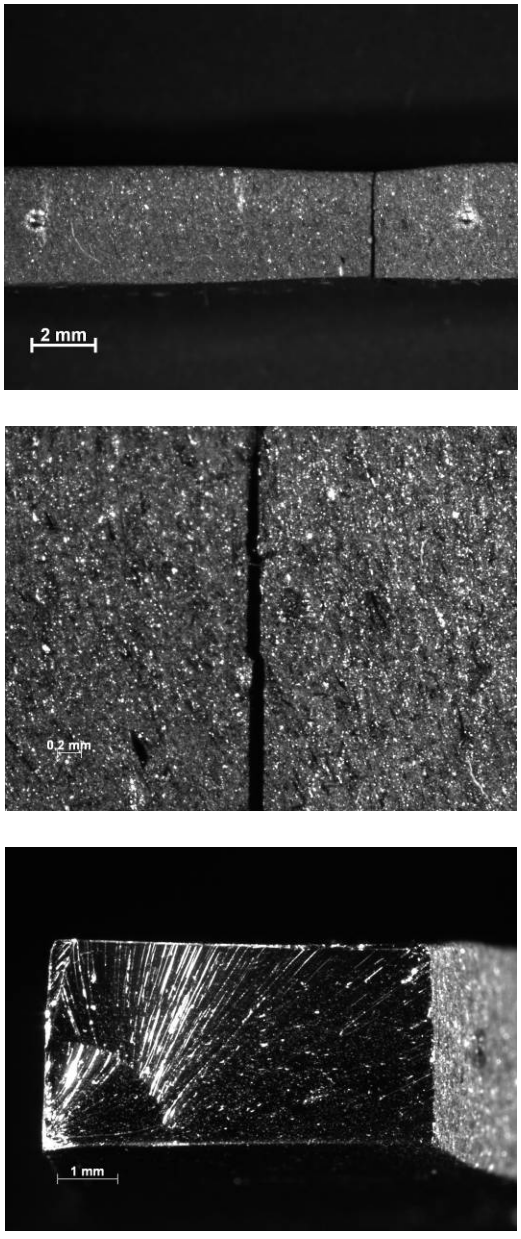

Figure 60 –Sample 10-01, PMR-15 neat resin aged in air for 10 h, T = 288°C, Creep stress = 20 MPa. Machined with water jet showing slight microcracking.

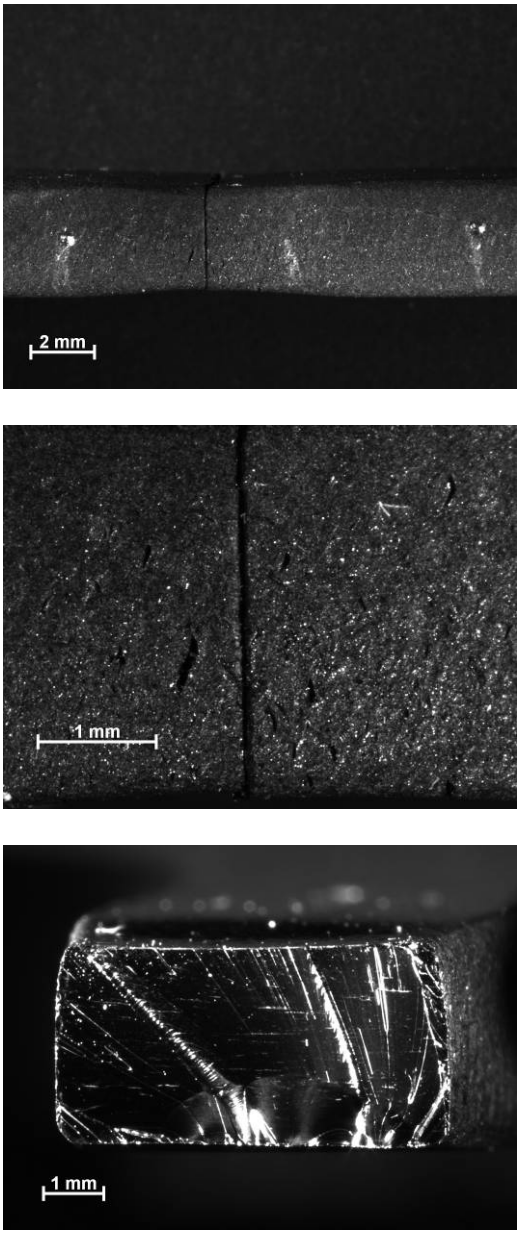

Figure 61 –Sample 12-17, PMR-15 neat resin aged in air for 10 h, T = 288°C, Creep stress = 20 MPa. Machined with water jet showing slight microcracking.

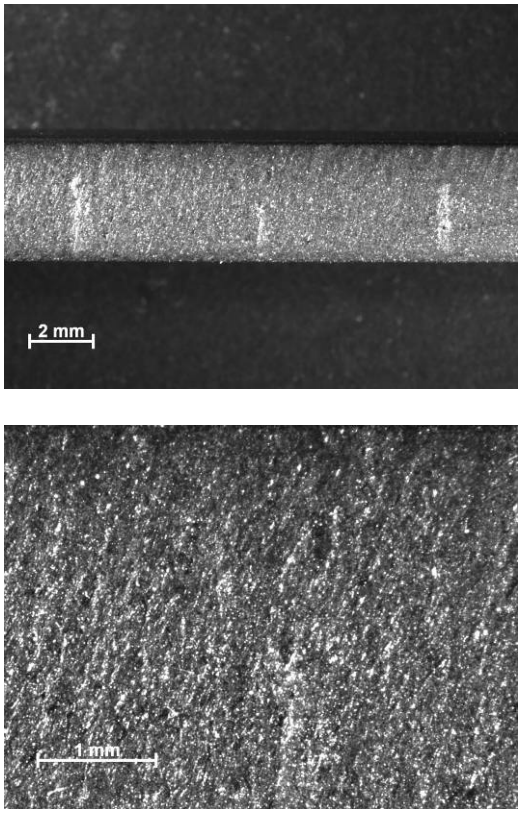

Figure 62 –Sample 12-05, PMR-15 neat resin aged in air for 10 h, T = 288°. Before testing, Machined with water jet.

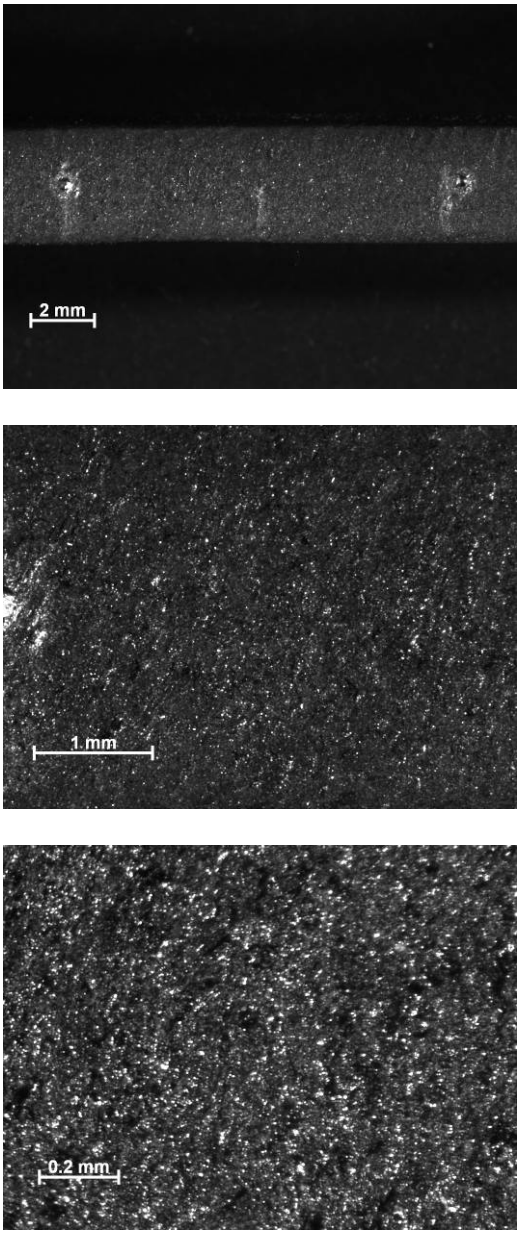

Figure 63 –Sample 12-05, PMR-15 neat resin aged in air for 10 h, T = 288°C, Creep stress = 10 MPa. =Machined with water jet showing slight microcracking.

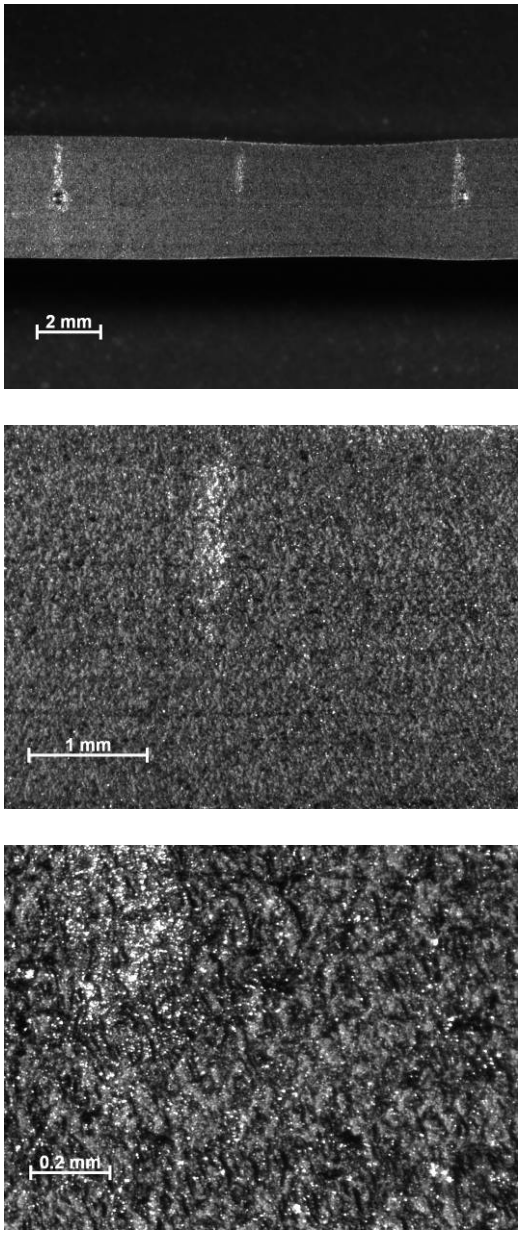

Figure 64 – Sample 11-05, PMR-15 neat resin aged in air for 10 h, T = 288°C, Creep stress = 20 MPa. Machined with diamond saw.

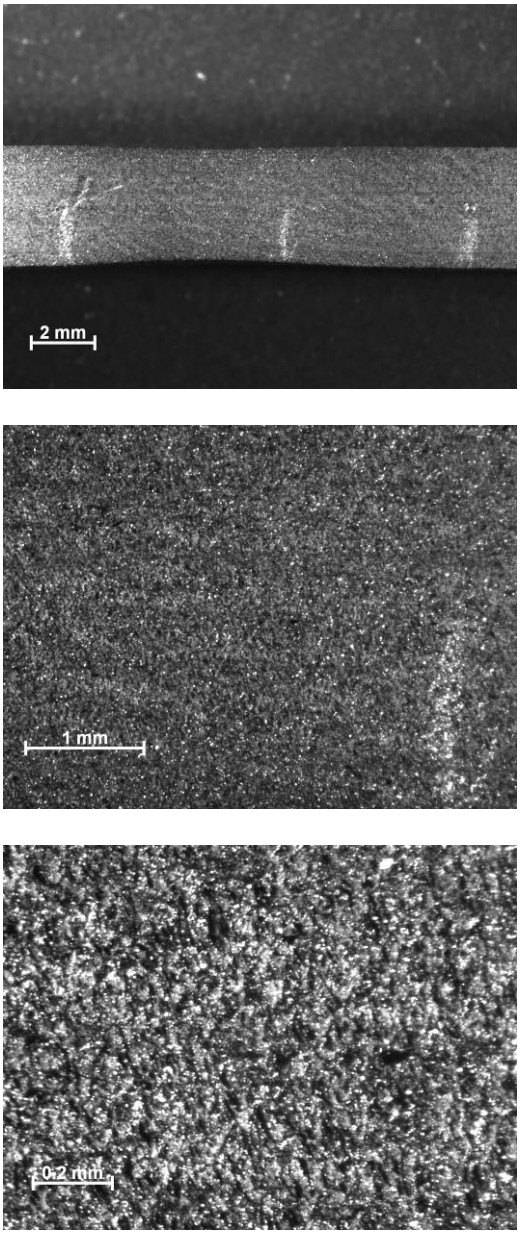

Figure 65 –Sample 02-02, PMR-15 neat resin aged in air for 50 h, T = 288°C, Creep stress = 20 MPa. Machined with diamond saw.

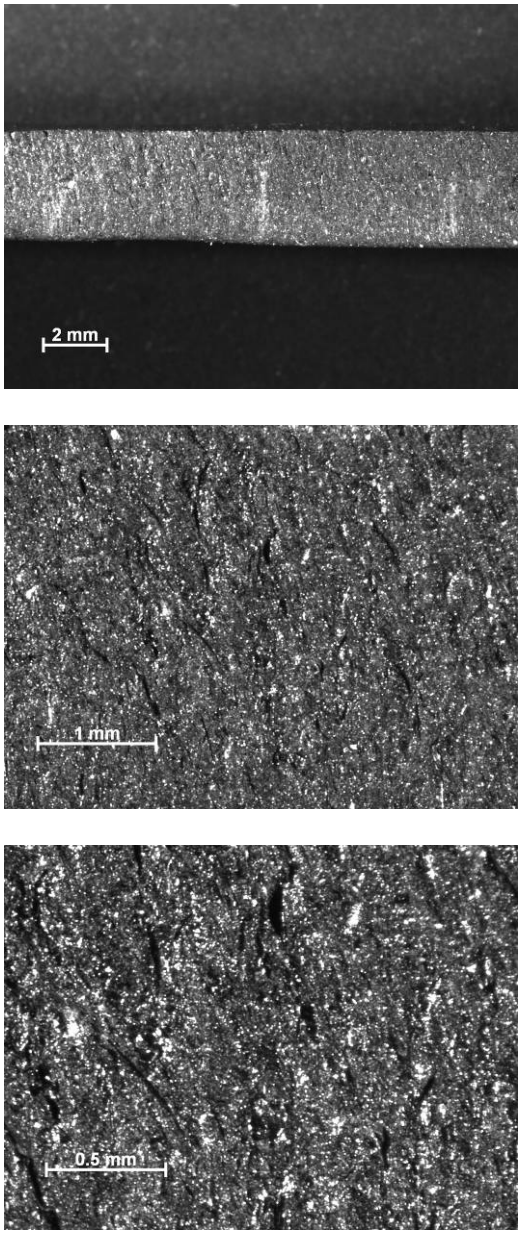

Figure 66 – Sample 13-12, PMR-15 neat resin aged in air for 50 h, T = 288°C, Creep stress = 20 MPa. Machined with water jet showing slight microcracking.

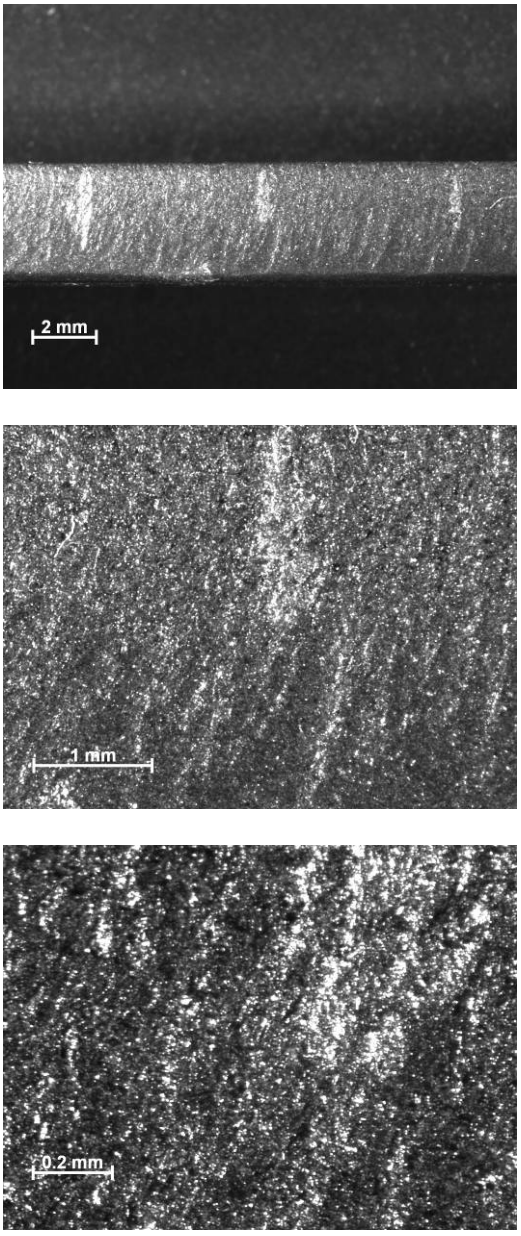

Figure 67 –Sample 12-02, PMR-15 neat resin aged in air for 50 h, T = 288°. Before testing, Machined with water jet.

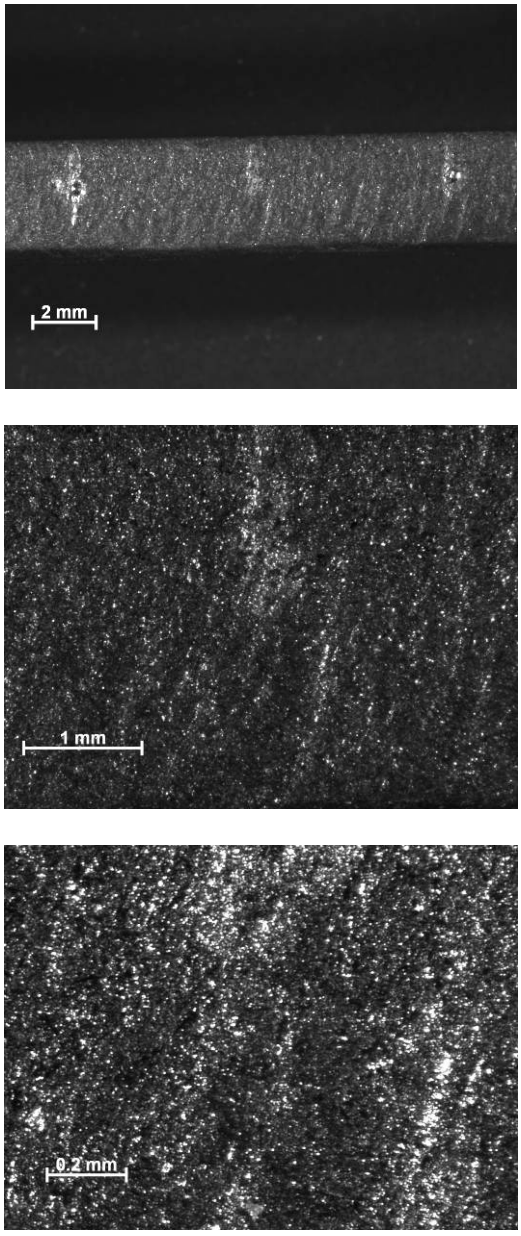

Figure 68 –Sample 12-02, PMR-15 neat resin aged in air for 50 h, T = 288°C, creep stress = 10 MPa. Machined with water jet.

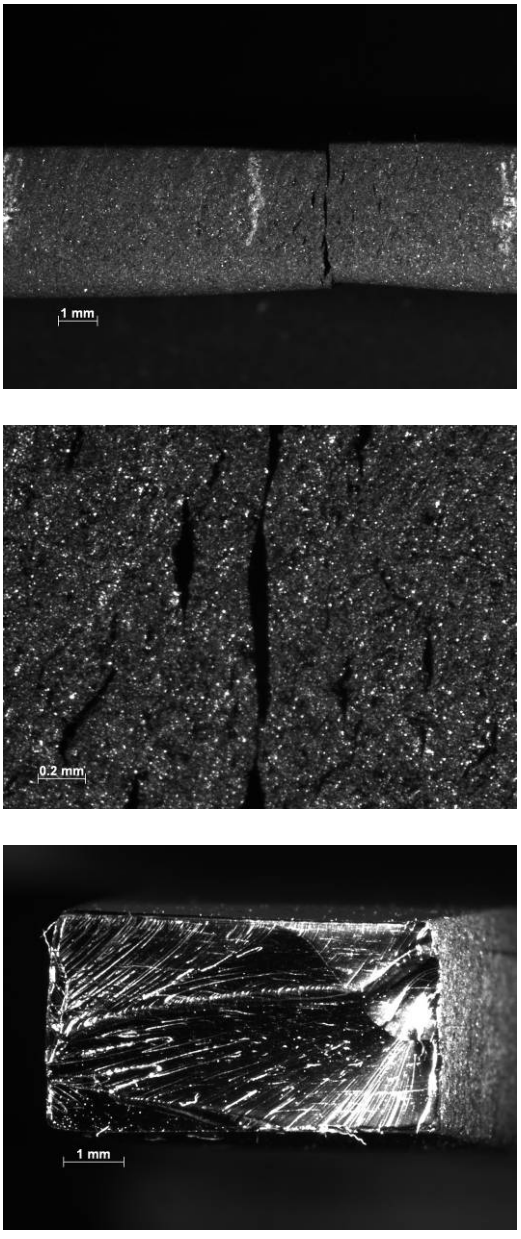

Figure 69 –Sample 12-18, PMR-15 neat resin aged in air for 100 h, T = 288°C, Creep stress = 20 MPa. Machined with water jet, showing slight microcracking.

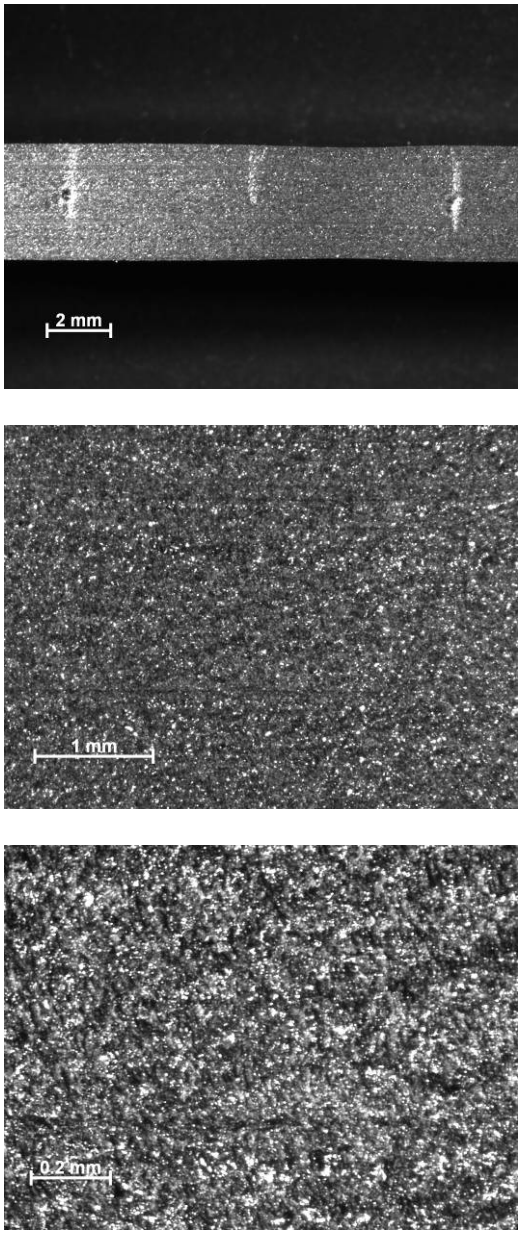

Figure 70 –Sample 02-04, PMR-15 neat resin aged in air for 100 h, T = 288°C, Creep stress = 20 MPa. Machined with diamond saw.

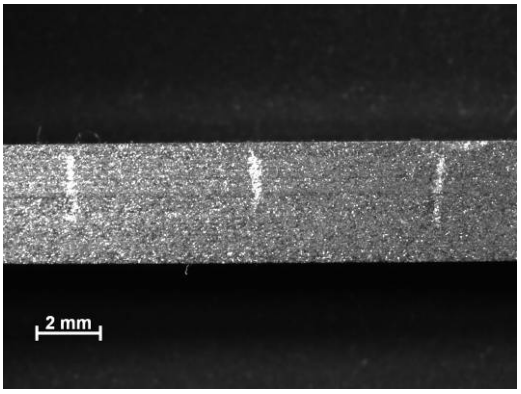

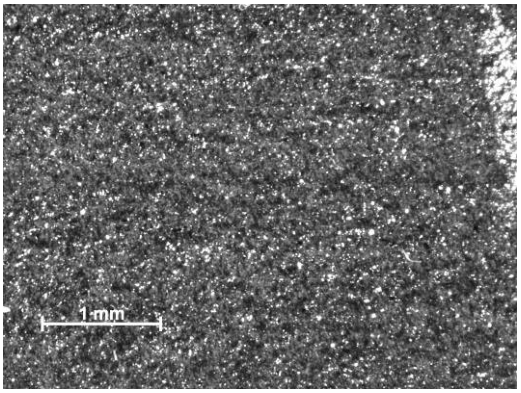

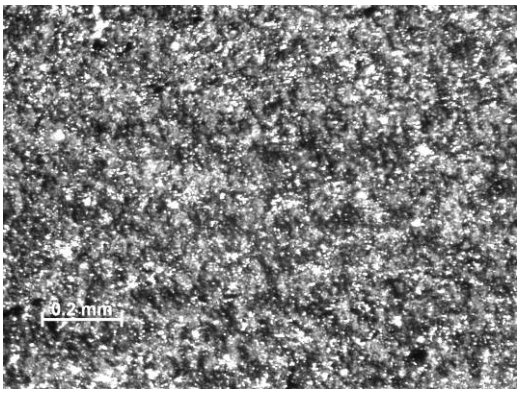

Figure 71 –Sample 11-16, PMR-15 neat resin aged in air for 100 h, T = 288°. Before testing, Machined with diamond saw.

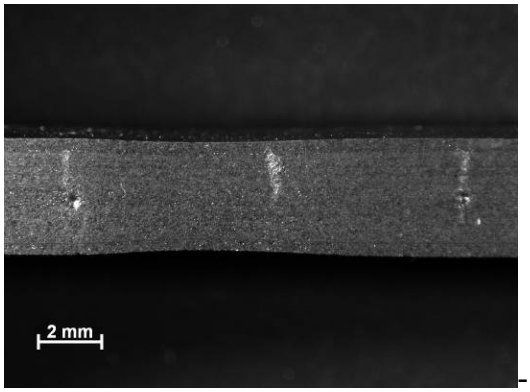

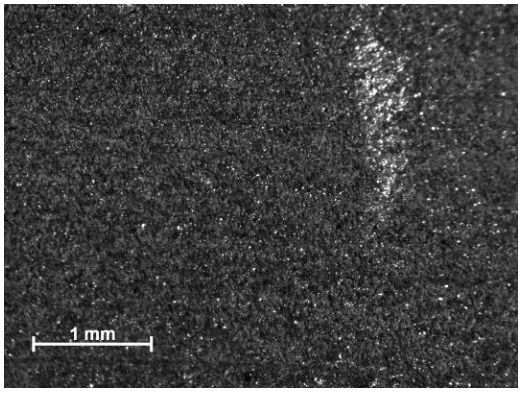

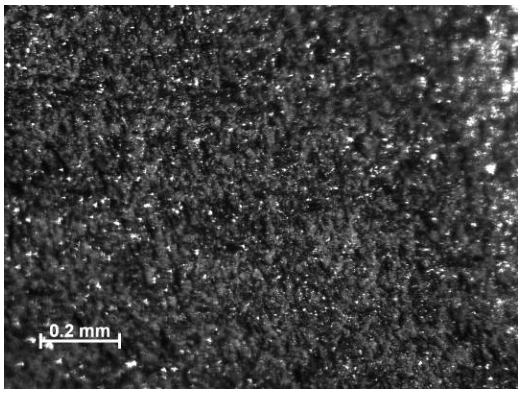

Figure 72 –Sample 11-16, PMR-15 neat resin aged in air for 100 h, T = 288°C, Creep stress = 20 MPa. Machined with diamond saw.

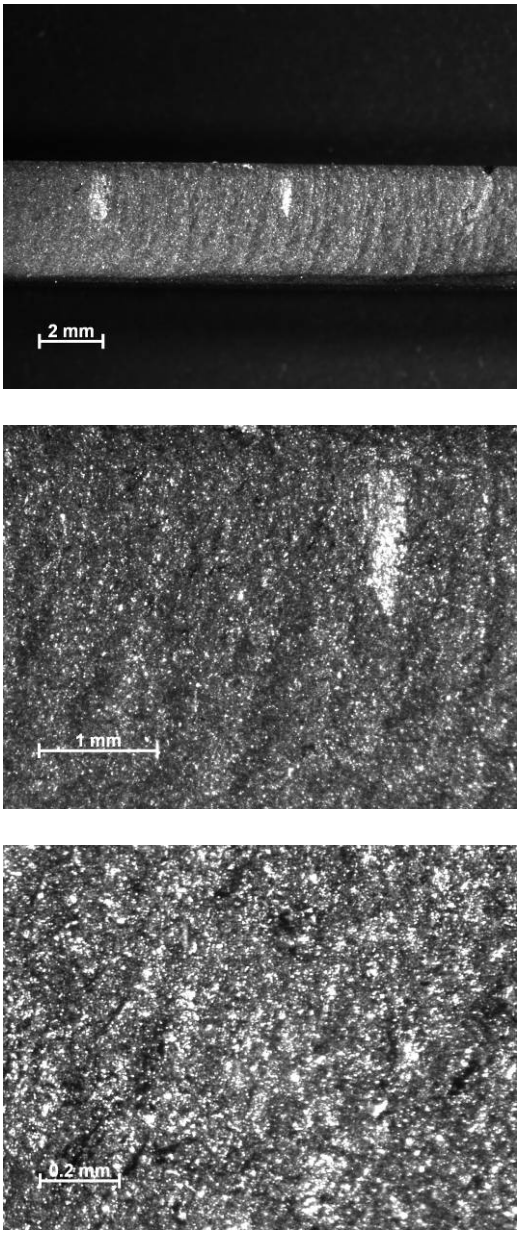

Figure 73 –Sample 12-16, PMR-15 neat resin aged in air for 100 h, T = 288°. Before testing, Machined with water jet.

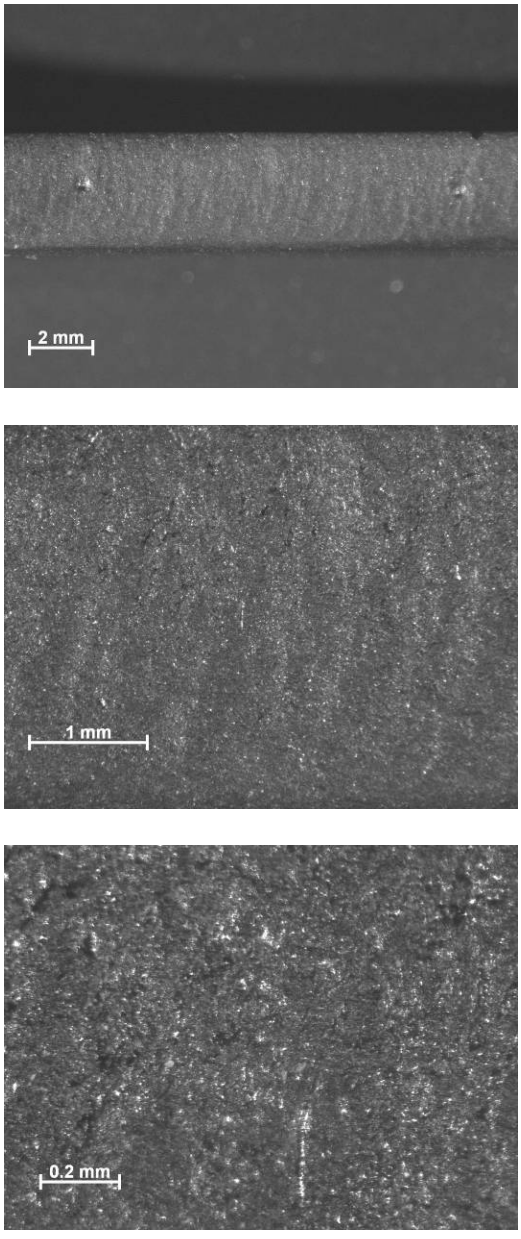

Figure 74 –Sample 12-16, PMR-15 neat resin aged in air for 100 h, T = 288°C, Creep stress = 20 MPa. Machined with water jet.

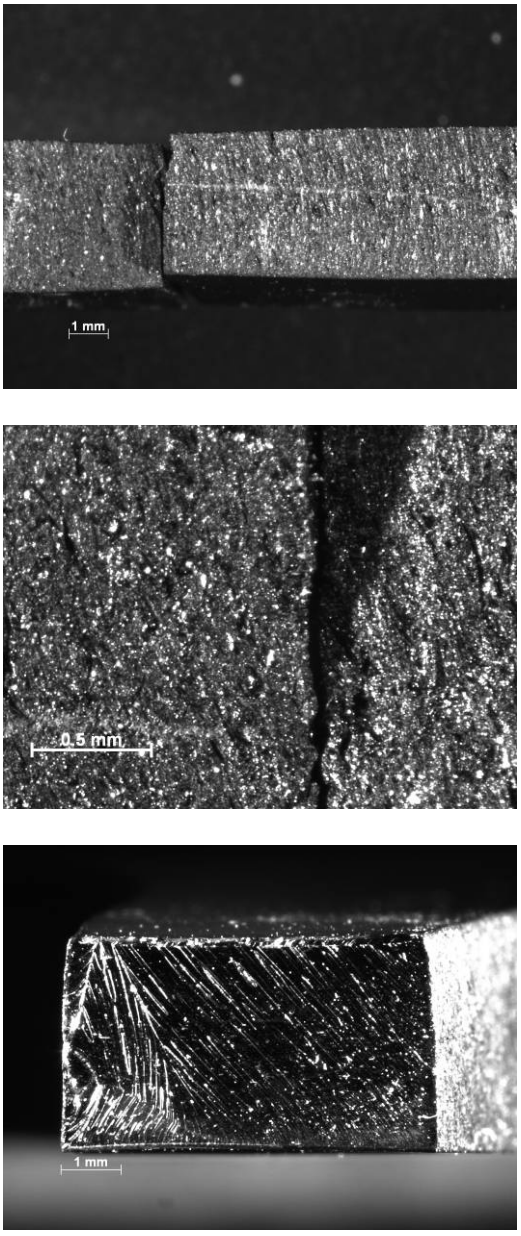

Figure 75 –Sample 13-09, PMR-15 neat resin aged in air for 250 h, T = 288°C, Creep stress = 20 MPa. Machined with water jet showing microcracking.

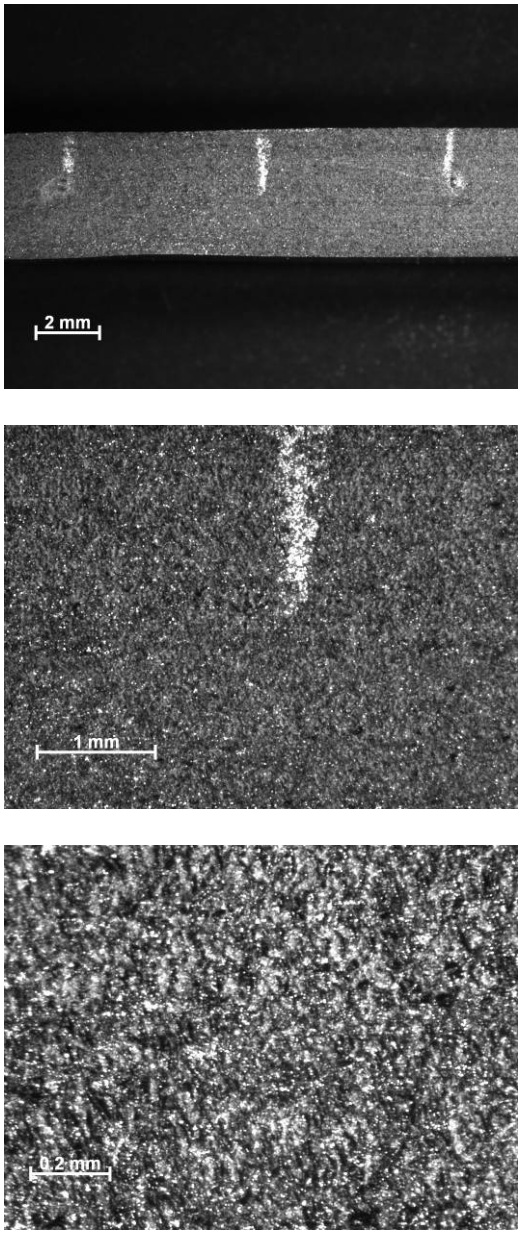

Figure 76 –Sample 12-04, PMR-15 neat resin aged in air for 250 h, T = 288°C, Creep stress = 20 MPa. Machined with diamond saw.

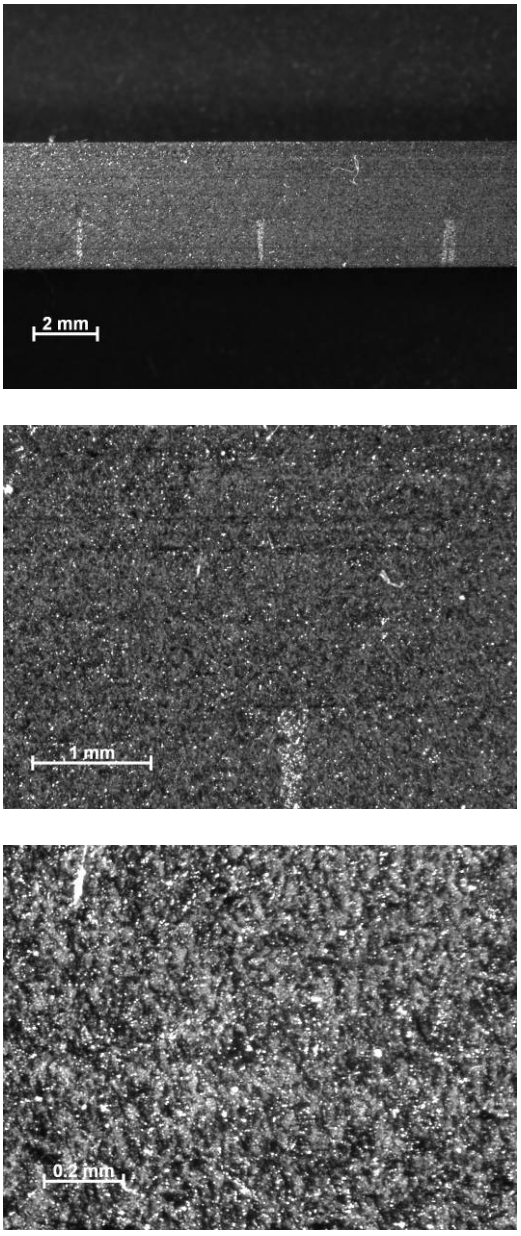

Figure 77 –Sample 02-05, PMR-15 neat resin aged in air for 250 h, T = 288°. Before testing, Machined with diamond saw.

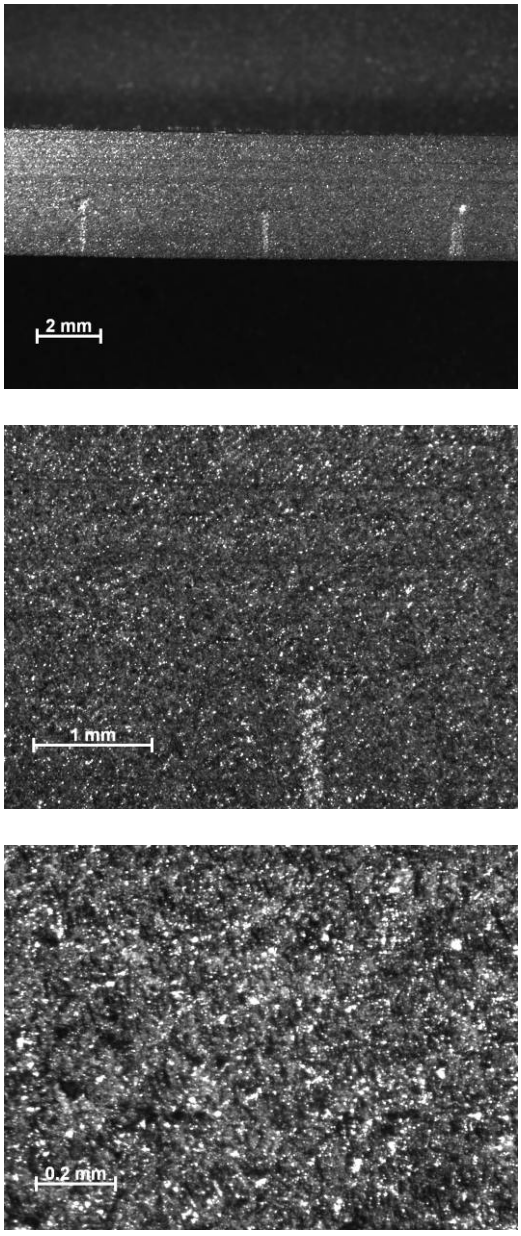

Figure 78 –Sample 02-05, PMR-15 neat resin aged in air for 250 h, T = 288°C, Creep stress = 10 MPa. Machined with diamond saw.

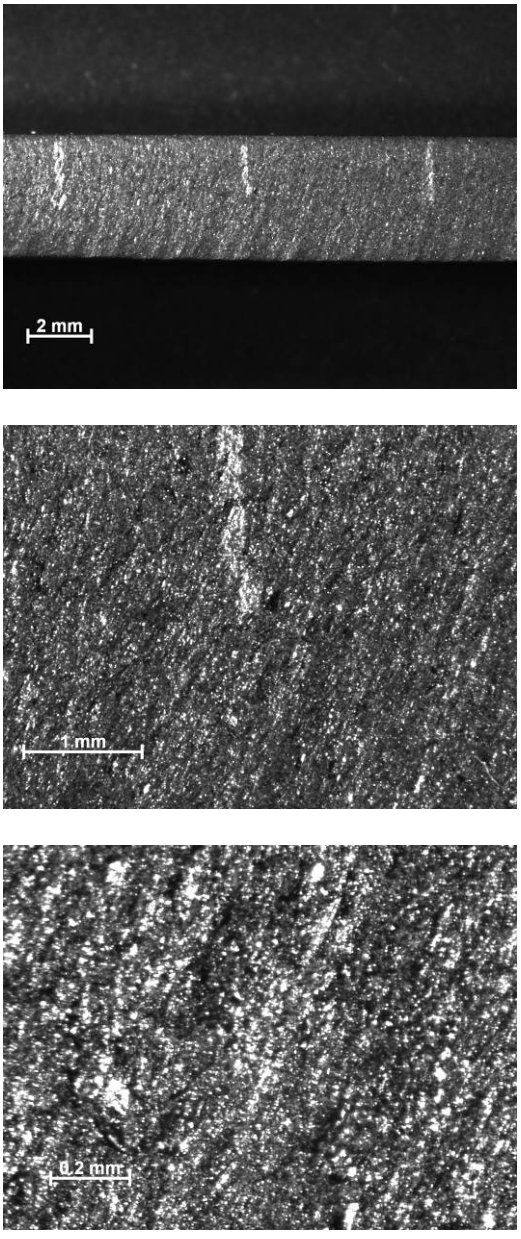

Figure 79 –sample 12-19, PMR-15 neat resin aged in air for 250 h, T = 288°. Before testing, Machined with water jet.

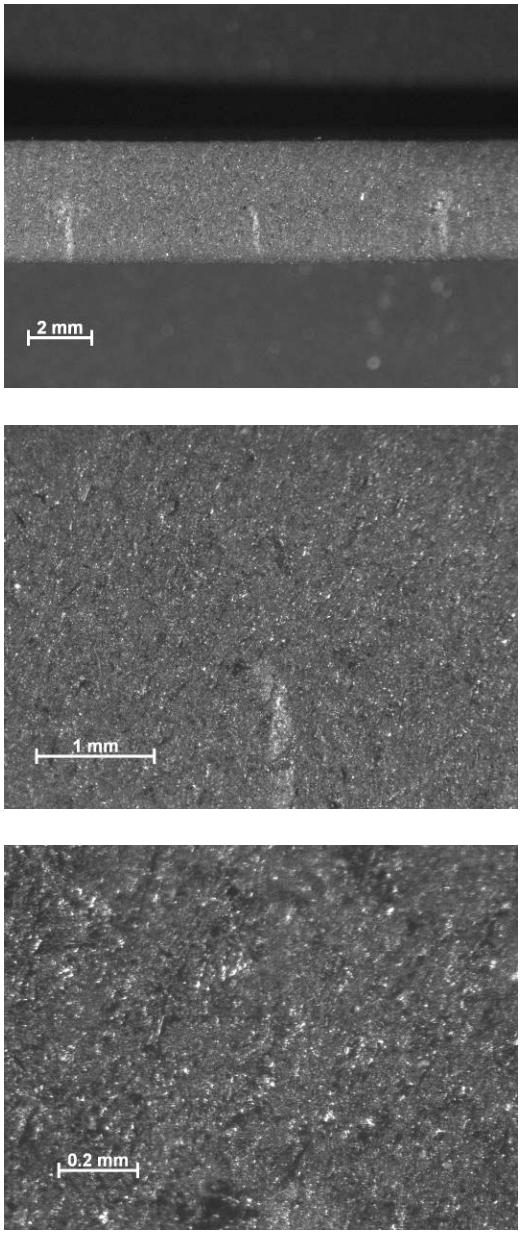

Figure 80 –Sample 12-19, PMR-15 neat resin aged in air for 250 h, T = 288°C, Creep stress = 10 MPa. Machined with water jet.

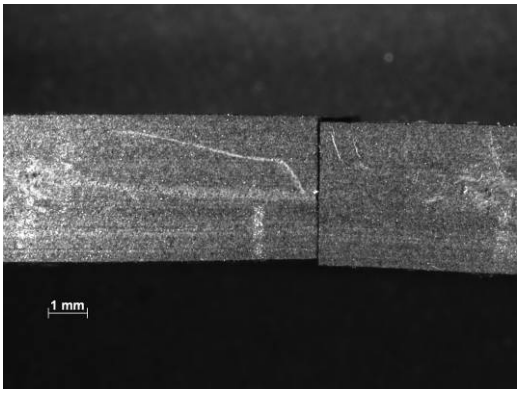

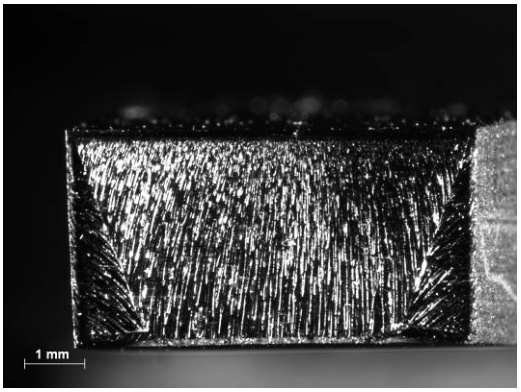

Figure 81 –Sample 02-06, PMR-15 neat resin aged in air for 500 h, T = 288°C, Creep stress = 20 MPa. Machined with diamond saw showing fracture line and surface.

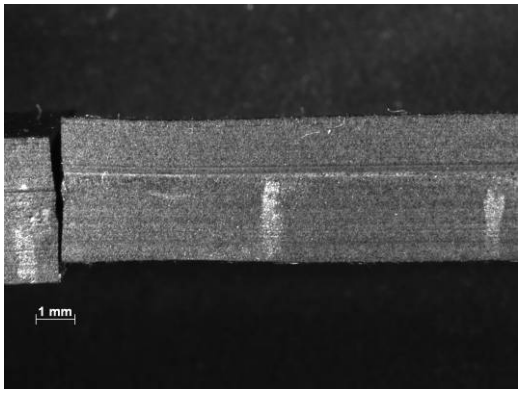

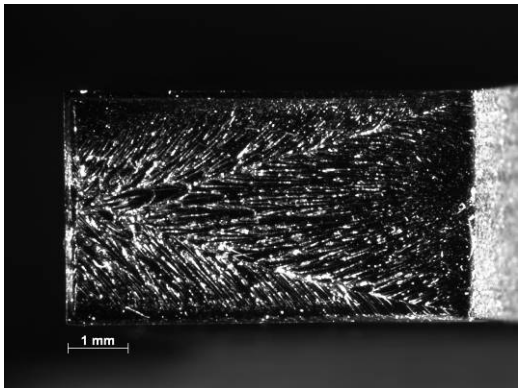

Figure 82 –Sample 11-18, PMR-15 neat resin aged in air for 500 h, T = 288°C, Creep stress = 20 MPa. Machined with diamond saw showing fracture line and surface.

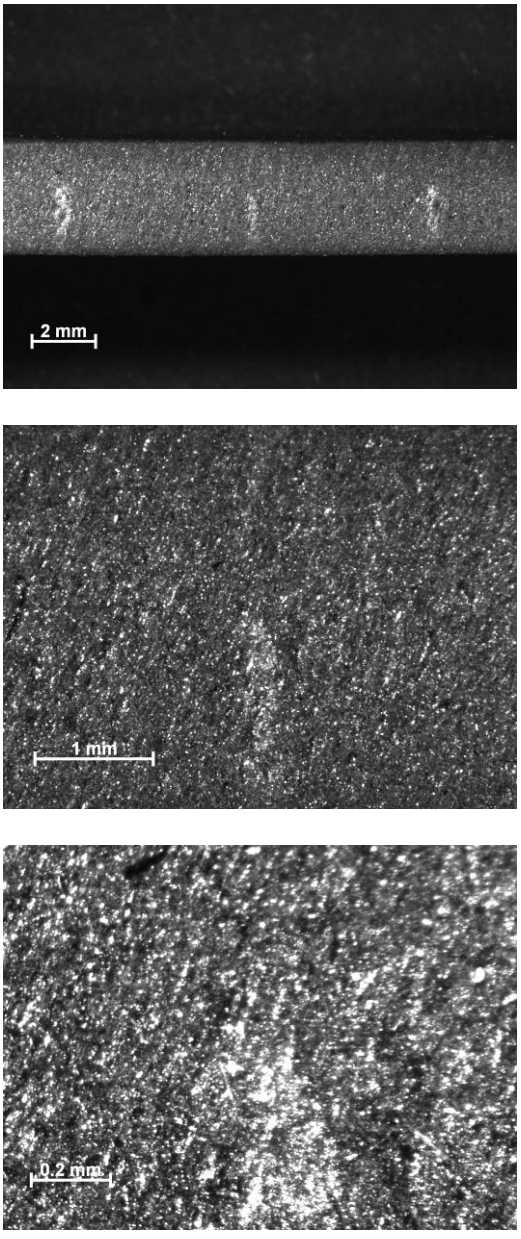

Figure 83 –Sample 12-08, PMR-15 neat resin aged in air for 500 h, T = 288°. Before testing, Machined with water jet.

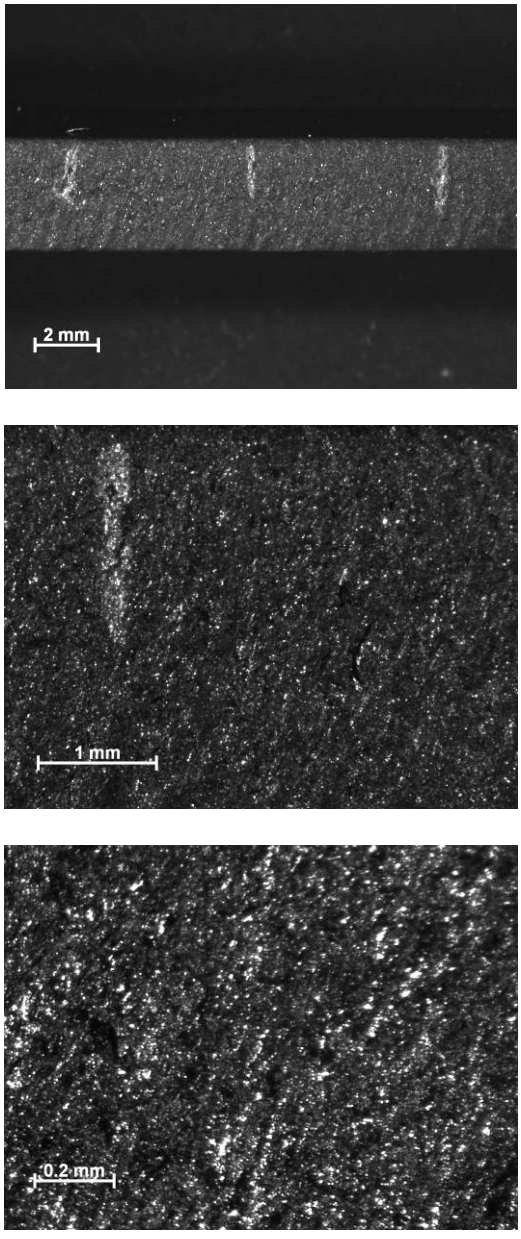

Figure 84 – Sample 12-08, PMR-15 neat resin aged in air for 500 h, T = 288°C, Creep stress = 10 MPa. Machined with water jet.

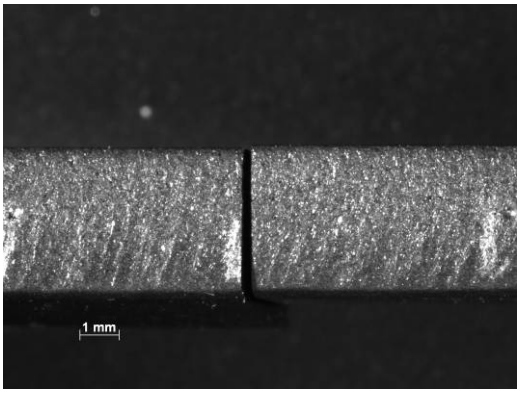

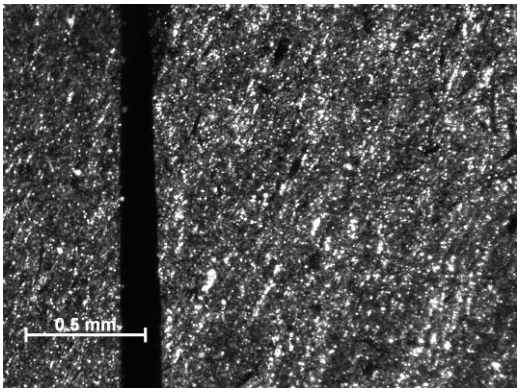

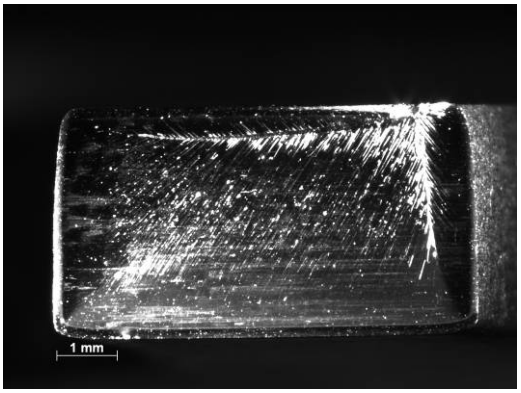

Figure 85 –Sample 12-01, PMR-15 neat resin aged in air for 1000 h, T = 288°C, Creep stress = 20 MPa. Machined with water jet showing slight microcracking around fracture line.

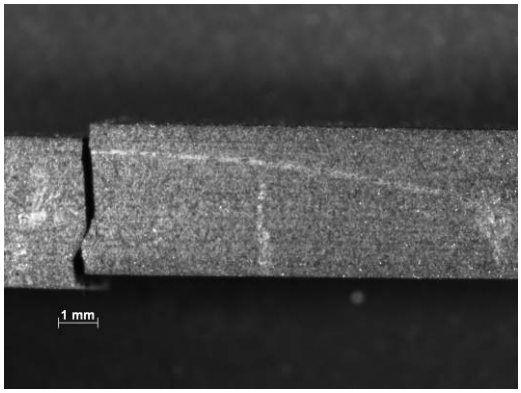

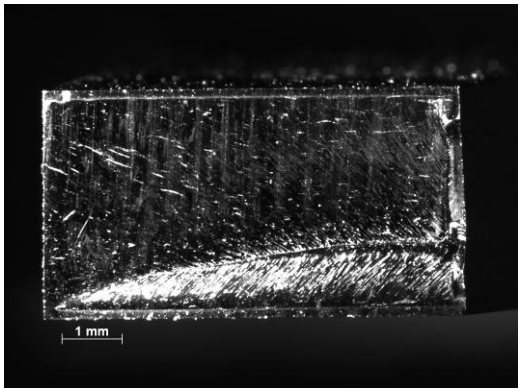

Figure 86 – Sample 12-13, PMR-15 neat resin aged in air for 1000 h, T = 288°C, Creep stress = 20 MPa. Machined with water jet showing fracture line and surface.

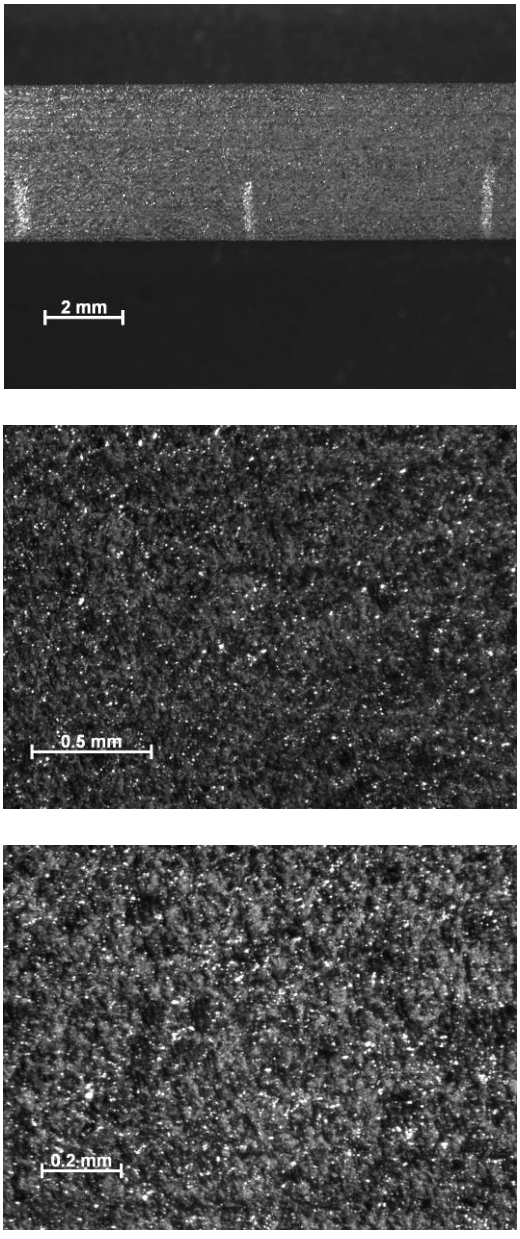

Figure 87 –Sample 02-07, PMR-15 neat resin aged in air for 1000 h, T = 288°. Before testing, Machined with diamond saw.

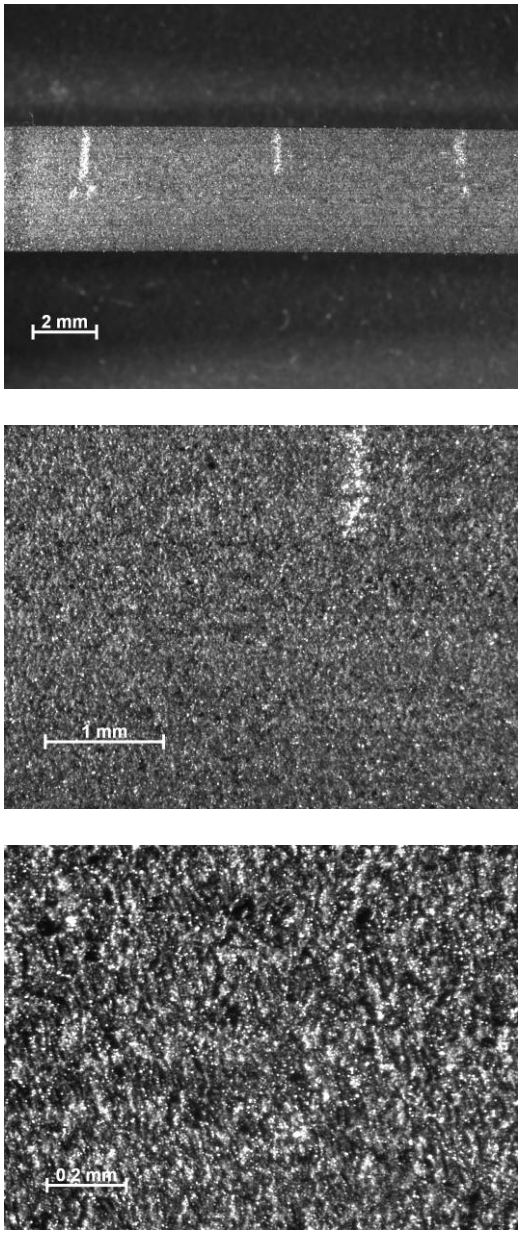

Figure 88 –Sample 02-07, PMR-15 neat resin aged in air for 1000 h, T = 288°C, Creep stress = 10 MPa. Machined with diamond saw.

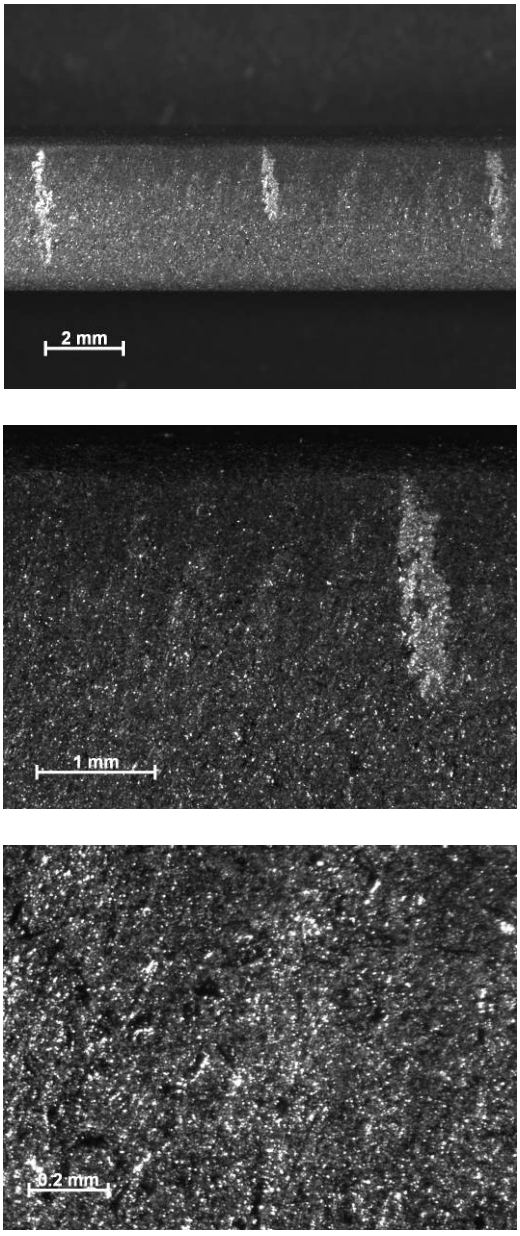

Figure 89 – Sample 12-06, PMR-15 neat resin aged in air for 1000 h, T = 288°. Before testing, Machined with water jet.

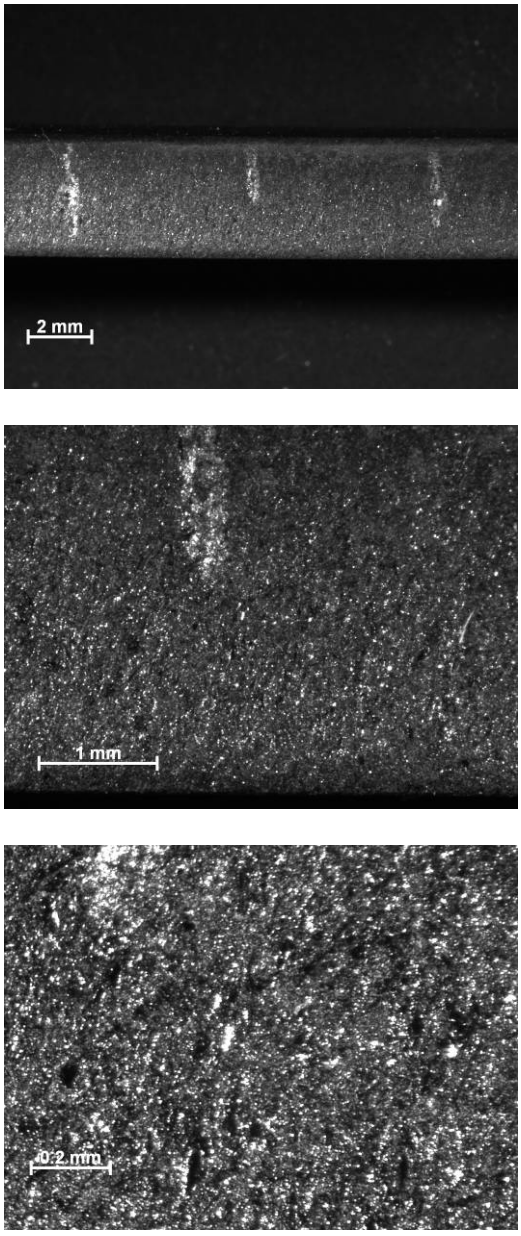

Figure 90 –Sample 12-06, PMR-15 neat resin aged in air for 1000 h, T = 288°C, Creep stress = 10 MPa. Machined with water jet showing slight microcracking..

Appendix B – Creep Sample Micrographs, Aged in Argon at 288°C

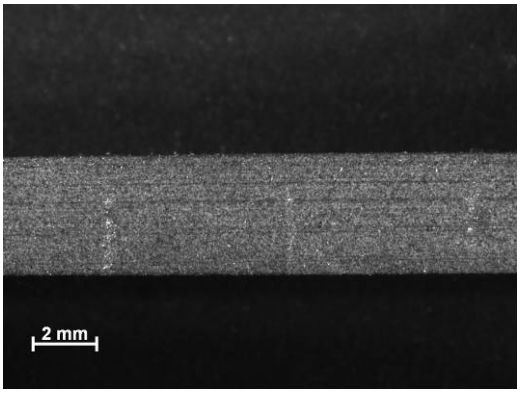

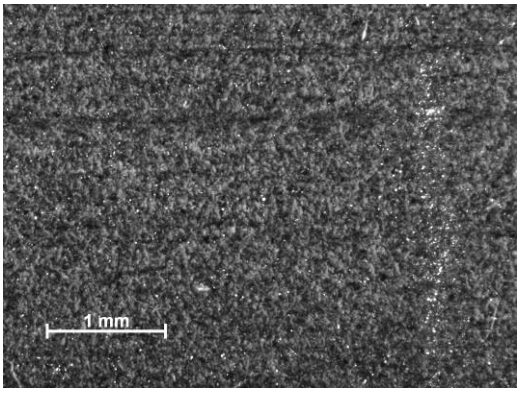

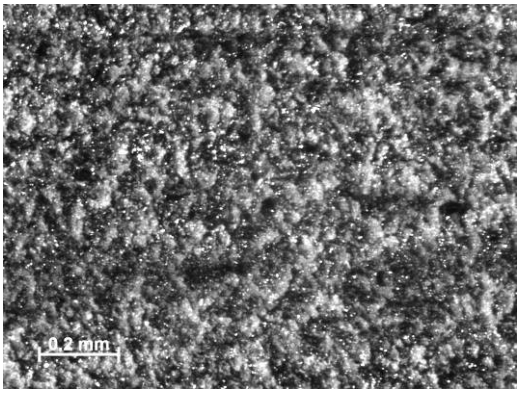

Figure 91 –Sample 11-10, PMR-15 neat resin aged in argon for 50 h, T = 288°. Before testing, Machined with diamond saw.

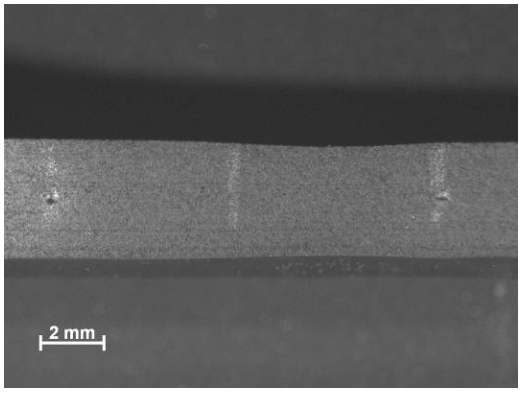

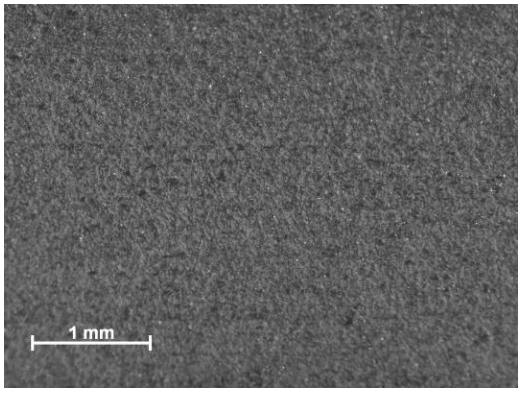

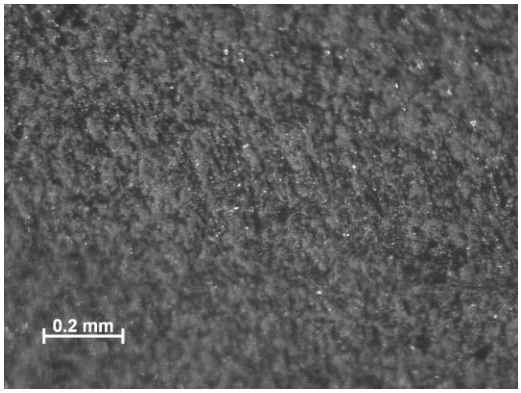

Figure 92 –Sample 11-10, PMR-15 neat resin aged in argon for 50 h, T = 288°C, Creep stress = 20 MPa. Machined with diamond saw.

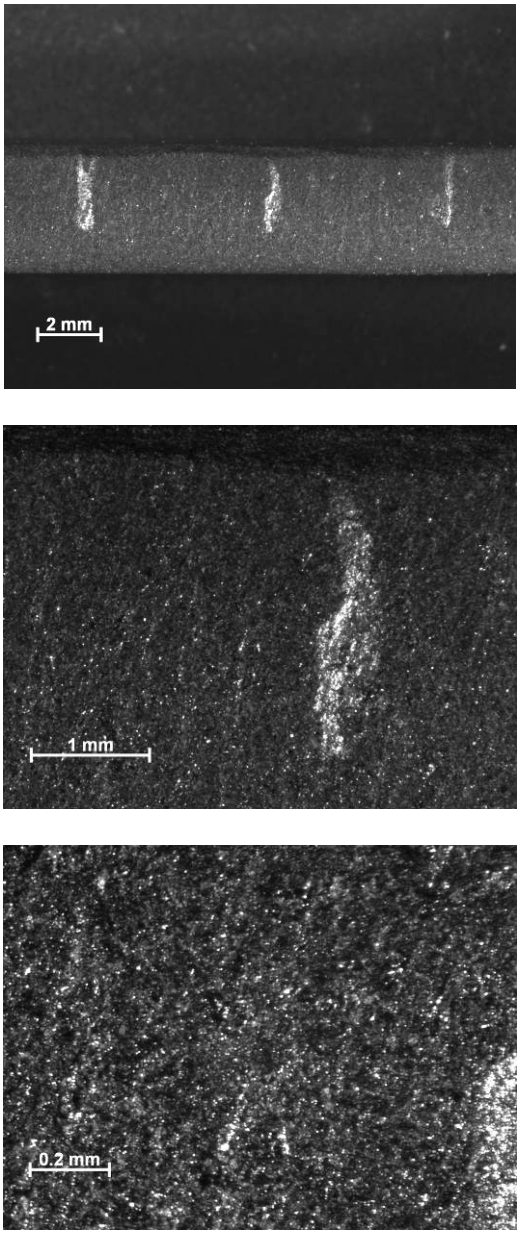

Figure 93 –Sample 12-07, PMR-15 neat resin aged in argon for 50 h, T = 288°. Before testing, Machined with water jet.

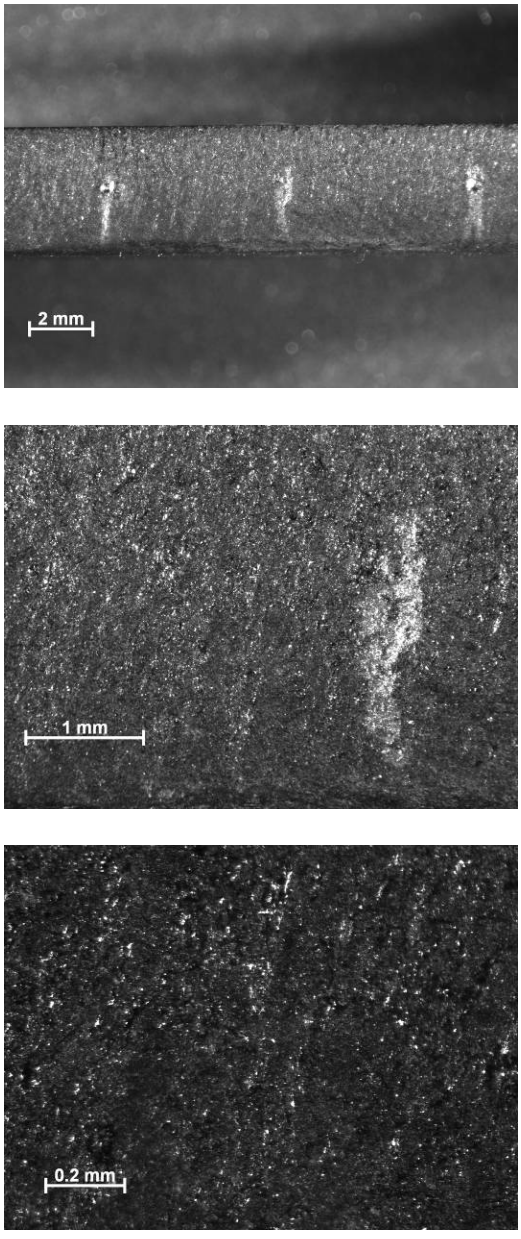

Figure 94 –Sample 12-07, PMR-15 neat resin aged in argon for 50 h, T = 288°C, Creep stress = 10 MPa. Machined with water jet.

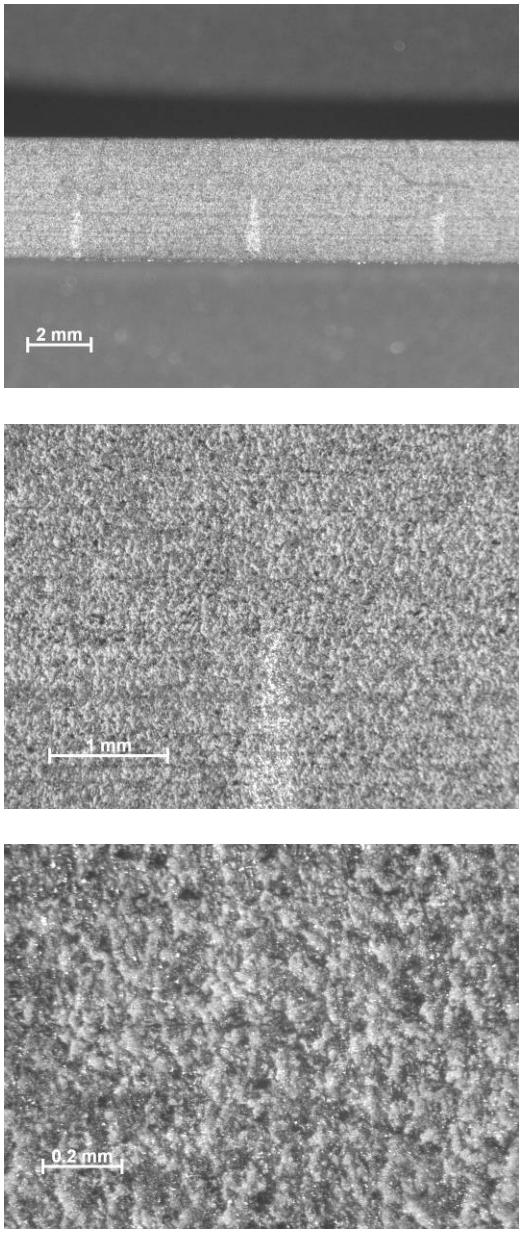

Figure 95 –Sample 11-03, PMR-15 neat resin aged in argon for 100 h, T = 288°. Before testing, Machined with diamond saw.

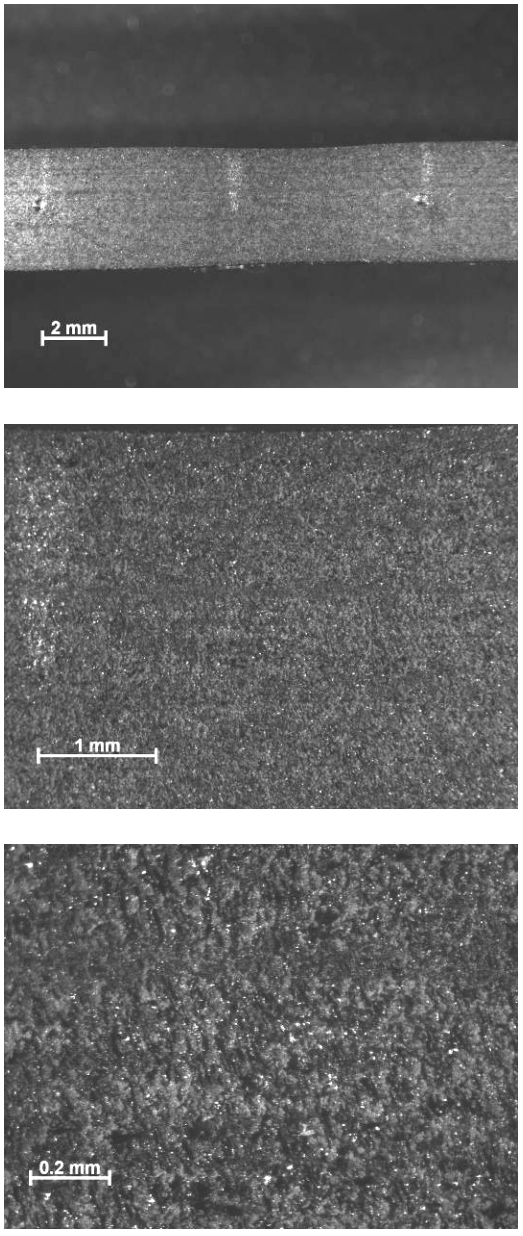

Figure 96 –Sample 11-03, PMR-15 neat resin aged in argon for 100 h, T = 288°C, Creep stress = 10 MPa. Machined with diamond saw.

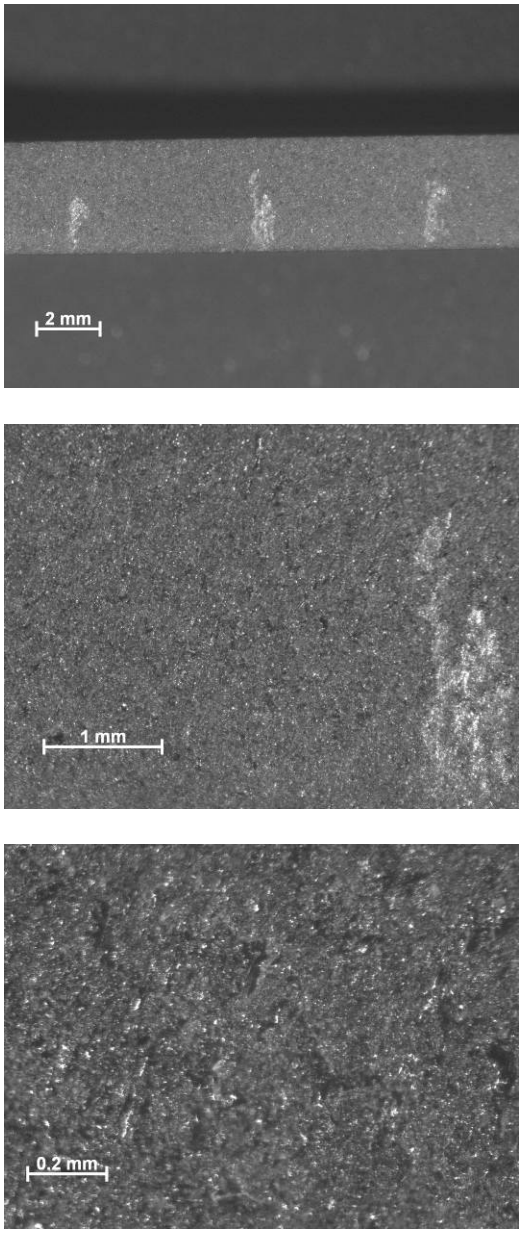

Figure 97 –Sample 12-14, PMR-15 neat resin aged in argon for 100 h, T = 288°. Before testing, Machined with water jet.

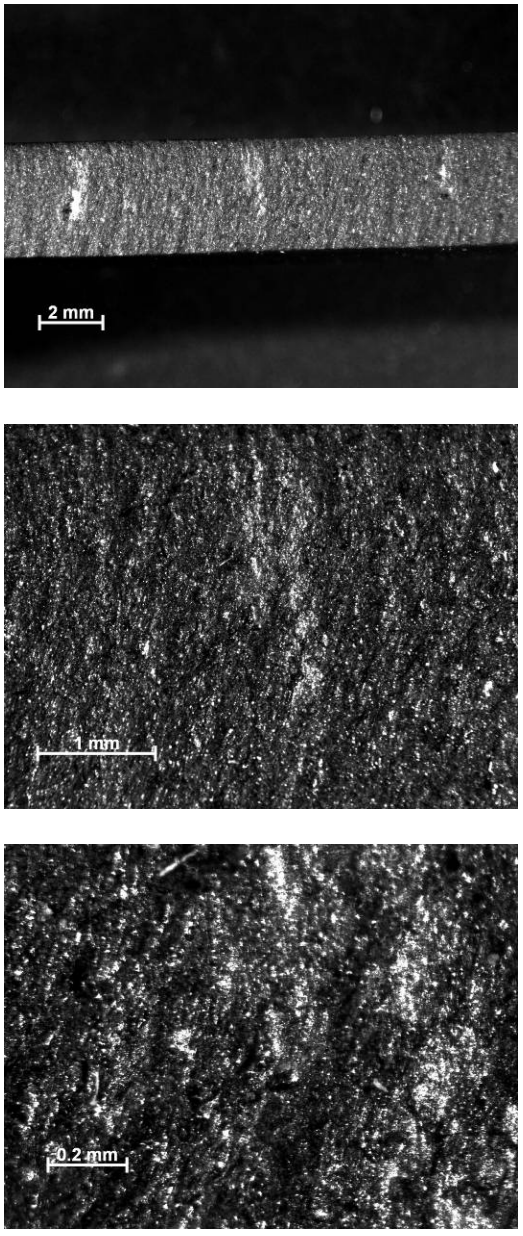

Figure 98 –Sample 12-14, PMR-15 neat resin aged in argon for 100 h, T = 288°C, Creep stress = 10 MPa. Machined with water jet.

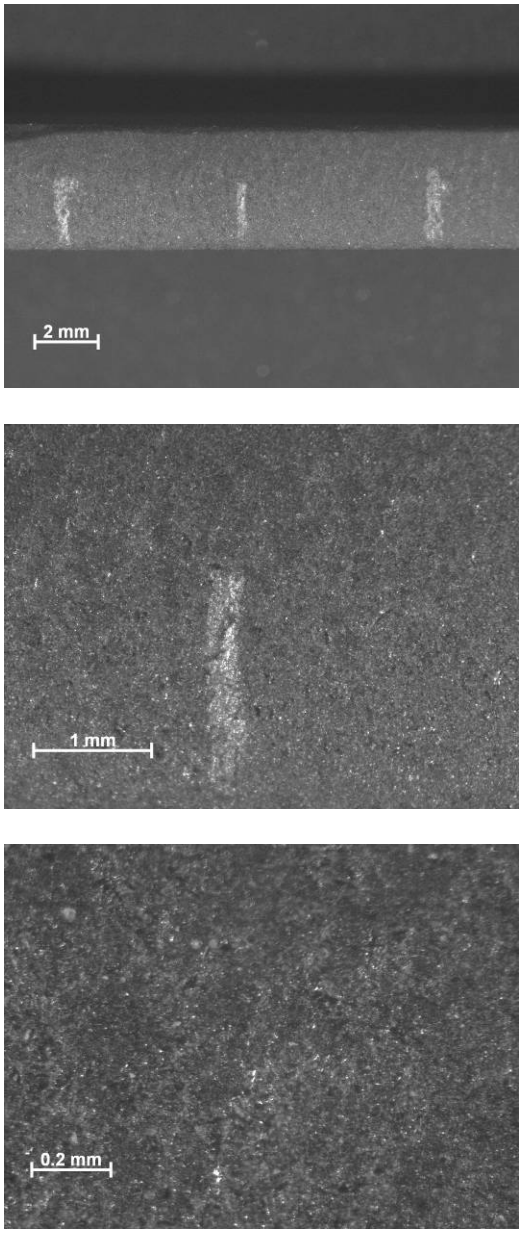

Figure 99 –Sample 12-15, PMR-15 neat resin aged in argon for 100 h, T = 288°. Before testing, Machined with water jet.

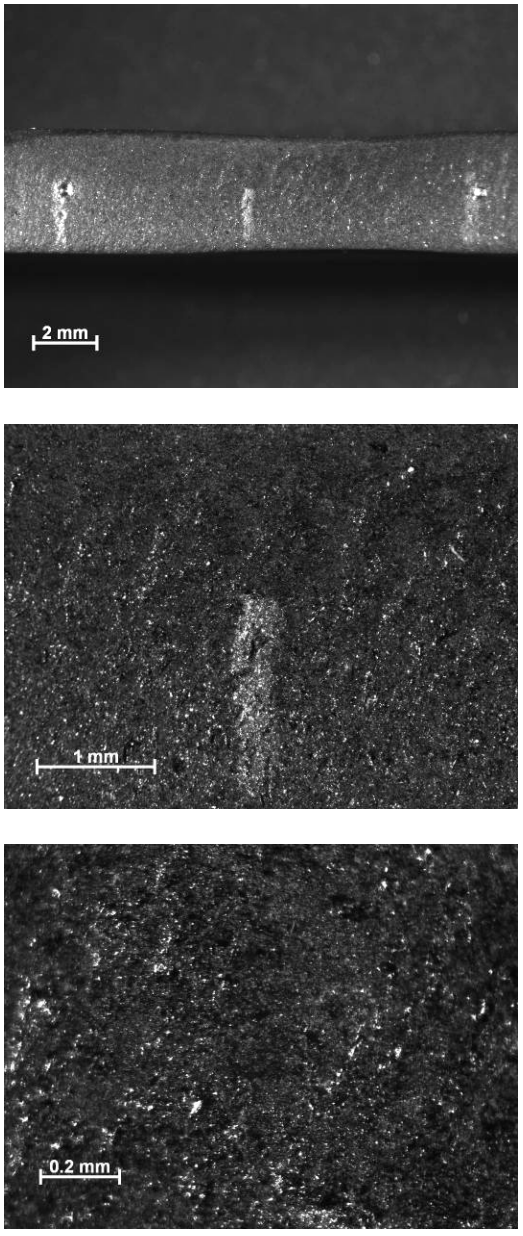

Figure 100 –Sample 12-15, PMR-15 neat resin aged in argon for 100 h, T = 288°C, Creep stress = 20 MPa. Machined with water jet.

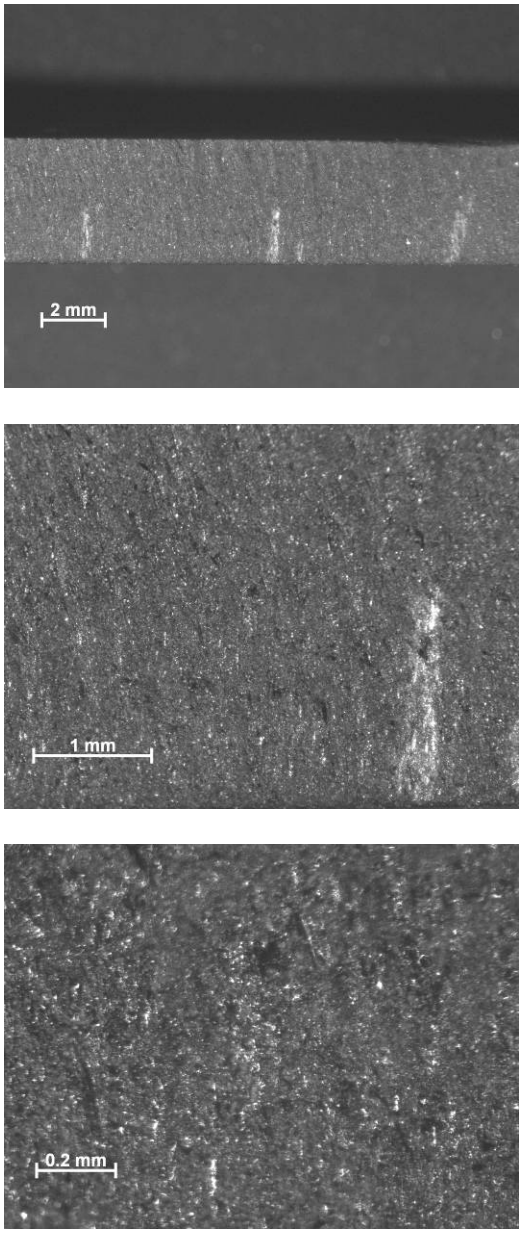

Figure 101 –Sample 13-03, PMR-15 neat resin aged in argon for 100 h, T = 288°. Before testing, Machined with water jet.

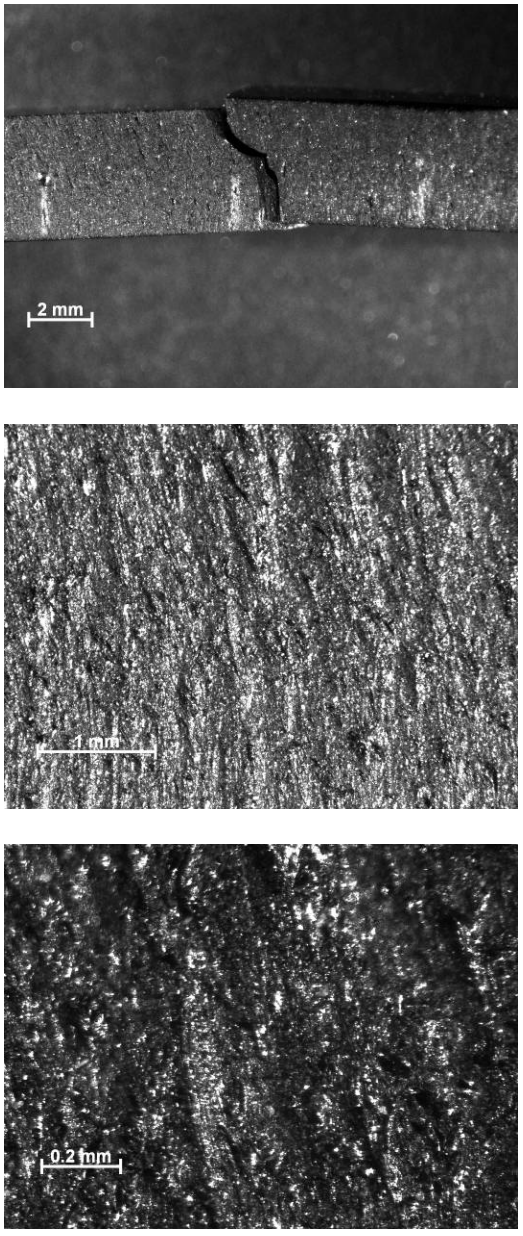

Figure 102 –Sample 13-03, PMR-15 neat resin aged in argon for 100 h, T = 288°C, Creep stress = 10 MPa. Machined with water jet.

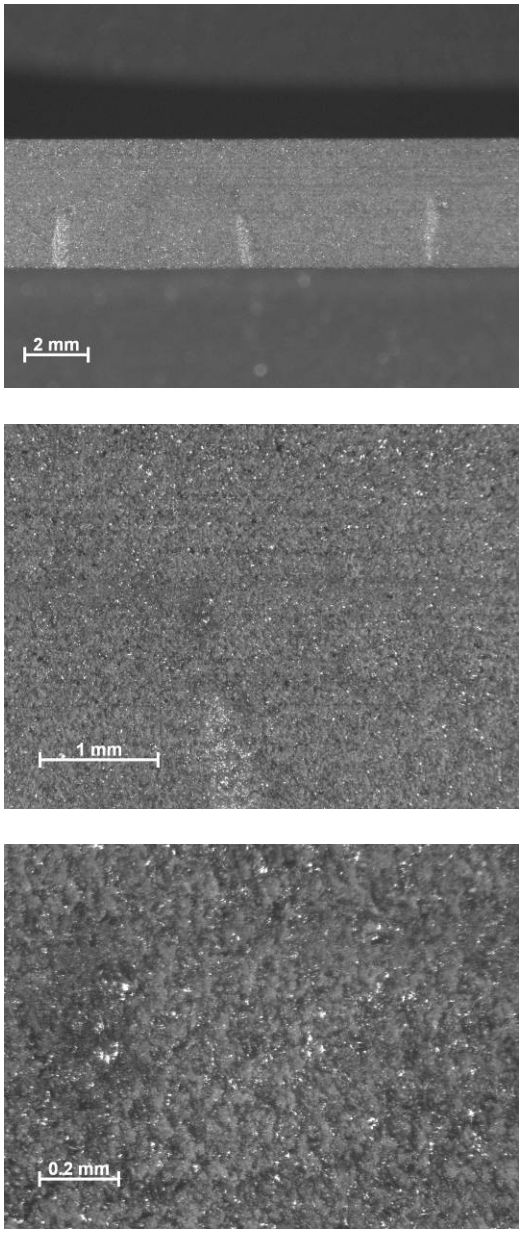

Figure 103 –Sample 11-18, PMR-15 neat resin aged in argon for 250 h, T = 288°. Before testing, Machined with diamond saw.

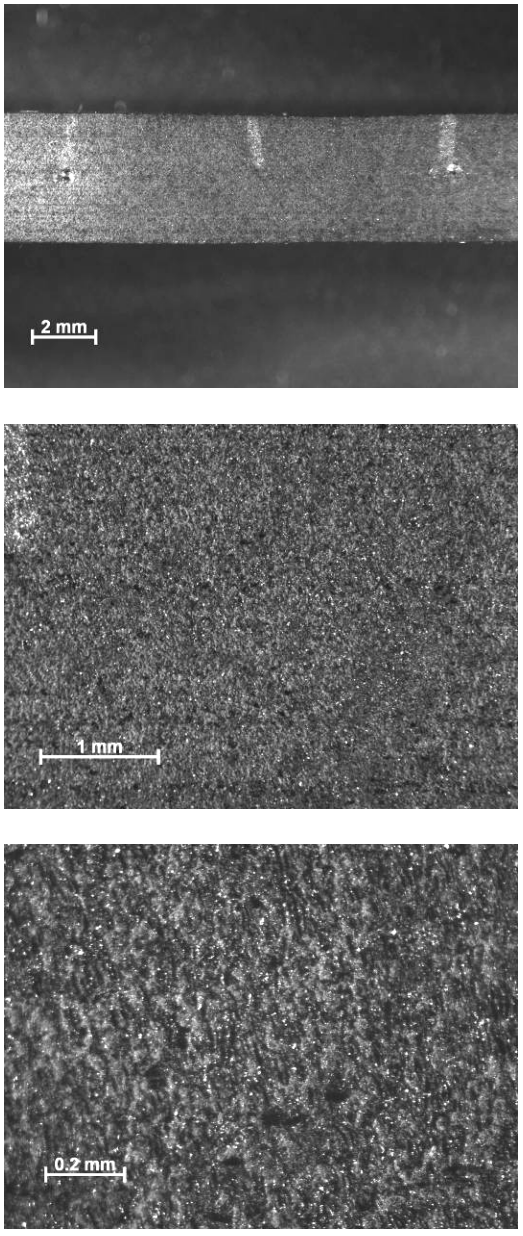

Figure 104 –Sample 11-18, PMR-15 neat resin aged in argon for 250 h, T = 288°C, Creep stress = 20 MPa. Machined with diamond saw.

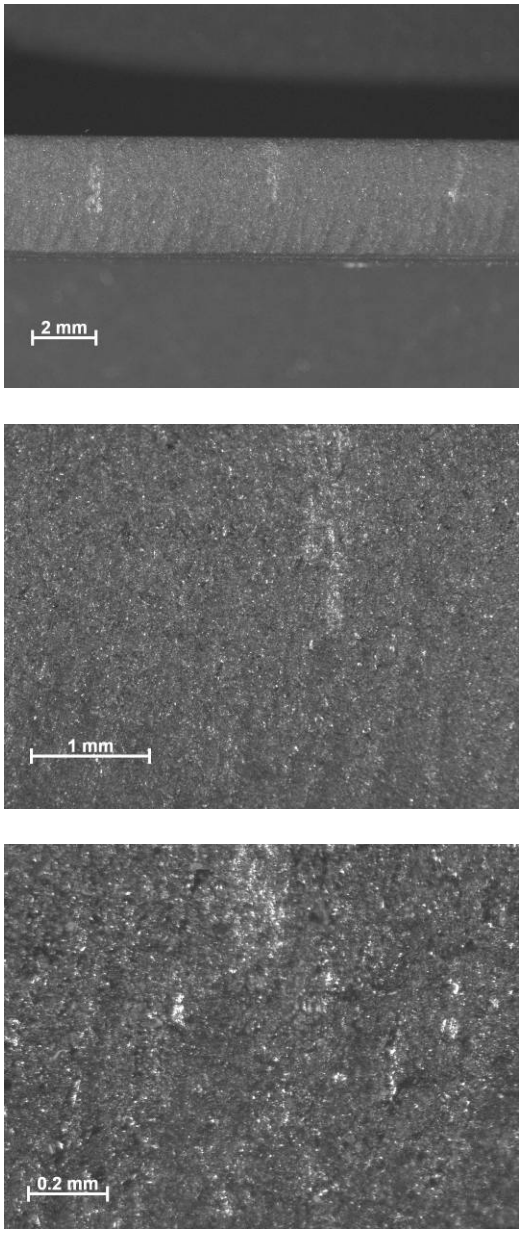

Figure 105 –Sample 12-12, PMR-15 neat resin aged in argon for 250 h, T = 288°. Before testing, Machined with water jet.

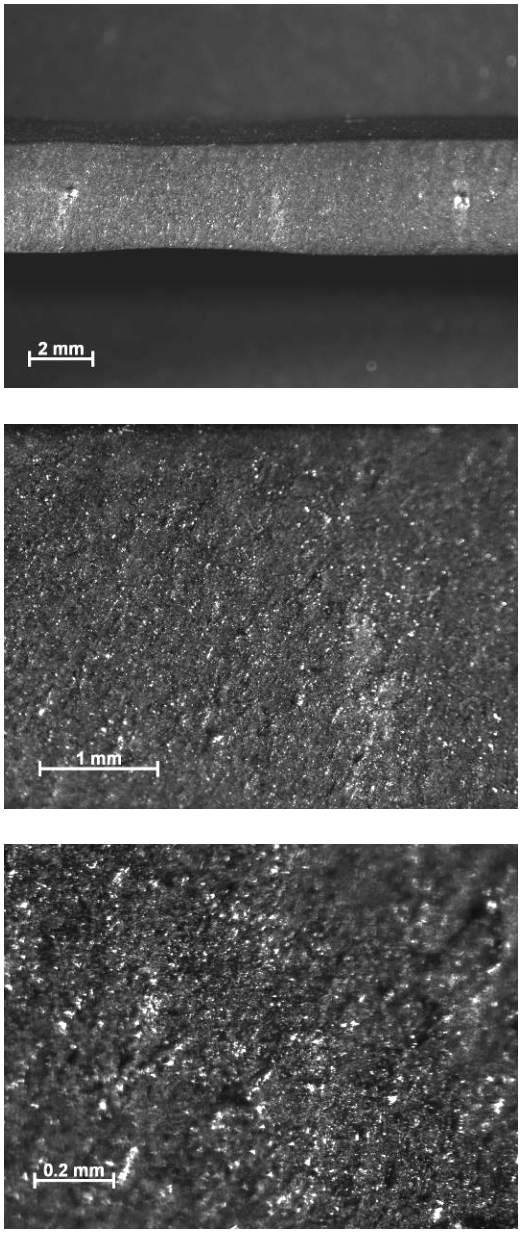

Figure 106 –Sample 12-12, PMR-15 neat resin aged in argon for 250 h, T = 288°C, Creep stress = 20 MPa. Machined with water jet.

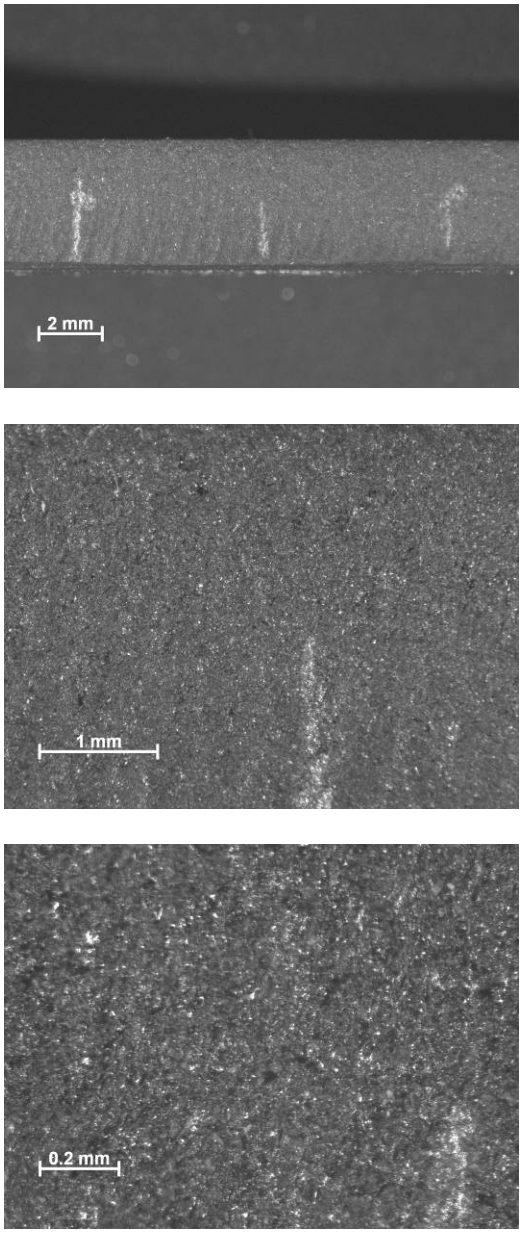

Figure 107 –Sample 12-13, PMR-15 neat resin aged in argon for 250 h, T = 288°. Before testing, Machined with water jet.

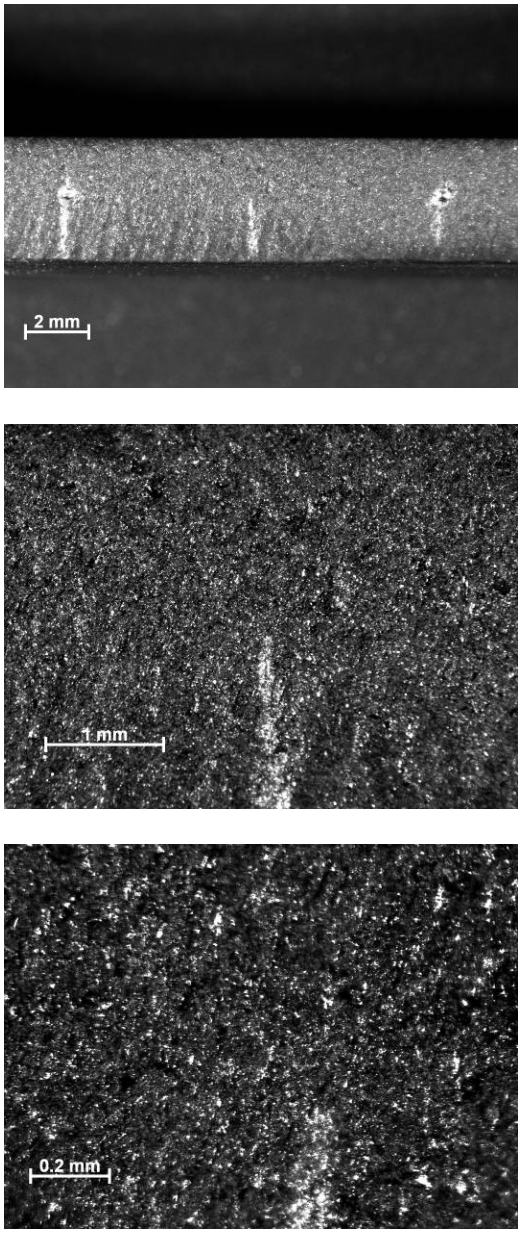

Figure 108 –Sample 12-13, PMR-15 neat resin aged in argon for 250 h, T = 288°C, Creep stress = 10 MPa. Machined with water jet.

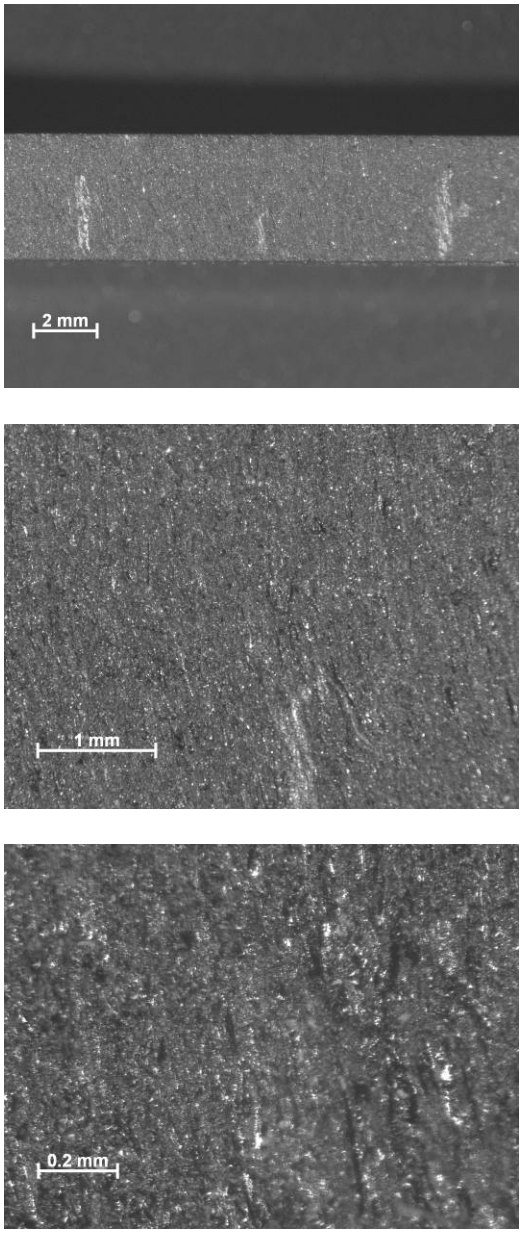

Figure 109 –Sample 13-04, PMR-15 neat resin aged in argon for 250 h, T = 288°. Before testing, Machined with water jet.

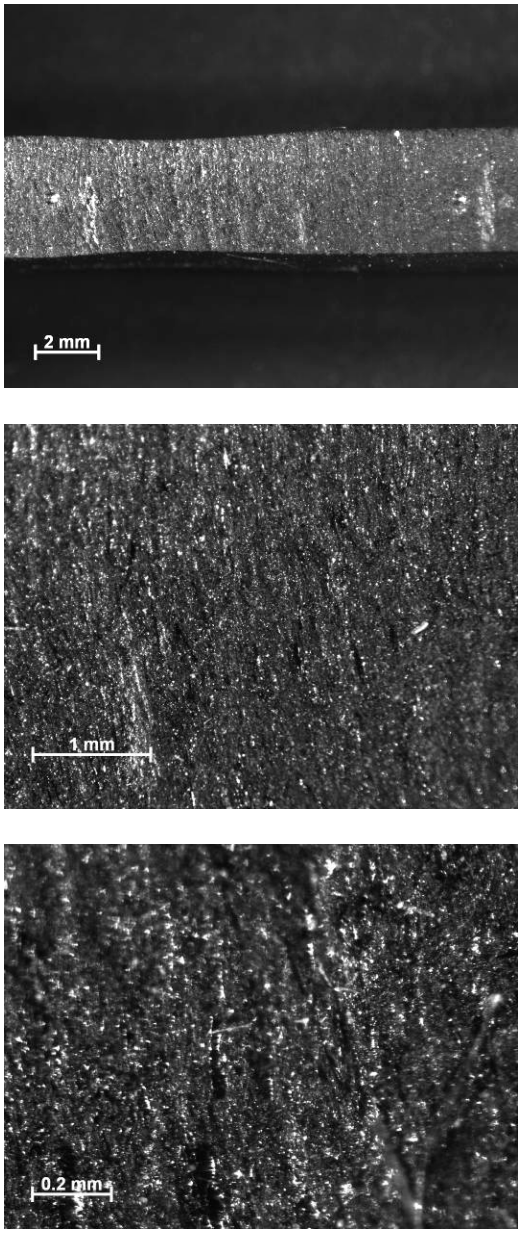

Figure 110 –Sample 13-04, PMR-15 neat resin aged in argon for 250 h, T = 288°C, Creep stress = 20 MPa. Machined with water jet showing slight microcracking.

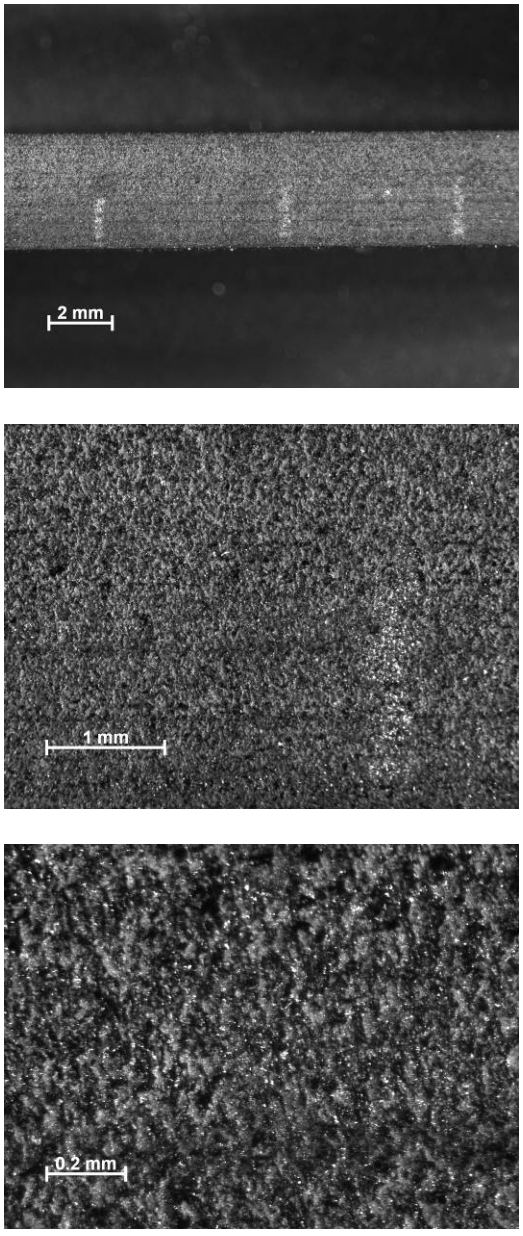

Figure 111 –Sample 11-09, PMR-15 neat resin aged in argon for 500 h, T = 288°. Before testing, Machined with diamond saw.

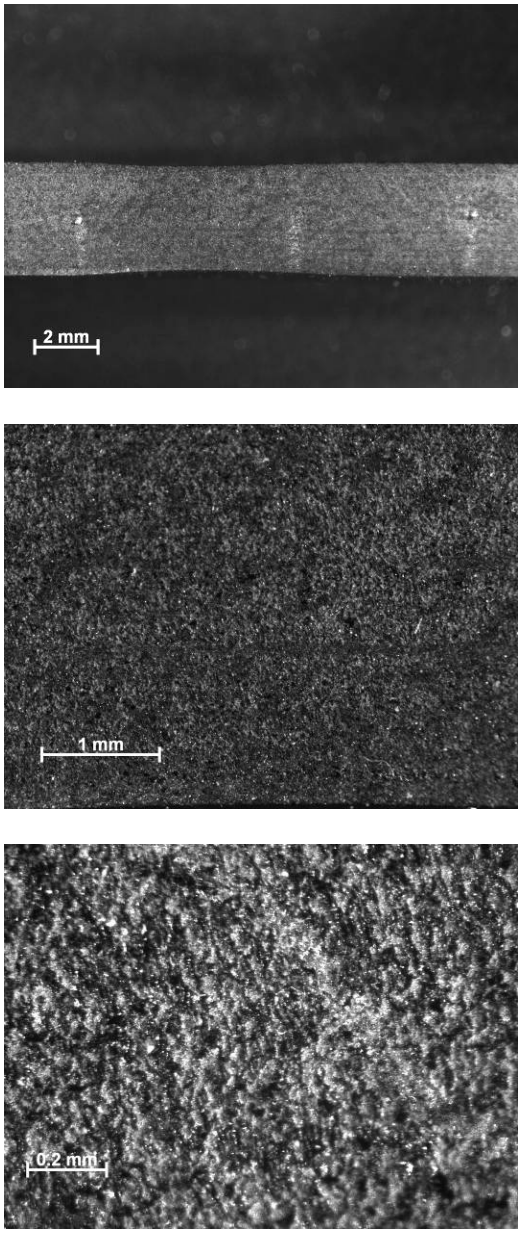

Figure 112 –Sample 11-09, PMR-15 neat resin aged in argon for 500 h, T = 288°C, Creep stress = 20 MPa. Machined with diamond saw.

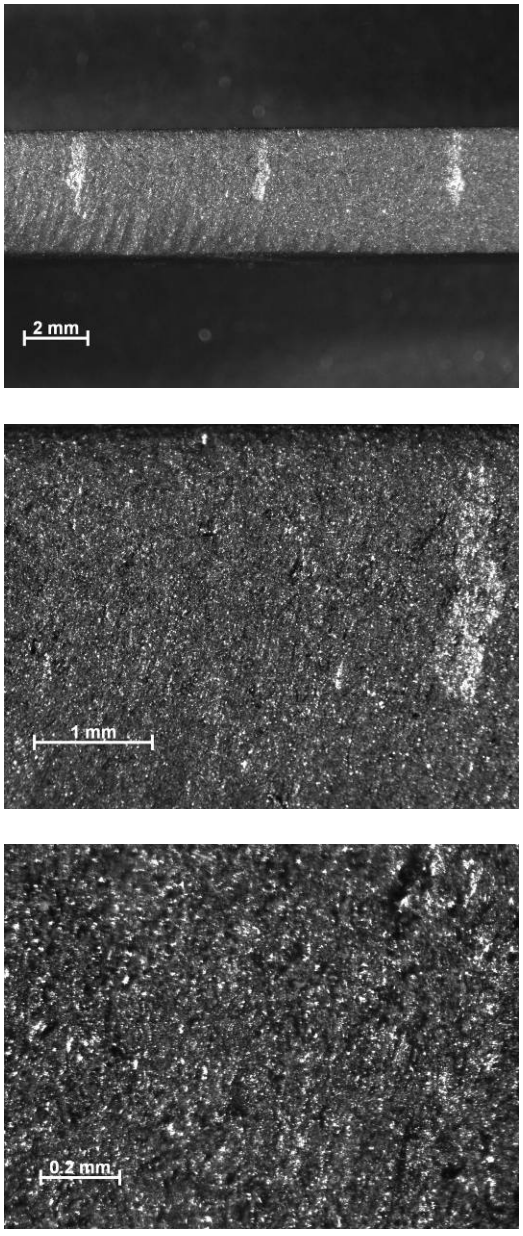

Figure 113 –Sample 12-04, PMR-15 neat resin aged in argon for 500 h, T = 288°. Before testing, Machined with water jet.

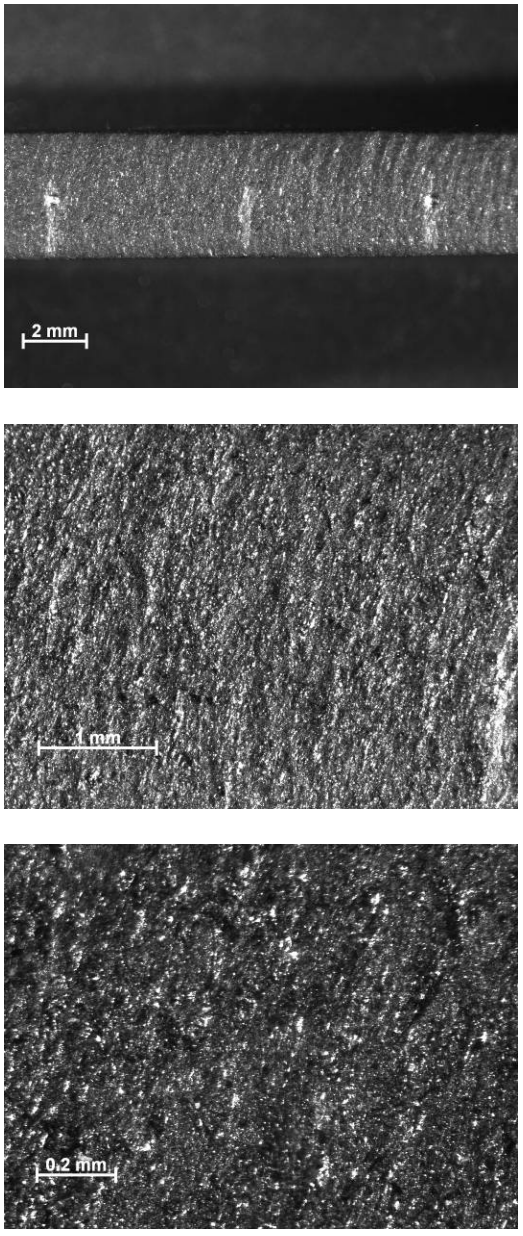

Figure 114 –Sample 12-04, PMR-15 neat resin aged in argon for 500 h, T = 288°C, creep stress = 10 MPa. Machined with water jet.

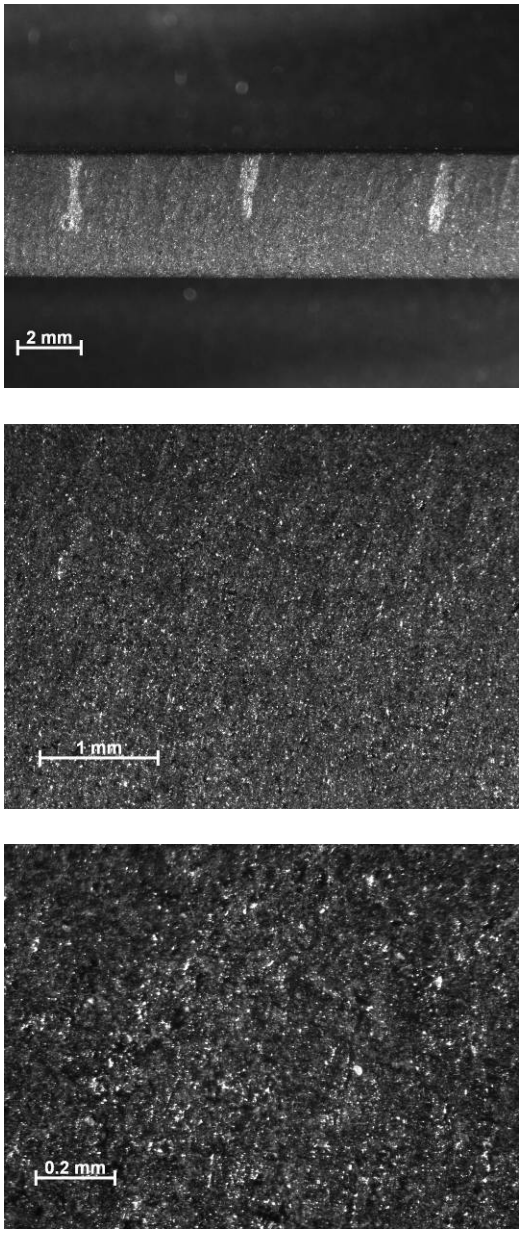

Figure 115 –Sample 12-20, PMR-15 neat resin aged in argon for 500 h, T = 288°. Before testing, Machined with water jet.

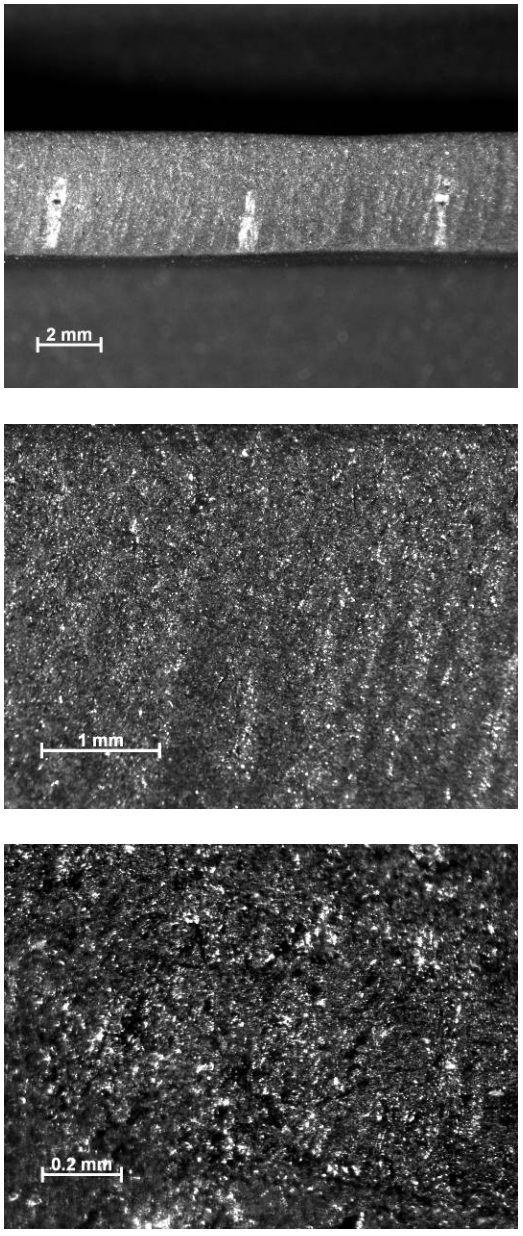

Figure 116 –Sample 12-20, PMR-15 neat resin aged in argon for 500 h, T = 288°C, Creep stress = 20 MPa. Machined with water jet showing very slight microcracking.

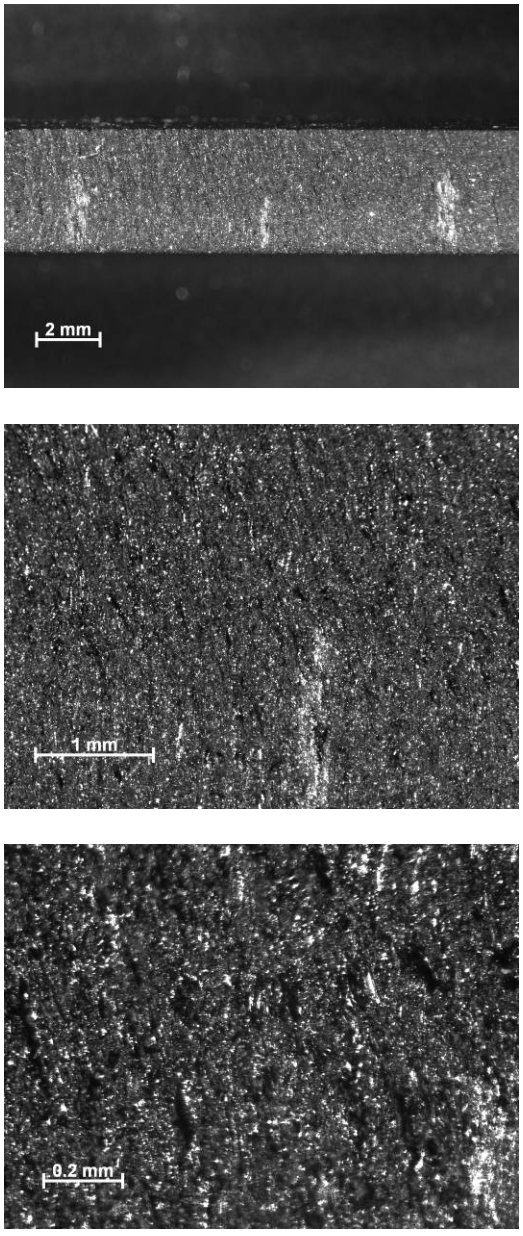

Figure 117 –Sample 12-06, PMR-15 neat resin aged in argon for 500 h, T = 288°. Before testing, Machined with water jet.

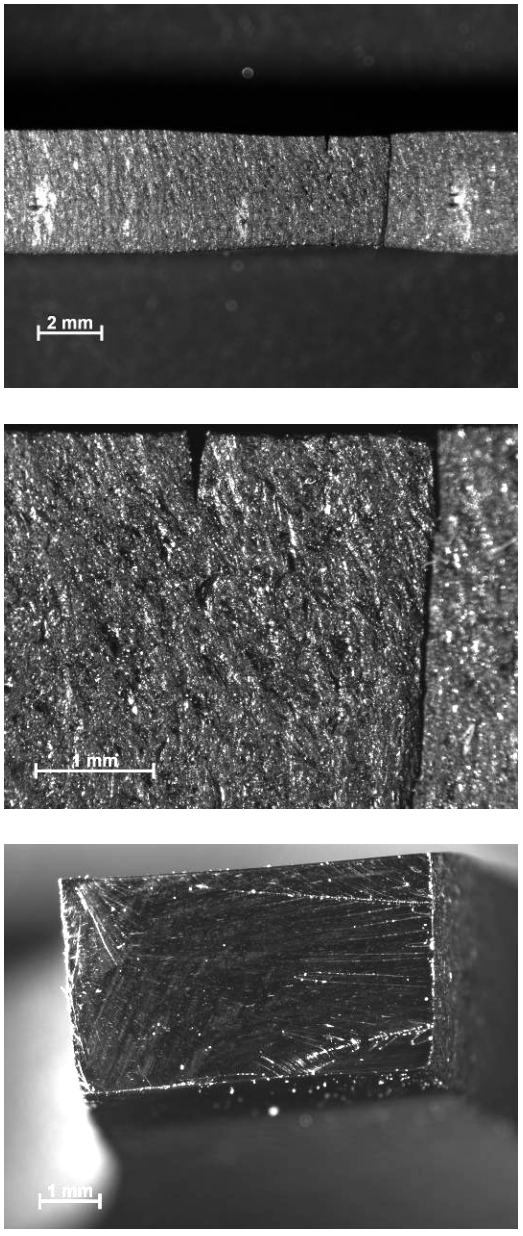

Figure 118 –Sample 13-06, PMR-15 neat resin aged in argon for 500 h, T = 288°C, Creep stress = 20 MPa. Machined with water jet showing microcracking around the fracture line and surface.

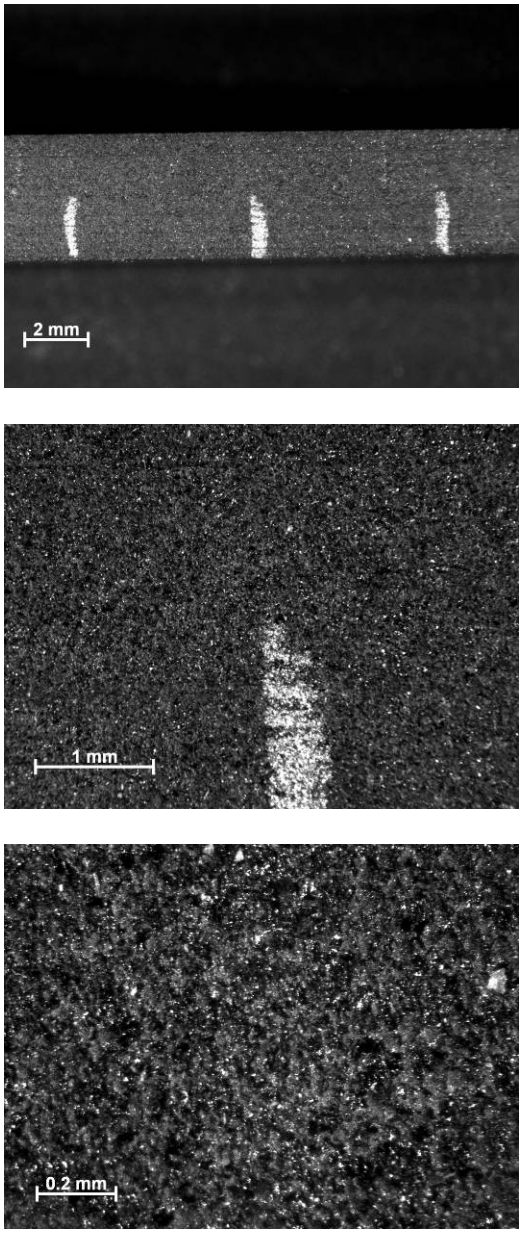

Figure 119 –Sample 11-02, PMR-15 neat resin aged in argon for 1000 h, T = 288°. Before testing, Machined with diamond saw.

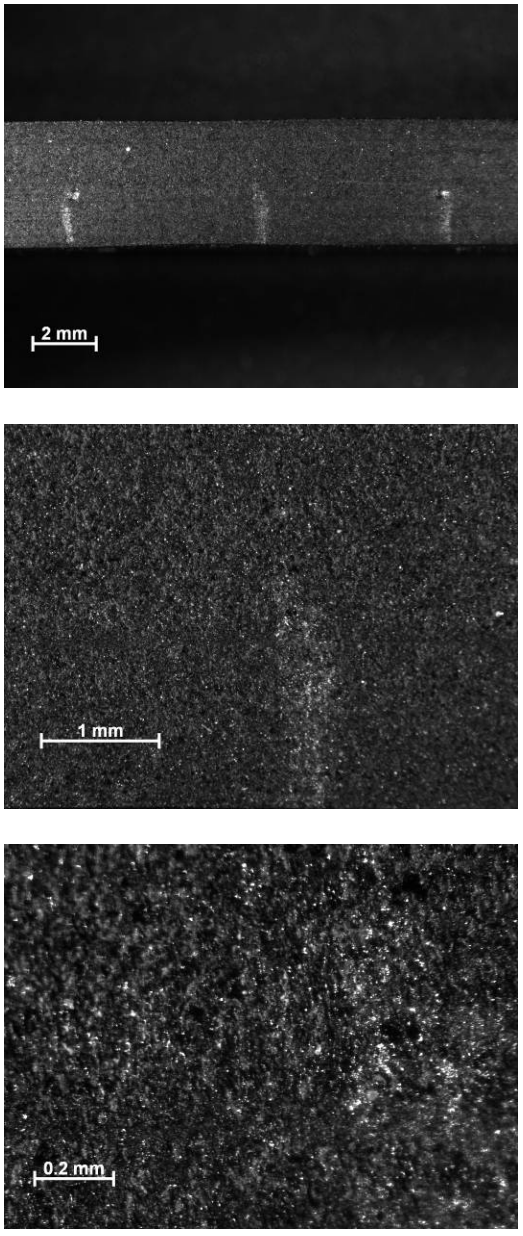

Figure 120 –Sample 11-02, PMR-15 neat resin aged in argon for 1000 h, T = 288°C, Creep stress = 20 MPa. Machined with diamond saw.

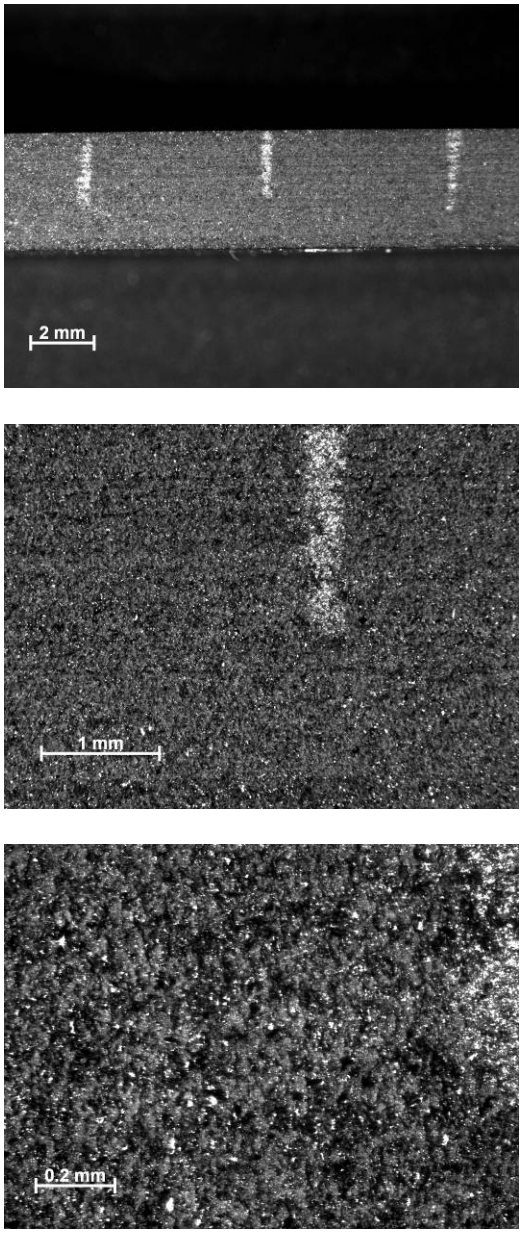

Figure 121 –Sample 11-14, PMR-15 neat resin aged in argon for 1000 h, T = 288°. Before testing, Machined with diamond saw.

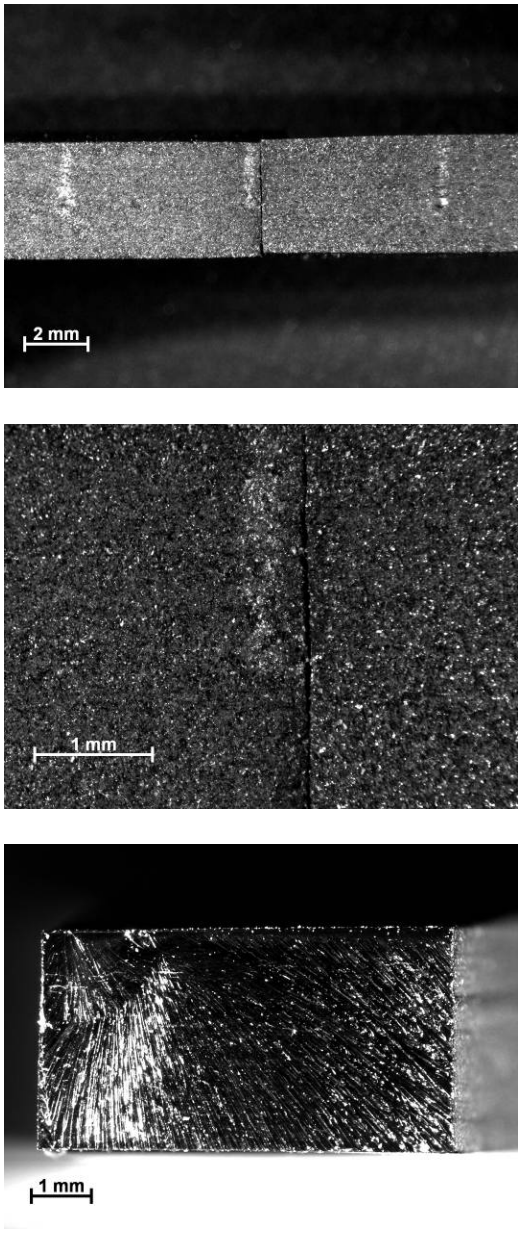

Figure 122 –Sample 11-14, PMR-15 neat resin aged in argon for 1000 h, T = 288°C, Creep stress = 20 MPa. Machined with diamond saw showing fracture line and surface.

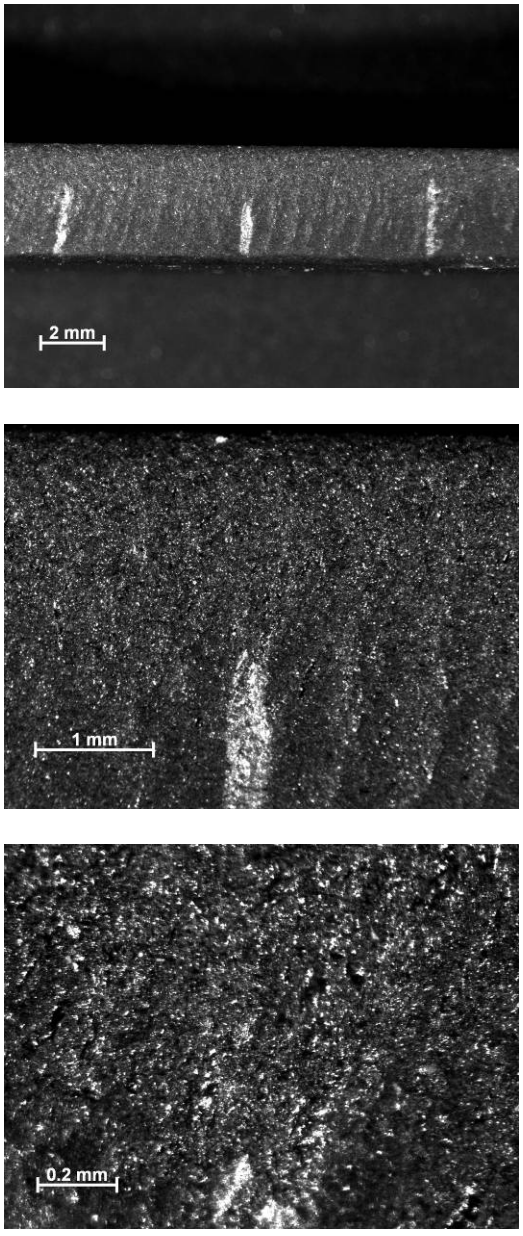

Figure 123 –Sample 12-03, PMR-15 neat resin aged in argon for 1000 h, T = 288°. Before testing, Machined with water jet.

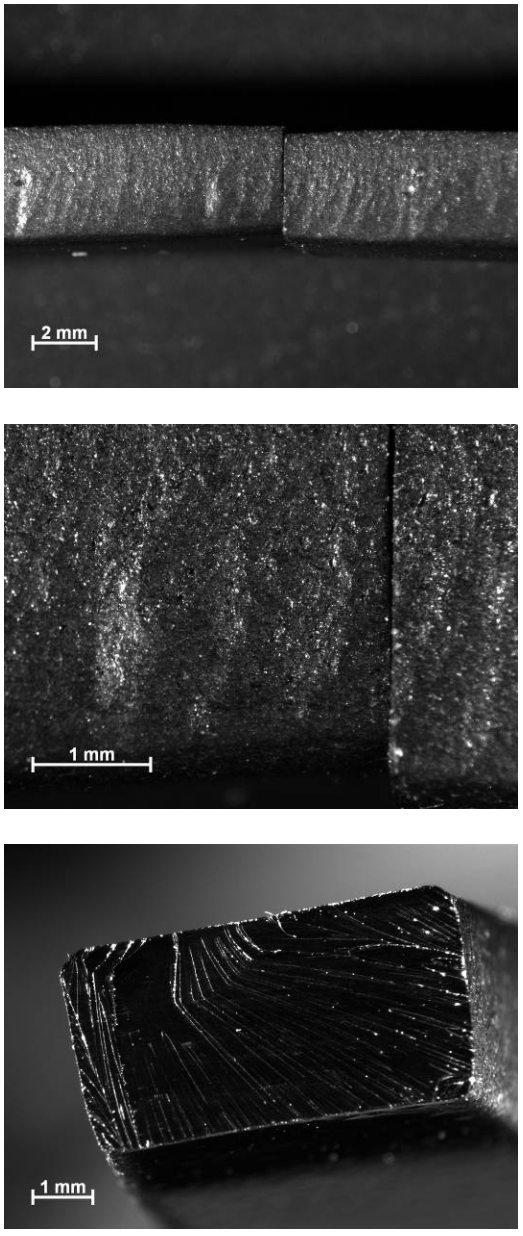

Figure 124 –Sample 12-03, PMR-15 neat resin aged in argon for 1000 h, T = 288°C, Creep stress = 20 MPa. Machined with water jet showing fracture line and surface.

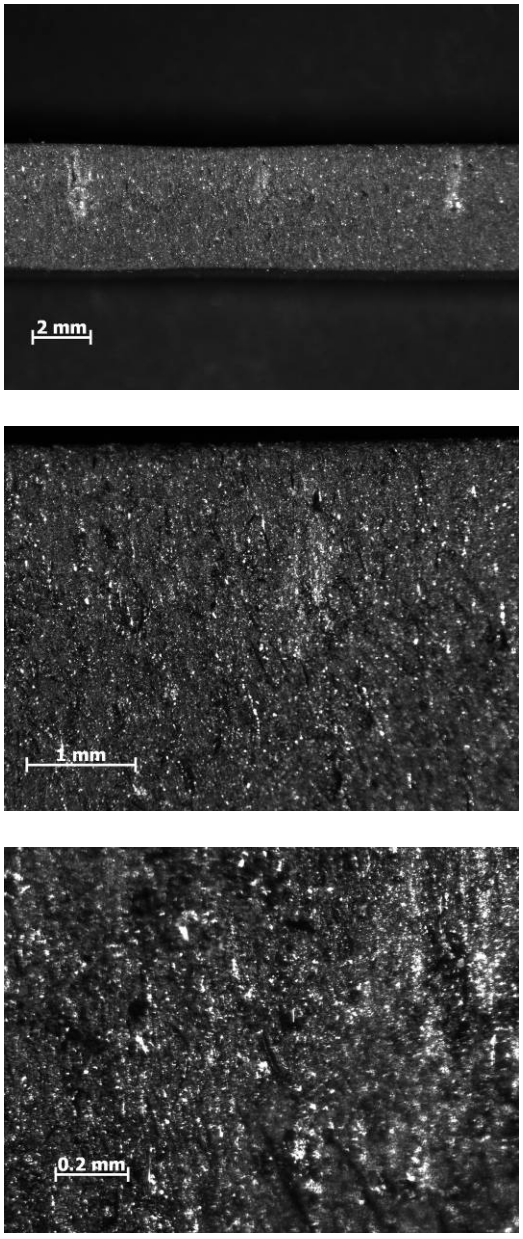

Figure 125 –Sample 12-07, PMR-15 neat resin aged in argon for 1000 h, T = 288°C, Creep stress = 10 MPa. Machined with water jet showing slight microcracking.

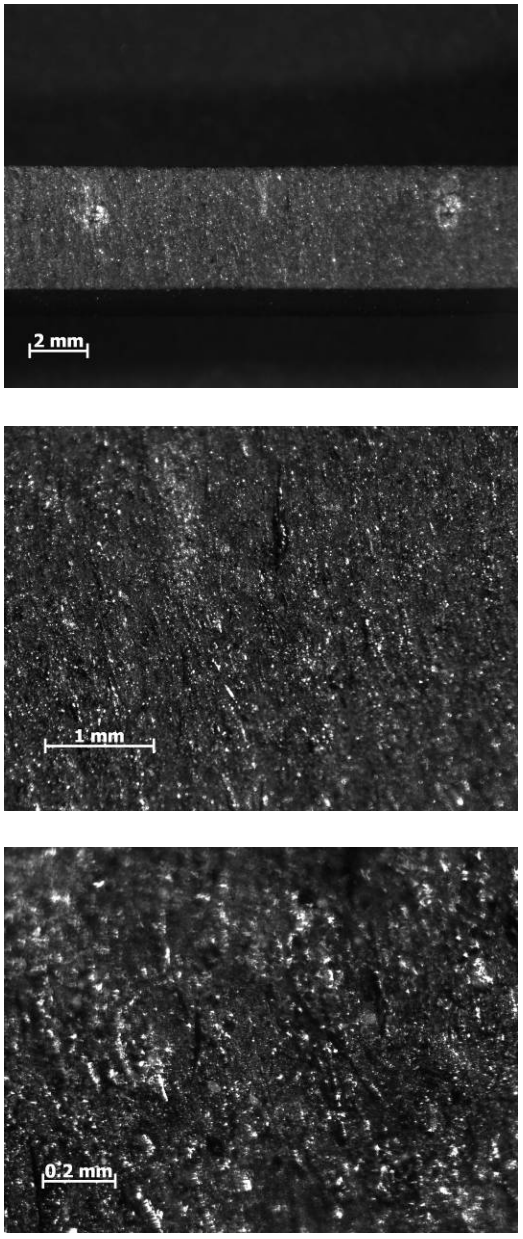

Figure 126 –Sample 13-08, as-processed PMR-15 neat resin, Creep stress = 10 MPa. Machined with water jet.

Appendix C - Fracture Surface Oxidation Layer Measurement

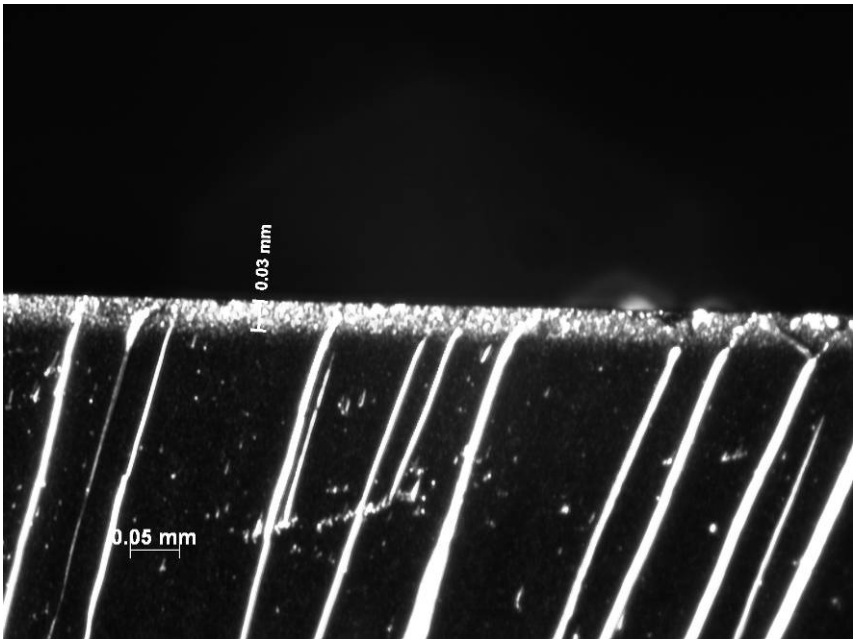

Figure 127 –Oxidation layer observed on fracture surface of sample aged in air at 288°C for 10 h. Showing formation of an oxidation layer 0.03 mm thick.

Figure 128 – Oxidation layer observed on fracture surface of sample aged in air at 288°C for 100 h. Showing formation of an oxidation layer 0.05 mm thick.

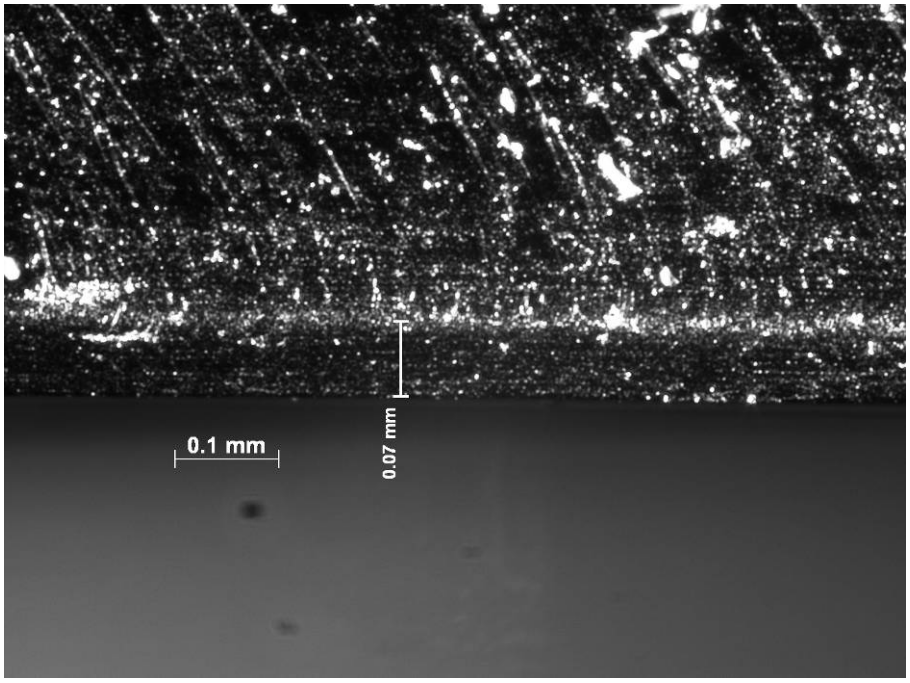

Figure 129 – Oxidation layer observed on fracture surface of sample aged in air at 288°C for 250 h. Showing formation of an oxidation layer 0.07 mm thick.

Figure 130 – Oxidation layer observed on fracture surface of sample aged in air at 288°C for 500 h. Showing formation of an oxidation layer 0.12 mm thick.

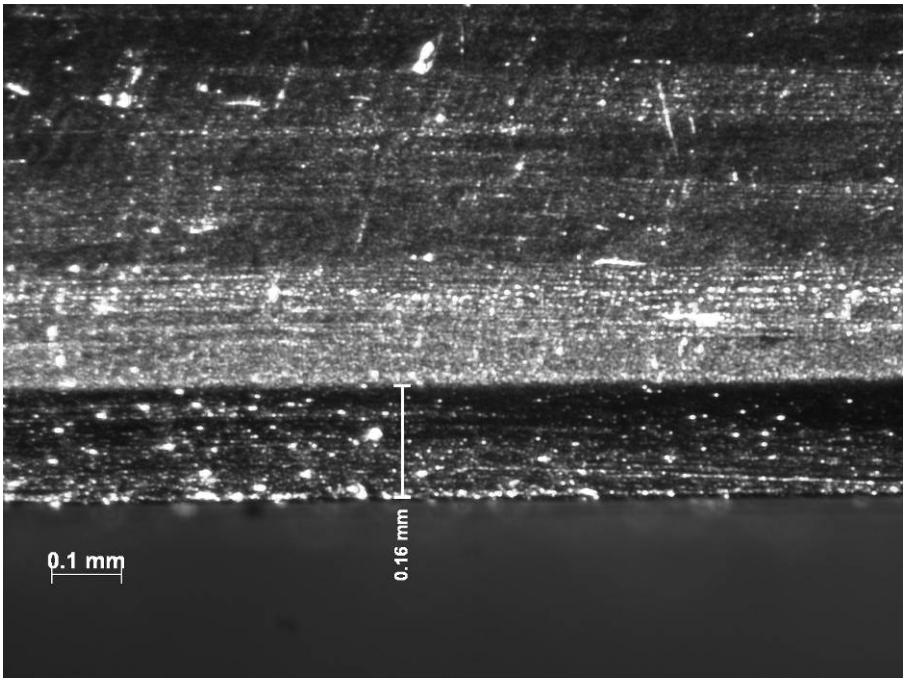

Figure 131 – Oxidation layer observed on fracture surface of sample aged in air at 288°C for 1000 h. Showing formation of an oxidation layer 0.16 mm thick.

Appendix D - Oxidation Layer Measurement by Microscopy

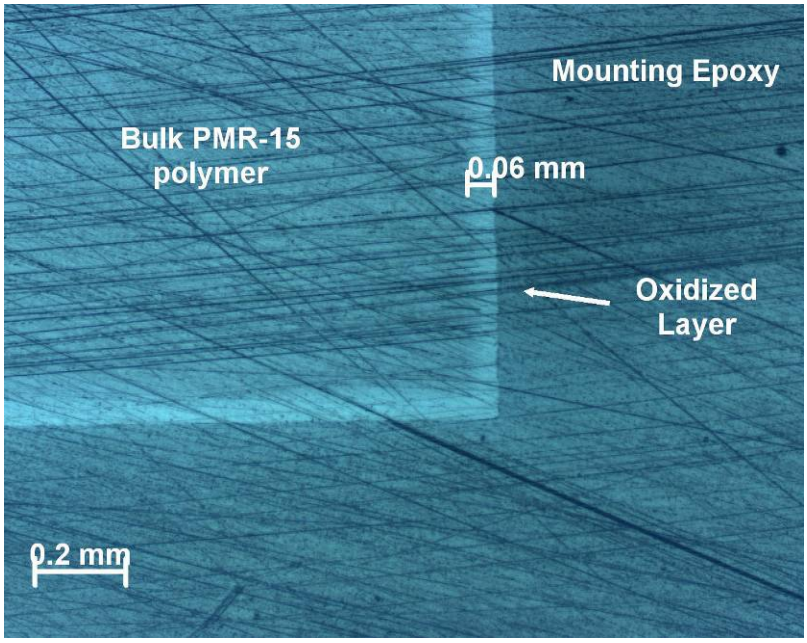

Figure 132 –Oxidation layer observed on polished section of sample aged in air at 288°C for 50 h. Showing formation of an oxidation layer 0.06 mm thick.

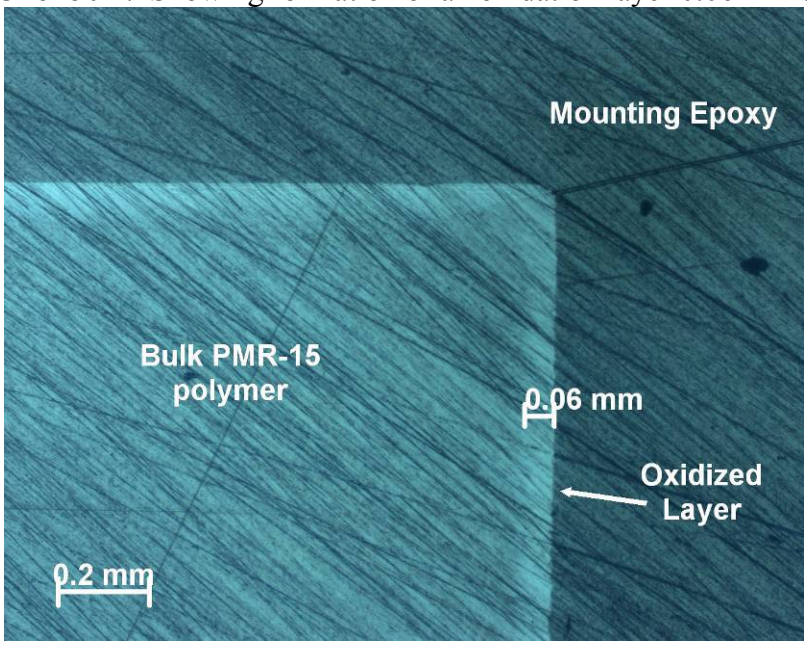

Figure 133 – Oxidation layer observed on polished section of sample aged in air at 288°C for 100 h. Showing formation of an oxidation layer 0.06 mm thick.

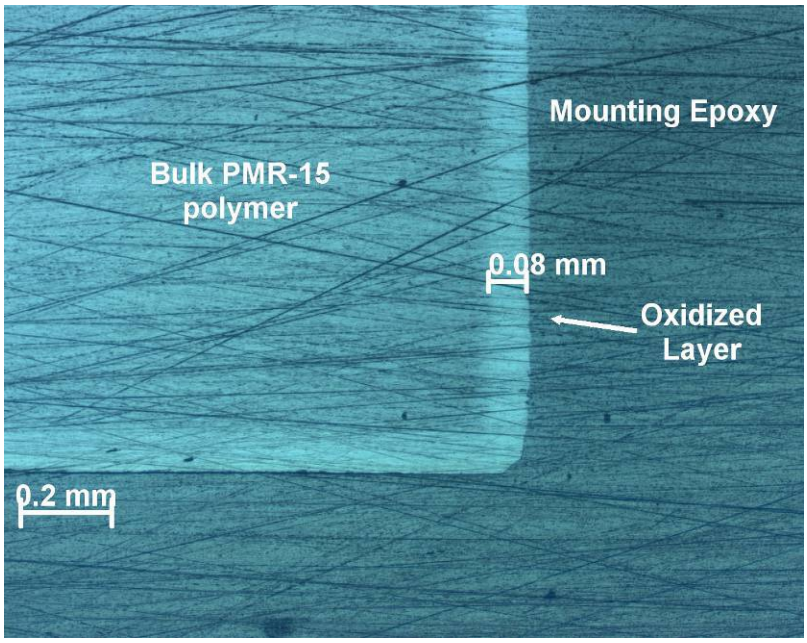

Figure 134 – Oxidation layer observed on polished section of sample aged in air at 288°C for 250 h. Showing formation of an oxidation layer 0.08 mm thick.

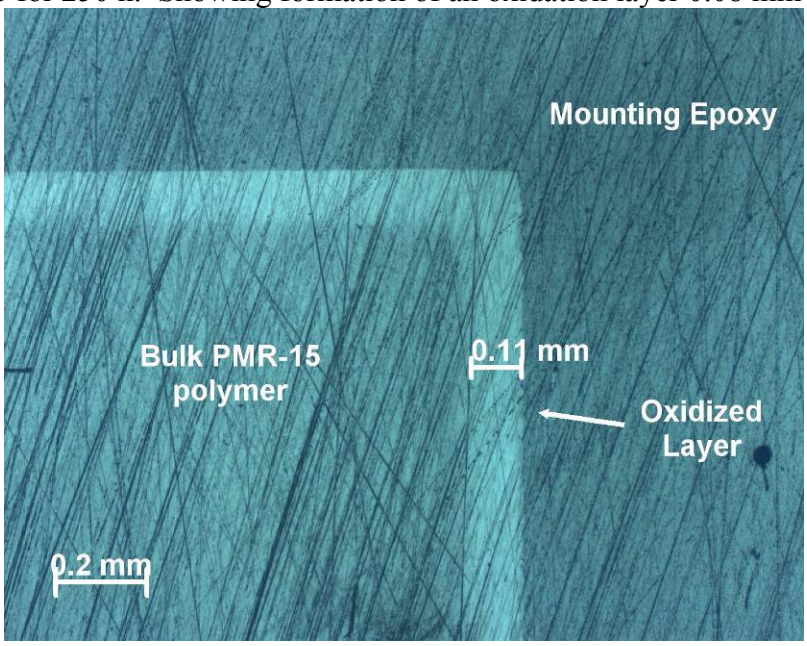

Figure 135 – Oxidation layer observed on polished section of sample aged in air at 288°C for 500 h. Showing formation of an oxidation layer 0.11 mm thick.

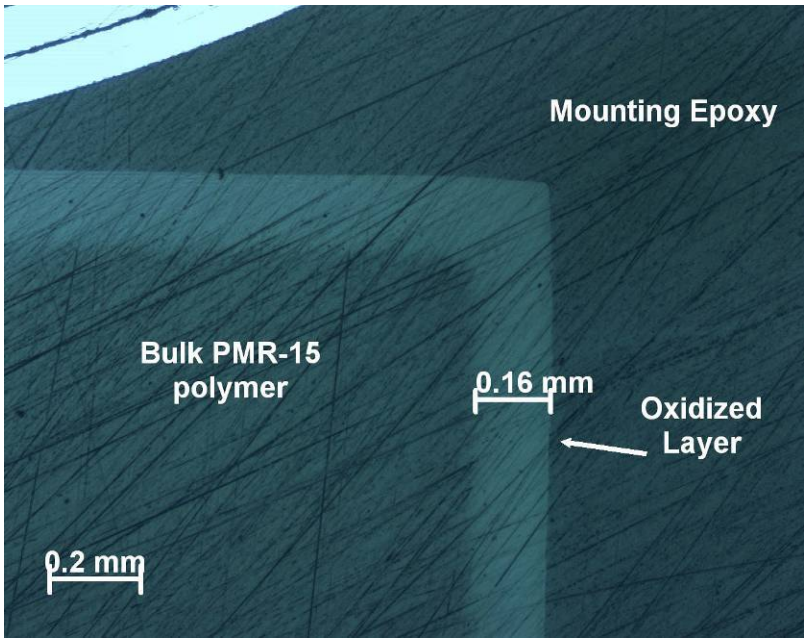

Figure 136 – Oxidation layer observed on polished section of sample aged in air at 288°C for 1000 h. Showing formation of an oxidation layer 0.16 mm thick.

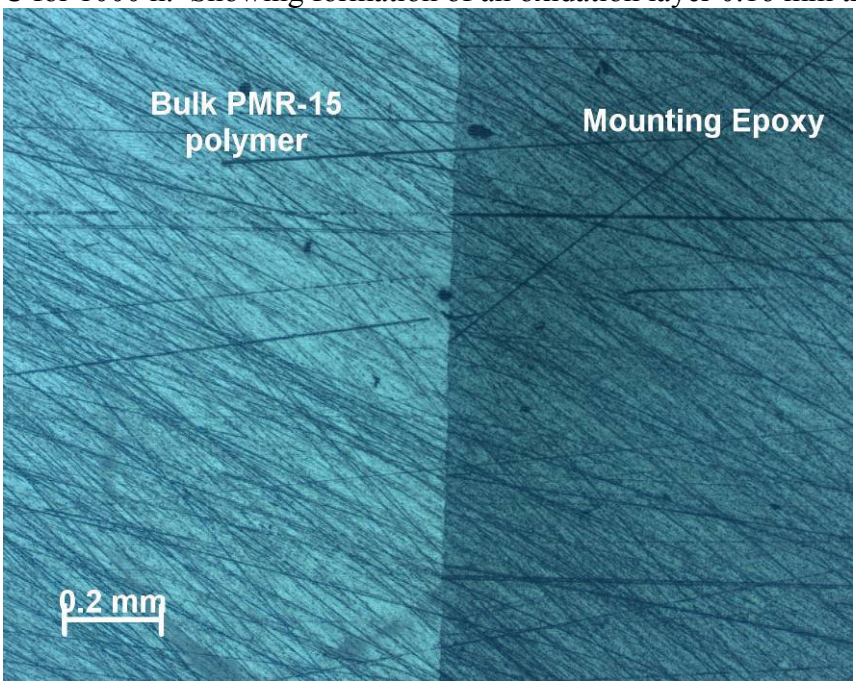

Figure 137 – Oxidation layer observed polished section of sample aged in argon at 288°C for 50 h. Showing absence of an oxidation layer.

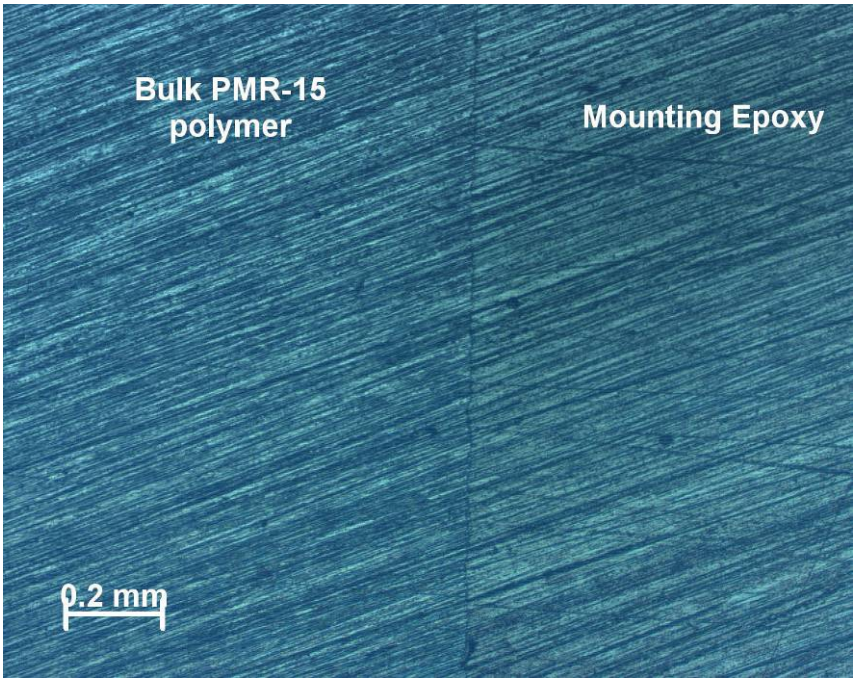

Figure 138 – Oxidation layer observed polished section of sample aged in argon at 288°C for 100 h. Showing absence of an oxidation layer.

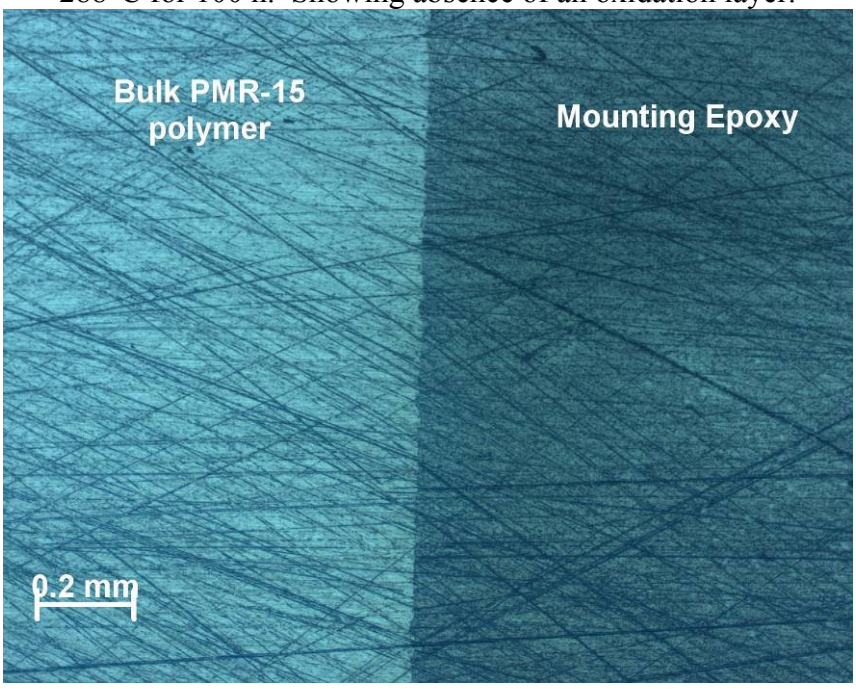

Figure 139 – Oxidation layer observed polished section of sample aged in argon at 288°C for 250 h. Showing absence of an oxidation layer.

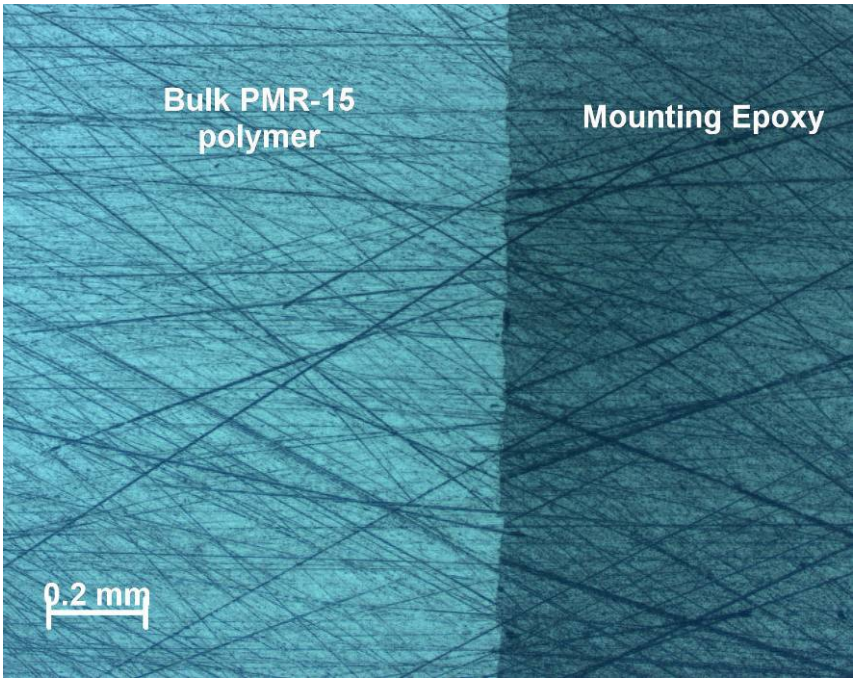

Figure 140 – Oxidation layer observed polished section of sample aged in argon at 288°C for 500 h. Showing absence of an oxidation layer.

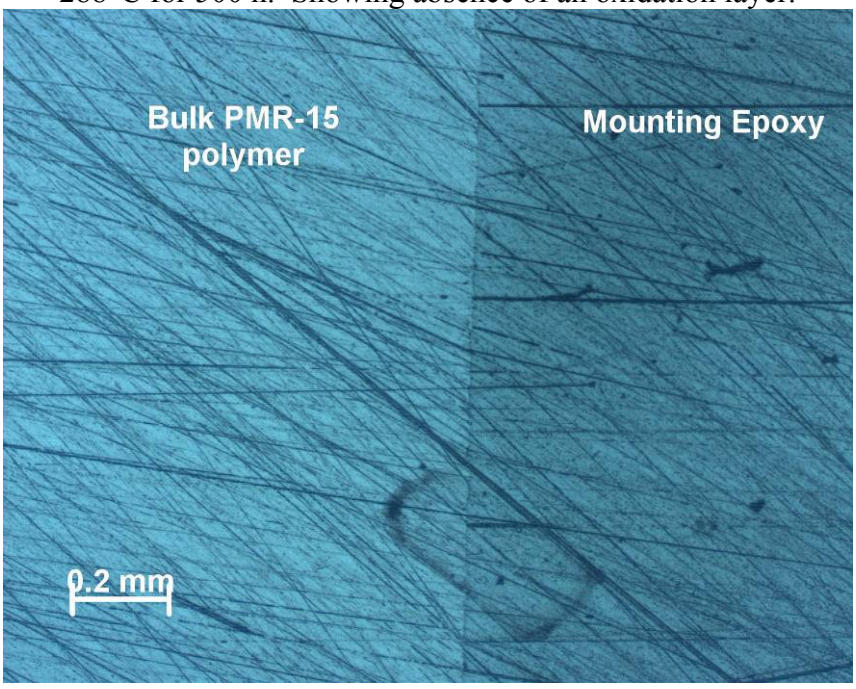

Figure 141 – Oxidation layer observed polished section of sample aged in argon at 288°C for 1000 h. Showing absence of an oxidation layer.

REPORT DOCUMENTATION PAGE

Form Approved
OMB No. 074-0188

The public reporting burden for this collection of information is estimated to average 1 hour per response, including the time for reviewing instructions, searching existing data sources, gathering and maintaining the data needed, and completing and reviewing the collection of information. Send comments regarding this burden estimate or any other aspect of the collection of information, including suggestions for reducing this burden to Department of Defense, Washington Headquarters Services, Directorate for Information Operations and Reports (0704-0188), 1215 Jefferson Davis Highway, Suite 1204, Arlington, VA 22202-4302. Respondents should be aware that notwithstanding any other provision of law, no person shall be subject to an penalty for failing to comply with a collection of information if it does not display a currently valid OMB control number.
PLEASE DO NOT RETURN YOUR FORM TO THE ABOVE ADDRESS.

1. REPORT DATE *(DD-MM-YYYY)*	**2. REPORT TYPE**	**3. DATES COVERED** *(From – To)*
22-03-2007	Master's Thesis	October 2005 – March 2007

4. TITLE AND SUBTITLE

EFFECTS OF PRIOR AGING AT ELEVATED TEMPERATURE IN AIR AND IN ARGON ENVIRONMENTS ON CREEP RESPONSE OF PMR-15 NEAT RESIN

5a. CONTRACT NUMBER

5b. GRANT NUMBER

5c. PROGRAM ELEMENT NUMBER

6. AUTHOR(S)

Broeckert, Joseph L., 1st Lt, USAF

5d. PROJECT NUMBER

5e. TASK NUMBER

5f. WORK UNIT NUMBER

7. PERFORMING ORGANIZATION NAMES(S) AND ADDRESS(S)
Air Force Institute of Technology
Graduate School of Engineering and Management (AFIT/EN)
2950 Hobson Way, Building 640
WPAFB OH 45433-8865

8. PERFORMING ORGANIZATION REPORT NUMBER

AFIT/GMS/ENY/07-M01

9. SPONSORING/MONITORING AGENCY NAME(S) AND ADDRESS(ES)
AFOSR/NE
Attn: Dr. Charles Y-C. Lee
875 N. Randolph Street, Suite 325
Arlington, VA 22203 DSN: 426-7779

10. SPONSOR/MONITOR'S ACRONYM(S)

11. SPONSOR/MONITOR'S REPORT NUMBER(S)

12. DISTRIBUTION/AVAILABILITY STATEMENT

APPROVED FOR PUBLIC RELEASE; DISTRIBUTION UNLIMITED.

13. SUPPLEMENTARY NOTES

14. ABSTRACT

Creep behavior of PMR-15 neat resin, a polyimide thermoset polymer, aged in air or argon gaseous environments at 288°C for up to 1000 h was evaluated. Creep tests were performed at 288°C at creep stress levels of 20 and 10 MPa. Creep periods of at least 25 h in duration were followed by recovery at zero stress. Weight loss and growth of the oxidation layer were also monitored and correlated with aging time. The aging time in both air and argon environments had a strong influence on the creep and recovery response of PMR-15 neat resin. Samples aged in argon for 1000 h and tested at a creep stress level of 20 MPa produced creep strain of 4%, while the as-processed samples accumulated creep strain of 16%. DMA tests were performed to examine any changes in the glass transition temperature (Tg) of the PMR-15 neat resin. DMA results revealed an increase in (Tg) from 331°C to 336.5°C after 1000 h in argon at 288°C. Increase in Tg, indicating an increase in crosslink density due to aging in both air and argon environments is likely behind the changes in elastic modulus and in creep and recovery behavior.

15. SUBJECT TERMS
polymer, PMR-15, creep, recovery, aging, argon, weight loss, glass transition temperature, Tg, DMA, crosslink density

16. SECURITY CLASSIFICATION OF:			**17. LIMITATION OF ABSTRACT**	**18. NUMBER OF PAGES**	**19a. NAME OF RESPONSIBLE PERSON**
a. REPORT	**b. ABSTRACT**	**c. THIS PAGE**			Dr. Marina Ruggles-Wrenn,
U	**U**	**U**	**UU**	176	**19b. TELEPHONE NUMBER** *(Include area code)* (937) 255-3636, ext 4641 (marina.ruggles-wrenn@afit.edu)

Standard Form 298 (Rev. 8-98)
Prescribed by ANSI Std. Z39-18